

UCLA

UCLA Previously Published Works

Title

Biosynthesis and synthetic biology of psychoactive natural products

Permalink

<https://escholarship.org/uc/item/4717h743>

Journal

Chemical Society Reviews, 50(12)

ISSN

0306-0012

Authors

Jamieson, Cooper S

Misa, Joshua

Tang, Yi

et al.

Publication Date

2021-06-21

DOI

10.1039/d1cs00065a

Peer reviewed



Published in final edited form as:

Chem Soc Rev. 2021 June 21; 50(12): 6950–7008. doi:10.1039/d1cs00065a.

Biosynthesis and Synthetic Biology of Psychoactive Natural Products

Cooper S. Jamieson^{1,4}, Joshua Misa^{2,4}, Yi Tang^{1,2}, John M. Billingsley^{2,3}

¹Department of Chemistry and Biochemistry, University of California, Los Angeles, Los Angeles, CA, USA

²Department of Chemical and Biomolecular Engineering, University of California, Los Angeles, Los Angeles, CA, USA

³Invizyne Technologies, Inc., Monrovia, CA, USA

⁴These authors contributed equally.

Abstract

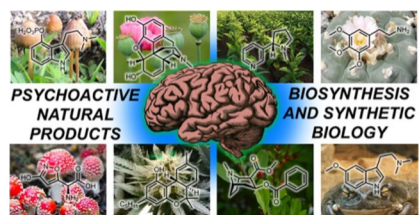
Psychoactive natural products play an integral role in the modern world. The tremendous structural complexity displayed by such molecules confers diverse biological activities of significant medicinal value and sociocultural impact. Accordingly, in the last two centuries, immense effort has been devoted towards establishing how plants, animals, and fungi synthesize complex natural products from simple metabolic precursors. The recent explosion of genomics data and molecular biology tools has enabled the identification of genes encoding proteins that catalyze individual biosynthetic steps. Once fully elucidated, the “biosynthetic pathways” are often comparable to organic syntheses in elegance and yield. Additionally, the discovery of biosynthetic enzymes provides powerful catalysts which may be repurposed for synthetic biology applications, or implemented with chemoenzymatic synthetic approaches. In this review, we discuss the progress that has been made toward biosynthetic pathway elucidation amongst four classes of psychoactive natural products: hallucinogens, stimulants, cannabinoids, and opioids. Compounds of diverse biosynthetic origin – terpene, amino acid, polyketide – are identified, and notable mechanisms of key scaffold transforming steps are highlighted. We also provide a description of subsequent applications of the biosynthetic machinery, with an emphasis placed on the synthetic biology and metabolic engineering strategies enabling heterologous production.

Graphical Abstract

⁷Conflicts of interest

The authors declare the following competing financial interest(s):

John Billingsley is an employee of Invizyne, Technologies (Monrovia, CA, USA), a company seeking to commercialize synthetic biochemistry.



1 Introduction

The consumption of psychoactive natural products predates recorded history.¹ For millennia, our ancestors subsisted by consuming materials foraged from the natural world. Over time, innumerable person-hours of trial and error resulted in a keen understanding of the expected physiological and psychological effects upon ingestion of specific plants, animals, and fungi.² This information propagated initially as traditional knowledge, forming the basis of valuable cultural practices and efficacious traditional medicine.³ The myriad of ethical concerns around the appropriation of indigenous knowledge, exploitation of slave labor, as well as inequitable access to natural product cultivation, sale, and use, typically go unanswered by mainstream science, and we encourage the reader to consult a selection of responsibly written articles on these subject matters.^{4–8} Scientists are beginning to recognize that natural products have mediated intimate evolutionary relationships between plants, animals, and fungi.⁹ For instance, over centuries, winemakers selected grapes harboring high-alcohol producing Crabtree-positive yeast, enabling the co-domestication of a plant-fungal symbiont pair.¹⁰ An additional, highly speculative example known as the “Stoned Ape Hypothesis” posits that the consumption of psychedelic mushrooms may have played a role in rapid increase of brain size in early hominids.¹¹

This push-pull relationship of humans with natural products continues to this day, as the adoption of single molecule constituents by Western culture has triggered the expansion of traditional cultivation practices to meet global demands.¹² Isolation of and characterization of organic plant extracts marked the beginnings of both organic chemistry and Western medicine. Prior to 20th century prohibition, efforts towards the total synthesis of commodified natural products provided a foundation for generations of organic chemists. Sir Robert Robinson’s 1917 route to the cocaine precursor tropinone is widely lauded as a classic in total synthesis,¹³ while Woodward’s innumerable contributions to the field of natural product total synthesis included a route to the lysergic acid diethylamide (LSD) precursor lysergic acid.¹⁴ Incorporation of this knowledge into semi-syntheses prompted researchers to think of biological materials as chemical factories, and beg the question: how do organisms synthesize natural products? Extraordinary progress has been made in the elucidation of the metabolic pathways underpinning the chemical composition of psychoactive substances. In the field of natural product biosynthesis, scientists investigate the biosynthetic logic that enables Nature to synthesize psychoactive natural products with high efficiencies and selectivities.¹⁵ Identification and reconstitution of key enzymatic steps uncovers Nature’s synthetic schema towards complex molecular scaffolds from simple metabolic precursors. The accumulation of such biosynthetic information is driven in part by advancements in synthetic biology; emerging biotechnologies promise to outperform

traditional synthetic methods in cost, safety, efficiency, and sustainability. Thus, significant achievements have been made in the heterologous expression of natural product pathways towards consumer products.

1.1 Four categories of psychoactive natural products

Only in the last half of a century have scientists begun to investigate the molecular mechanisms of psychoactivity – the alterations in perception, consciousness, and behavior, associated with such small molecules.¹⁶ Prior to the 1950s, most scientists believed that synaptic activity was dictated entirely through electrical impulses, and little evidence existed on the role of chemical signaling.¹⁷ Our current understanding of psychopharmacology has been directly facilitated by the use of natural products. The extraordinary protein receptor binding affinities of psychoactive natural products allowed scientists to deduce the role of neurotransmitters in the central nervous system.¹⁸ We now know that neuroreceptors are the key signal transducers able to integrate chemical signals into biological systems. It is the selective receptor binding and activation by native and non-native chemical ligands that causes modulation of neural pathways, resulting in altered perception.¹⁹ These receptors are differentially expressed in different populations of neurons, and may exist as splice variants or exhibit single-nucleotide polymorphisms between individuals.²⁰ Further, differential activation of receptor subtypes by a given ligand makes it difficult to categorize psychoactive drugs based strictly on the physiological target. For example, activation of μ -opioid receptors (MORs) by agonists like morphine (Section 5.2) results in analgesia and sedation,²¹ whereas activation of κ -opioid receptors (KORs) by the potent ligand salvinorin A (Section 2.9) results in dissociation.²² Thus, while formally an opioid, the consumer of *Salvia divinorum* would classify the shrub as a *bona fide* hallucinogen based on perceived psychological effect. As a result, psychoactive drugs have traditionally been categorized based simply on the experience of the user, as opposed to complex molecular mechanisms of psychoactivity. The natural products discussed herein fall within one of four well-recognized classes: hallucinogens, stimulants, cannabinoids, and opioids (Fig. 1).

The utility of psychoactive natural products, if used safely, cannot be questioned. Selective, potent binding of a ligand to a target is a hallmark feature of a pharmaceutical agent. While immense pharmaceutical potential has been ascribed to many psychoactive natural products, evidence-based drug development campaigns are largely hindered by regulatory status.²³ Natural products in the Schedule I Controlled Substance category have been designated as having no accepted medical use, hindering clinical trials, even though many compounds on the list exhibit great potential for clinical success. For example, evidence implicates psilocybin **1** as a promising candidate for treatment-resistant depression²⁴ and post-traumatic stress disorder,²⁵ whereas the alkaloid ibogaine **2** has undergone development as anti-addictive agent.²⁶ Meanwhile, a recent meta-analysis concluded that the natural product derivative lysergic acid diethylamide (LSD) **3** has strong potential in the treatment of alcoholism.²⁷ These three compounds fall into the category of hallucinogenic natural products, invoking psychedelic, introspective effects. Alkaloidal stimulants are also of great societal value, and include the world's most widely consumed psychoactive drug, caffeine **4**.²⁸ Nicotine **5** and cocaine **6**, two other well-known alkaloidal stimulants, exhibit high potential for dependence, but are each approved for specific medicinal indications.^{29,30}

While the legal status of *Cannabis* is currently in flux, the primary constituents tetrahydrocannabinol (THC) **7** and cannabidiol (CBD) **8** are FDA approved medications.³¹ State-by-state deregulation has resulted in the ongoing cannabinoid boon driving academia and industry to discover additional applications for THC, CBD, and other rare cannabinoids. Finally, opioid analgesics are included on the World Health Organization's List of Essential Medicines. Despite the ongoing opioid crisis, morphine **9** plays a critical role in pain management and palliative care.³² Kratom, which contains the potent MOR agonist mitragynine **10**, has emerged recently as an alternative to opium-derived substances. Given its potential for abuse, additional epidemiological studies of kratom are warranted.³³ As opioid dependence soars, public health organizations have described the importance of research into pain management and addiction. We advocate for an unbiased, evidence-based evaluation of the risks and benefits of psychoactive natural product use in order to maximize societal value.

1.2 Overview of biosynthesis of psychoactive compounds

As with most natural products isolated from microorganisms and plants, the psychoactive compounds discussed in this review are biosynthesized from simple, primary metabolites such as acetate, isoprene, and amino acids.¹⁵ With the exception of cannabinoids and a few others, most of the compounds covered are alkaloids derived from the decarboxylation of a small set of amino acids. For example, L-tryptophan **11** is the precursor to ibogaine **2** and psilocybin **3**; L-tyrosine **12** is the precursor to mescaline (Section 2.6) and morphine **10**; while the nonproteinogenic amino acid L-ornithine **13** is the precursor to nicotine **5** and cocaine **6**. The decarboxylation of amino acids is catalyzed by an enzyme family known as amino acid decarboxylase (AADC), which uses pyridoxal-5'-phosphate (PLP) as a cofactor. A few of the compounds contain isoprenoid building blocks, such as the C5 prenyl unit in lysergic acid (Section 2.5) and the C10 geranyl unit in cannabinoids (Section 4.2). The C–C bonds between the isoprenes and the rest of the molecules in these compounds are catalyzed by a group of enzymes known as prenyltransferases. Prenyltransferases are one type of group transfer enzyme used by nature to transfer functional groups from thermodynamically activated carriers to natural product biosynthetic intermediates. Other group transfer enzymes include acyltransferases and *S*-adenosylmethionine (SAM) dependent methyltransferases, which are frequently found in biosynthetic pathways. Nature also uses redox reactions extensively to modify the natural products to their final, bioactive forms. The enzymes catalyzing these reactions are collectively referred to as oxidoreductases, and include examples such as cytochrome P450s, ketoreductases and amine oxidases.³⁴ The enzymology of these enzymes has been well-studied and the reader can refer to other reviews for more information.^{35,36} Here we will briefly summarize a few enzyme-catalyzed or enzyme-mediated reactions that will be found throughout the review.

1.2.1 Decarboxylation of amino acids—The aromatic amino acids L-tryptophan **12**, L-tyrosine **13** and to a less extent, L-phenylalanine, are commonly used precursors for alkaloid natural product biosynthesis. For example, the indole ring in L-tryptophan **11** is preserved in compounds such as psilocybin **1** and ibogaine **2**; while the *para*-hydroxybenzene side chain in L-tyrosine **12** can be found in mescaline (Section 2.6) and morphine **9**. The terminal amine-containing L-lysine and L-ornithine **13** are also used as

precursors. Relevant to this review, the four-carbon side chain of L-ornithine **13** is required for the formation of pyrrolidines and tropanes. The first step in the utilization of these amino acids for alkaloid biosynthesis is decarboxylation to give the corresponding primary amines, although in lysergic acid biosynthesis L-tryptophan is used without decarboxylation. The decarboxylation products of L-tryptophan, L-tyrosine and L-ornithine are tryptamine **14**, tyramine **15**, and putrescine **16**, respectively (Fig. 2A). In the case of tyramine **14**, hydroxylation of one of the *meta* positions in the *para*-phenol ring gives the metabolite dopamine **17**. Dopamine **17** is a natural product building block, but also a neurotransmitter in mammals. The chemical logic for the early decarboxylation is straightforward: to facilitate intra- and intermolecular Mannich reactions with aldehydes and ketones using the nucleophilic amine (see section 1.2.2). This decarboxylation-Mannich two step rapidly sets up the (poly)-heterocyclic scaffold of many alkaloidal natural products.

The decarboxylation reactions are catalyzed by dedicated amino acid decarboxylases. For example, in the case of L-tryptophan, a tryptophan decarboxylase is involved. These enzymes typically use the PLP cofactor, as expected for many enzymes that perform C_α, C_β and C_γ modifications on amino acids.³⁷ The mechanism of the reaction is shown in Fig. 2B. The aldehyde of PLP modifies an active site lysine to form the resting aldimine in the decarboxylase active site. A transaldimination step takes place next in which the amine of the substrate amino acid attacks the aldimine and forms the amino acid-PLP aldimine. The PLP then serves as an electron sink in the enzyme-catalyzed cleavage of the C_α-COO⁻ bond via a quinonoid species. Reprotonation of the C_α then generates the product aldimine, which can undergo another transaldimination with the active site lysine to release the product amine and regenerate the resting aldimine.

1.2.2 Mannich/Pictet-Spengler reactions—Following decarboxylation of the amino acids to the corresponding primary amines, a common next step is the Mannich reaction involving the primary amine. The Mannich reaction is a two-step reaction that yields an alkylated amine.³⁸ In the first step, the primary amine reacts with either an aldehyde or a ketone to form the Schiff base. The C=N double bond is then attacked by a carbon nucleophile, such as the acidic C_α of a carbonyl to form the β-amino-carbonyl product. Two examples of an intramolecular Mannich reaction can be found in the formation of the tropane unit in cocaine **6** (Section 3.4).^{39,40} Starting from putrescine **16**, methylation of one of the primary amines gives the intermediate *N*-methylputrescine **18**; oxidation and hydrolysis of the other amine yields *N*-methylaminobutanal **19**, which is in equilibrium with the cyclic *N*-methylpyrrolinium **20**. Attack of the imine by the enolized 3-oxo-glutaric acid **21** yields the adduct pyrrolidine tropane scaffold precursor (Fig. 3A). A subsequent dehydrogenation generates a new pyrrolinium species that can be attacked with C_α of the 1,3-diketo unit in a second Mannich reaction (Section 3.4).

One variation of the Mannich reaction that is central to the biosynthesis of plant alkaloids is the Pictet-Spengler (PS) reaction involving β-arylethylamines such as tryptamine **14** and dopamine **17**. In the PS reaction, after the amine reacts with an aldehyde or ketone to form the Schiff base, a carbanion resonance structure of the indole in tryptamine or the *para*-hydroxy phenol ring in dopamine can attack the imine to form the new C–C bond. This can

be followed by rearrangements to form the stable tricyclic tetrahydro- β -carboline or bicyclic tetrahydroisoquinoline, respectively. The tryptamine-derived tetrahydro- β -carboline is found in harmala alkaloids (Section 2.4) and iboga alkaloids (Section 2.8). To generate the harmala family of compounds, tryptamine **14** is condensed with pyruvic acid **22**, followed by attack of the imine by C3 from the indole ring to form a spirocycle, which collapses via single bond migration to complete the PS reaction (Fig. 3B).⁴¹ Similarly, the condensation between the aldehyde donor secologanin **24** and tryptamine **14** is catalyzed by a dedicated Pictet-Spenglerase, yielding strictosidine, the universal precursor to monoterpene indole alkaloids (MIAs) including ibogaine.⁴² In the biosynthesis of benzyloquinoline alkaloids (BIAs) such as morphine **9**, the PS reaction takes place between dopamine **17** and 4-hydroxyphenylacetaldehyde **26**, both oxidation products of tyramine **15**, to form the key intermediate *S*-norcoclaurine **27**, precursor to *R*-reticuline **28** and morphine **9**. (Fig. 3C).⁴³

1.2.3 Common group transfer reactions—Group transfer reactions are widely used by Nature in the biosynthesis of natural products. Functional groups that are frequently transferred from donor molecules to biosynthetic intermediates include methyl, acetyl, small, medium and long alkyl-substituted acyl chains, isoprenyl, glucosyl, etc. These reactions serve a multitude of purposes, including i) increasing the size and complexity of the molecules; ii) changing the lipophilicity of molecules; iii) altering the reactivity of functional groups; iv) serving as a transient chemical protection group for downstream modifications; v) acting as leaving groups in elimination reactions; and vi) changing the biological properties of the natural product. Hence, these reactions are indispensable to the structural diversity of natural products that have been isolated to date.

The donor molecules, those that “carry” the groups to be transferred, are kinetically stable and thermodynamically activated: the molecules are high in energy and therefore releasing the groups is a highly exergonic reaction; yet the molecules are stable under cellular conditions and enzyme catalysis is required to overcome the kinetic barriers. We recently reviewed eight such molecules that power cellular metabolism, which include ATP, NAD(P)H, acetyl-CoA, SAM, carbamoyl phosphate, isoprenyl pyrophosphate, UDP-glucose and molecular oxygen.⁴⁴ NAD(P)H and molecular oxygen are involved in the redox reactions and will be summarized in the next section. Among the remaining six, carbamoyl-phosphate is involved in nitrogen metabolism and is not directly involved in natural product biosynthesis.

The remaining five, however, are frequently used group transfer donor molecules, and examples can be found throughout the review. ATP, the universal cellular energy currency, is the donor in the transferring of phosphate groups to nucleophilic oxygen in the presence of a phosphotransferase. This reaction is ubiquitous in primary metabolism but is quite rare in natural product biosynthesis (or secondary metabolism). One such example can be found in the psilocybin pathway (see section 2.3). Acetyltransferases catalyze the transfer of acetyl groups from the acetyl-CoA thioester to a variety of O and N nucleophiles (Fig. 4A). SAM-dependent methyltransferases use *S*-adenosylmethionine to transfer a methyl group from the trivalent sulfonium group to C, O, N, and S nucleophiles in an S_N2 type substitution reaction (Fig. 4B). This reaction can be found in the majority of biosynthetic pathways described herein. For example, iterative *N*-methylation of tryptamine yields the psychoactive molecule

N,N-dimethyltryptamine **29** (DMT, see Section 2.2). UDP-glucose is an activated glucose donor in cells for the assembly of oligosaccharides and polysaccharides. UDP-glucose is thermodynamically activated but kinetically stable in the absence of glucosyltransferases.⁴⁴ In the presence of glucosylating enzymes, UDP dissociates via cleavage of the C–O bond in an S_N1 fashion to yield a C1 oxocarbenium ion, which can be attacked by incoming nucleophiles (Fig. 4C). A notable example of substrate glucosylation is in the biosynthetic pathway of strictosidine **25**, the precursor to ibogaine (Section 2.8). The enzyme 7DLGT glucosylates the hemiacetal in 7-deoxyloganetic acid **30** to give 7-deoxyloganic acid **31**.⁴⁵ The glucose moiety serves as a protecting group to prevent formation of the aldehyde, and remains in strictosidine **25**. In order to transform strictosidine **25** into different scaffolds, a glucosidase removes the glucose moiety, unmasking the aldehyde and leading to subsequent rearrangements towards structurally diverse monoterpene indole alkaloids.

The final group transfer reaction that is relevant to this review is the transfer of prenyl groups from isoprenyl pyrophosphate to different nucleophiles in small molecules. These reactions are catalyzed by a family of enzymes known as prenyltransferases. The prenyl unit that is transferred from the pyrophosphorylated donor to the substrate can be as small, as in the five-carbon dimethylallyl (most common), or the more elongated oligoprenyl groups such as the ten-carbon geranyl, fifteen-carbon farnesyl, etc. In the enzyme active site, the prenyl pyrophosphate donors can undergo C–O bond cleavage to yield the C1 carbocation, which is stabilized by delocalization of the positive charge. Attack of the carbocation by a nucleophile carbon forges the new bond and completes the prenyl transfer reaction (Fig. 4D). Electron rich aromatic rings, such as hydroxybenzenes and indoles can serve as nucleophiles to attack the allyl cation to perform in essence an electrophilic aromatic substitution. Two examples in this review illustrate this reaction. The first is the dimethylallyl tryptophan synthase (DMATS) in lysergic acid biosynthesis, which prenylates the C4 position in *L*-tryptophan **11** to give 4-dimethylallyl-*L*-tryptophan (4-DMAT, Section 2.4).⁴⁶ This modification introduces an olefin-containing five carbon unit into *L*-tryptophan, which can be further oxidized and cyclized into the hallucinogenic lysergic acid. The mechanism of this reaction has been thoroughly studied, and is likely a two-step reaction.⁴⁷ The C3 position of the indole ring is the most nucleophilic due to resonance with the indole nitrogen lone pair. Attack on the allyl cation can occur at either C1 or C3; this attack is proposed to take place at the more stable C3 position of the allyl cation. This generates a “reverse”-prenylated product that is proposed to undergo a nonenzymatic sigmatropic Cope rearrangement to yield the “forward”-prenylated 4-DMAT. In addition to serving as the starting point for lysergic acid (Section 2.5), indole prenylation of early pathway intermediates is commonly observed in the biosynthesis of other fungal indole alkaloids.

The second notable pathway that involves prenyl transfer is in cannabinoid biosynthesis (Section 4.2).⁵³ Starting with the first intermediate in the pathway, olivetolic acid **32** which is a resorcinol derivative, the aromatic prenyltransferase transfers the ten-carbon geranyl group from geranyl pyrophosphate to the C3 position in the ring to give cannabigerolic acid (CBGA, **33**). As in the lysergic acid example, the introduced ten-carbon unit can undergo oxidative intramolecular cyclization, providing a variety of cannabinoids (Section 4.2).

1.2.4 Oxidative and reductive reactions—Natural product biosynthetic pathways employ powerful redox enzymes to modify the intermediates *en route* to the final product. The redox modification can directly modify the molecular scaffolds, or trigger rearrangement cascades, to introduce considerable structural complexities.³⁴ On the reductive side, the NAD(P)H utilizing enzymes dominate as one would expect. These include ketoreductases, short-chain dehydrogenase/reductases (SDRs), ene-reductases, and imine reductases, etc. The two-electron reduction of C=C, C=O or C=N bonds are initiated through the attack by a hydride equivalent from either the dihydropyridine ring of NAD(P)H or the hydroquinone form of flavin adenine dinucleotide (FADH₂). On the oxidative side, aerobic organisms use an assortment of enzymes and molecular oxygen as the oxidant to perform a dazzling array of chemical modifications.¹⁵ Both single electron (radical) and two electron manifolds are used by enzymes. These enzymes include the large family of heme-dependent cytochrome P450 monooxygenases that are abundant in plants and fungi; nonheme, iron and α -ketoglutarate dependent oxygenases, copper-dependent oxidases (such as the amine oxidase mentioned above), and flavin-dependent monooxygenases and oxidases. In two-electron oxidation of substrates catalyzed by oxidases, molecular oxygen is reduced to hydrogen peroxide. In monooxygenases where oxygen is reduced fully to water (four electron reduction), the substrate undergoes a two-electron oxidation, while NADPH is oxidized to NADP⁺. Here, the substrate can incorporate one of the oxygen atoms via hydroxylation or epoxidation, or alternatively the substrate can be oxidized without incorporation of oxygen atoms. Hence, depending on the mechanism of the redox enzyme, the outcome of the reaction can be very different. This topic has been extensively reviewed in the literature,^{15,34,54} and will not be discussed in detail here. However, we will highlight two reactions to illustrate the enzymatic prowess of the P450s, a staple of the plant biosynthetic pathways.

P450 enzymes use heme as a coenzyme to bind molecular oxygen. The coordinated iron is reduced to the Fe(II) state by an associated cytochrome P450 reductase (CPR). Binding of molecular oxygen and electron transfer from the Fe(II) and CPR leads to a hydroperoxy Fe(III)–O–O–H species. Cleavage of the O–O bond and the loss of water generates the high valent Fe(IV)=O porphyrin cation radical, which is also referred to as Compound I. This is a highly oxidizing species that can abstract hydrogen from substrate C, O, and N atoms to generate substrate radicals, including “unactivated” *sp*³ carbons. This generates the Fe(IV)–OH species also known as Compound II. Radical OH transfer to the substrate carbon radical produces the hydroxylated product in a process known as oxygen rebound. In many P450-catalyzed reactions in biosynthesis, the substrate radical can migrate to other atoms in the molecule through internal reactions and delocalization through π -bonds. This can lead to rearrangement of the carbon skeleton, as well as oxygen atom incorporation at distal positions from the initial abstraction site. In some cases, the Fe(IV)–OH can abstract a second hydrogen atom from the substrate to generate a second radical in the substrate that can recombine with the first one to terminate the reaction cycle. In this scenario, no oxygen atom is incorporated yet molecular oxygen is consumed. An additional feature of some biosynthetic P450s is the ability to iteratively oxidize a substrate, either at a single carbon or at nearby atoms. For example, it is not uncommon to find a single P450 that can perform the

six-electron oxidation of a methyl group into a carboxylic acid in both fungal and plant biosynthetic pathways.

One notable example of P450 catalysis in this review is the secologanin synthase (SLS) found in the strictosidine biosynthetic pathway that ultimately leads to ibogaine (Section 2.8).^{55,56} The substrate is loganin **34** which contains the iridoid core. SLS performs hydrogen abstraction followed by oxygen rebound at the methyl group on the cyclopentanol ring to give a primary hydroxyl group. This species then undergoes a Grob fragmentation-like reaction to cleave the C–C bond which reveals both an aldehyde and a terminal olefin in the product secologanin **24** (Fig. 5A).⁵⁷ This aldehyde then participates in the aforementioned Pictet-Spengler reaction with tryptamine **14** to give strictosidine **25**. Hence, although this example illustrates a “standard” P450 reaction, the hydroxylation modification triggers a significant skeletal rearrangement.

A second example that illustrates oxidation without oxygen incorporation is found in the morphine biosynthetic pathway, in which the salutaridine synthase catalyzes the phenyl coupling in *R*-reticuline **28** to yield salutaridine **35** (Fig. 5B).⁵⁸ A radical addition mechanism is currently favored for this reaction: hydrogen abstraction from one of the phenol group generates an oxygen radical that is delocalized throughout the aromatic ring. The carbon radical then adds into the isoquinoline ring and recombines with the second radical that is generated by the P450 through the second hydrogen abstraction step. This forms a C–C bond that couples the two phenolic rings and gives rise to the rigidified morphinan scaffold of salutaridine **35** that is found in morphine **9** and related opioids.

1.3 Synthetic biology of psychoactive natural products

The psychoactivity of a given plant or fungi is often attributed to a short list of molecules. In reality, psychoactive natural products are produced as complex mixtures of metabolites and frequently have partially undefined compositions.⁵⁹ Variability in growth conditions, in addition to pests, disease, agrochemicals, and climate may introduce further inconsistencies in product composition.⁶⁰ In the event that a single psychoactive constituent is desired by the consumer and isolation from the native host is costly, total synthesis may be one strategy to establish a robust supply chain. In the last two decades, advances in DNA technologies have resulted in the development of an alternative production strategy: synthetic biology.^{61,62} Synthetic biologists use genetic tools to build designed biological systems with useful functionality. Whether or not synthetic biology can produce a viable process depends on the economic, environmental, and societal cost of alternative production strategies. However, as novel DNA-related technologies continue to arise, capabilities of molecular biologists are expected to expand. In 2010, Gibson assembly,⁶³ DNA microarrays,⁶⁴ and zinc-finger nucleases⁶⁵ were considered state-of-the-art. A PhD student that graduated in 2020, however, would have witnessed cost-efficient gene synthesis,⁶⁶ RNA-seq,⁶⁷ and CRISPR/Cas9⁶⁸ emerge as routine. The substantial unrealized potential of synthetic biology is evidenced by continued investments across industry and academia.

As these technologies expand, successful refactoring of a biosynthetic pathway relies on the use of well-characterized “genetic parts” – these DNA-based elements permit coordinated expression of genes of interest in a heterologous host.⁶⁹ Following the standardization of

genetic engineering protocols and genetic parts, reliable metabolic engineering techniques have been established that enable improvements in engineered systems. The general methodology for synthetic biology-based heterologous production of natural products is outlined in Fig. 6. First, a biosynthetic pathway must be elucidated such that a heterologous production strategy can be envisaged. Second, an appropriate biosynthetic chassis must be selected. Finally, the engineer must iterate through the design, build, test, learn (DBTL) cycle until sufficiently high titers, production rates, and yields are reached.

1.3.1 Pathway elucidation and design—Biocatalytic production methods benefit greatly from fully elucidated biosynthetic pathways; a single missing biosynthetic step may completely derail heterologous production efforts. Identification of natural product biosynthetic logic is the primary focus of Sections 2 – 5. Early biosynthetic investigations involved demonstrating that isotope labeled precursors could be site-specifically incorporated into final products, which provided connections between primary metabolism and natural product biogenesis. Now, genomic sequencing and synthetic biology toolkits permit gene knockouts in the native host or expression in a heterologous host for functional analysis. “Reconstitution” of the activity of a recombinantly expressed enzyme activity *in vitro* affords the most unequivocal evidence of a biosynthetic sequence. It should be mentioned that availability of transcriptomics data has provided a quantum leap in the ability to identify candidate enzymes, particularly in unclustered plant pathways. Whereas bacterial and fungal biosynthetic pathways are frequently colocalized in a “gene cluster,” examples of clustered plant pathways are scarce.^{70–72} Meanwhile, the differential abundance of RNA across plant tissues and cultivars gives metabolic engineers precise spatiotemporal gene expression data, which can be mined for information about biosynthetic pathways. In recent years, RNA-Seq has been used to identify a wide range of plant natural product biosyntheses, including a number of key conversions in psychoactive natural product pathways.^{45,73} For instance, Facchini and coworkers utilized RNA-Seq to discover neopinone isomerase, which catalyzes a reaction previously believed to occur spontaneously in morphine biosynthesis.⁷⁴ As an additional example, Luo *et al.* identified a functional prenyltransferase enabling cannabinoid production in *S. cerevisiae* by interrogating *Cannabis sativa* transcriptome data.⁷⁵

In some cases, a biosynthetic step from the native organism cannot be identified, or functional expression of a known pathway gene may not be feasible in a given organism. In this event, bioprospecting or mining the genomes of alternative organisms to identify functional proteins that carry out key reactions has been successfully applied. For example, incorporation of genes from *Gallus gallus* (chicken) and *Rattus norvegicus* (rat) in place of missing or non-functional yeast metabolic steps was a crucial advancement in the development of MIA and BIA producing strains.^{76,77} Alternatively, protein engineering strategies may be employed to alter the regiospecificity or substrate specificity of other well-characterized proteins in order to generate *de novo* suitable replacements for missing or nonfunctional steps. Dueber and coworkers employed this method to engineer a L-tyrosine hydroxylase, which normally requires a cofactor not produced in yeast, and used the evolved enzyme to produce a morphine precursor.⁷⁸ The field of directed evolution is now well

established,⁷⁹ which can be implemented prior to DBTL or integrated into the DBTL pipeline.

Following partial or complete pathway elucidation, a biosynthetic strategy may be designed. For many psychoactive natural products, especially those which can be easily constructed from primary metabolites, *de novo* production from minimal media will provide the most cost-efficient route to a final product. Stephanopoulos and coworkers recently highlighted an alternative approach: the use of a late-stage pathway entry point to circumvent troublesome early biosynthetic steps.⁸⁰ Such “mixed carbon” feeding strategies may prove useful if an intermediate is commercially available or accessible via facile chemical synthesis. Efficient uptake of the late-stage entry point is another requirement, as transport limitations may prevent efficient substrate incorporation. The terms biotransformation (single step) and bioconversion (multistep) are commonly used to refer to this type of hybrid synthetic approach, which has been leveraged in the biosynthesis of psilocybin⁸¹ and an ibogaine precursor.⁸² Lastly, many *in silico* pathway design algorithms have been described in recent years, which perform automated retrobiosynthetic analyses to predict novel or optimized pathways.^{83,84} This approach has been successfully applied to primary metabolic products, highlighting the demand for continued investigation of secondary metabolic pathways.^{85,86,87} Machine-learning technologies linked to databases of reactions using automated DBTL are predicted to play a role in the future of natural product biomanufacturing.⁸⁸

1.3.2 Chassis selection—A critical parameter in the successful refactoring of a natural product pathway is the selection of a suitable biosynthetic chassis. Five representative biosynthetic chassis are shown in Fig. 6. The model bacterium *Escherichia coli* has become a foundation of biotechnology as a DNA bearing model organism. *E. coli* laboratory strains have been customized for plasmid propagation and protein expression. Production of drugs with relatively short biosynthetic pathways has been shown,^{81,89} with stepwise mixed-strain cultures leveraged for longer pathways.⁹⁰ *Saccharomyces cerevisiae* (brewer’s yeast) was initially the subject of genetic studies, but has become a favorite organism in academia to demonstrate heterologous production of an impressive variety of plant or fungus-derived psychoactive drugs.^{73,75,77,91,92} The model ascomycete *Aspergillus nidulans* has also been used for the production of bioactive molecules due to its robust secondary metabolism and ability to splice fungal introns.^{93–95} *Nicotiana benthamiana* has proven useful in characterizing and reconstituting difficult plant pathways, and is particularly attractive due to the well-established and modular transient gene expression technologies.^{96–99} The fifth chassis is synthetic biochemistry, wherein long-lived “cell-free” enzymatic reactions have enabled high-titer flux through lengthy biosynthetic pathways.^{53,100–102}

One must carefully consider the features of a given pathway before deciding if a particular chassis meets the biosynthetic requirements. Many natural product pathways evolved in the context of highly specialized organelles, cells, or tissues.¹⁰³ In this case, pathway compartmentalization may be required in order to sequester reactive biosynthetic intermediates from endogenous metabolism. Currently, sub-cellular localization is possible through the use of organelle-targeting peptide signals fused to the N-terminus of pathway enzymes, or the use of intracellular protein scaffolds.^{104,105} The recent production of tropane alkaloids in yeast required extensive localization across six sub-cellular locations.⁷³

Tissue specific pathway localization in multicellular model organisms has yet to be employed but will require the implementation of intercellular metabolite transport. Special attention must be given to enzymes that are membrane associated, including the cytochrome P450s.¹⁰⁶ Even in the most appropriate chassis, functional expression of trafficked proteins may require extensive engineering. Galanie *et al.* employed a protein chimera strategy to ameliorate improper processing of a P450 for opioid biosynthesis in yeast.⁷⁷ Solubilization of membrane anchored P450s has been successfully demonstrated, but a general strategy guaranteeing functional soluble expression of P450s is still a major technological hurdle.¹⁰⁷ It is also important to consider the primary metabolite building blocks required for construction of the secondary metabolite to be produced. Individual organisms exhibit variable fluxes towards given metabolic pools, dictating initial maximum titers prior to strain engineering. To address this limitation, “metabolic chassis strains” – strains with increased flux towards dedicated natural product building blocks – have been developed. Microbial chassis for the production of *N*-methylpyrrolinium **20**,¹⁰⁸ strictosidine **25**,⁷⁶ (*R*)-reticuline **28**,^{90,109} and a number of other psychoactive natural product precursors have been established in the last decade.

The availability of a robust synthetic biology toolkit is another important factor to consider when selecting a production host. An ideal suite of molecular biology tools permits accurate and rapid genomic edits, precisely controlled gene expression, and diversity generation using libraries of genetic parts. More industrially “robust” organisms may also be utilized. These may be proprietary strains that outperform laboratory strains, but oftentimes lack the synthetic biology toolkit characteristic of the previously described model organisms. Proprietary methods may be developed for rational engineering, or random mutagenesis may be employed for nonrational diversity generation. Additional properties of robust chassis are faster growth, resistance to contamination, and a tailored metabolic profile. Predictable scalability and ease of downstream purification costs should also be considered when assessing platform commercialization.¹¹⁰ For academic purposes, however, it is most common to recapitulate biosynthetic pathways in model organisms as a proof-of-concept.

1.3.3 Design, Build, Test, Learn—Iterative design methodologies are now commonplace in deploying synthetic biology-based engineering. In natural product production chassis, first generation strain prototypes almost never produce compounds in sufficient quantities to compete with alternative production strategies. As a result, many iterations of design, build, test, and learn (DBTL) are required before a process is cost competitive. The industrial feasibility of bioprocess is often measured by titer (mass per volume), rate (mass per volume per time), and yield (mass product per mass substrate) as these metrics relate to cost of goods sold (COGS).¹¹¹ In addition to improving titers on the strain engineering front, large improvements in productivity can be made through bioprocess engineering, which has benefitted immensely from automated design of experiment methodologies. The ability to iterate through the DBTL process is dependent on the biosynthetic chassis, engineering strategy, and screening strategy, among other factors. Novel metabolic engineering approaches aim to reduce the cost or duration of some aspect of the DBTL cycle.^{112,113} As previously mentioned, “automated design” and “machine learning” technologies have only recently been deployed in metabolic engineering studies.

Thus, we focus below on methodologies which streamline the “build” and “test” phases of iterative design.

Within the DBTL cycle, synthetic biology toolkits have had the greatest impact on the “build” phase. Rapid and precise diversity generation, including the construction and integration of expression assemblies into a platform, is a vital prerequisite to screening. Libraries of well characterized genetic parts provide metabolic engineers with a set of elements that can precisely control the expression of a pathway gene. To this end, vector sets, promoter sets, terminator sets, and signal peptide sets are the most common control elements used. A vector is a circular fragment of DNA that harbors pathway genes, a selection marker, and an origin of replication which dictates copy number and plasmid stability. Integration of synthetic biology constructs directly into the genome may obfuscate the use vectors, however shuttle vectors for cloning of constructs are generally still employed. Promoters are regulatory elements directly upstream of a gene of interest, which recruit transcriptional elements for gene expression. Promoters may be constitutive (always on) or inducible (turned on by a condition). The promoter “strength” correlates to the copy number of mRNA upon induction; promoters are often referred to as tight (no basal expression) or leaky (measurable basal expression). Terminators are the regulatory elements downstream of the protein coding sequence, signaling transcriptional termination, and impact the half-life of mRNA. Signal peptides may be employed to direct expression to an organelle for localization or secretion. Prior to use, these genetic parts must be assembled into a single contiguous DNA fragment. Sequence independent cloning techniques such as Gibson assembly and yeast homologous recombination have replaced traditional methods such as digestion-ligation.⁶³ Furthermore, gene fragments can now be affordably synthesized, circumventing strain procurement and DNA isolation.⁶⁶ A once tedious and unpredictable process, heterologous gene expression has been streamlined using reliably functional elements; gene expression is now definitively “engineerable”. As we gain a more comprehensive understanding of sophisticated cellular programs, we will be able to assemble even more robust and dynamic synthetic biology circuits. Once such systems are constructed, integration into the heterologous host is the final hurdle in the “build” phase. The recent discovery of CRISPR/Cas9 has ameliorated this challenge. Cas9, an RNA-guided DNA endonuclease, enables genomic modifications with unprecedented precision, greatly accelerating strain construction.⁶⁸

Following the “build” phase, a screening approach is required in order to “test” the performance of synthetic constructs. Screening throughput is dependent on the strategy used to quantify production of a natural product. Direct measurement of product titer using chromatography, mass spectrometry, and spectrophotometry and comparison to an authentic standard is the most accurate quantification method. Advancements in instrumentation have increased the throughput and accuracy while decreasing costs, however these methods are still considered low-to-medium throughput, requiring 1 minute – 1 hour per sample. Meanwhile, indirect measurements of product titer employing biological readouts have enabled high-throughput testing of strains. So called “biosensors” transduce chemical inputs into physiological outputs in order to establish a correlation between a titer and a selectable phenotype. Biosensors enable screening of constructs on the order of seconds or less per sample. In rare circumstances, a natural product is produced in sufficient quantities and has a

unique enough absorbance spectrum to function directly as the selectable chromophore. More typically, a genetically-encoded biosensor must be engineered that robustly actuates a signal that can be correlated to the metabolite's concentration. Biosensors consist of a sensor-actuator pair and are either RNA-based or protein-based. The sensor-input consists of binding of the biosensor to the secondary metabolite. Then, an actuator-output is generated resulting in modulation of transcription or translation of a selectable protein. The genetic circuit may also encode Boolean logic in order to improve biosensor properties such as dynamic range or sensitivity.¹¹⁴ Selection is then performed either *in situ* (cell viability) or *ex situ* (high-throughput cell sorting). For example, a cell viability screen can be established by tying a biosensor output to expression of an antibiotic resistance gene or complementation of an auxotroph. On the other hand, biosensor-dependent expression of a fluorescent protein enables high-throughput fluorescence-activated cell sorting (FACS) for rapid analysis of entire populations of cells. Microbial opioid production has benefited greatly from the use of biosensors, as both RNA and protein based metabolite sensors have been reported for benzylisoquinoline alkaloid pathway intermediates.^{78,115} Adaptive laboratory evolution (ALE) has also emerged as an efficient method to circumvent traditional DBTL strain construction. ALE employs natural selection and *in vivo* diversity generation for population-wide engineering, and has been primarily applied to primary metabolic products.¹¹⁶ Although several generalizable biosensor development platforms have been proposed, research towards rapid expansion of the variety of sensed metabolites is ongoing.

Compared to organic synthesis and biochemical engineering, synthetic biology is a relatively nascent applied science. Despite this, immense progress has been made in the last 20 years, and a number of recent success stories illustrate the field's potential. Research groups now routinely refactor pathways with more than 10 steps in *A. nidulans* and *N. benthamiana*, and pathways with more than 20 steps have been reconstituted using both *S. cerevisiae* and synthetic biochemistry. The ongoing challenge for these platforms is to improve titers and reduce costs sufficiently to compete with traditional production methods. General strategies range from improving flux through pathway bottlenecks to ameliorating growth defects from metabolic burden or toxicity, however a more nuanced engineering approach is often required. In depth discussions of the engineering strategies enabling benchmark production of the psychoactive natural products described in this review accompany the biosynthetic pathway descriptions.

2. Hallucinogenic natural products

Of all the psychoactive compounds that are either isolated as natural products or produced synthetically, hallucinogens may impart the most dramatic shifts in one's psyche. This broad class of substances can induce potent alterations to consciousness, mood, and perception resulting in vivid visual hallucinations, synesthesia, and a warped sense of time and space.¹¹⁷ The precise mixture of perceptual and somatic effects of hallucinogens is highly compound specific and thus has led to many debates on accurate nomenclature. There is yet to be a consensus with terms such as "psychedelic" and "entheogen" often used interchangeably with "hallucinogen" in different contexts.

Natural sources of hallucinogens famously include “magic mushrooms” of the *Psilocybe* genus and other fungi such as ergot and fly agaric. Other well-known sources of hallucinogens are from the spineless cactus, peyote, the psychoactive brew, ayahuasca, and with a recent resurgence, nutmeg.¹¹⁸ Most natural hallucinogens are alkaloids derived from amino acids such as L-tryptophan **11**, L-tyrosine **12**, and L-glutamic acid **36** (Fig. 7), with one notable exception being the terpenoid salvinorin A **37**. Numerous extensive reviews exist on the history, pharmacology, and potential as therapeutics of hallucinogens which we recommend.^{117,119,120}

2.1 Serotonin Receptors

The serotonin or 5-hydroxytryptamine (5-HT) receptors, named for their native ligand, serotonin **38**, have been implicated in the modulation of sensory perception, mood, cognition, memory, and more through the peripheral and central nervous systems (Fig. 7).¹²¹ There are many subtypes, and with the exception of 5-HT₃ which is a ligand-gated ion channel, the rest are G-protein-coupled receptors, each with unique spatial distribution and localization in the brain.¹²² Phylogenetic analysis and low sequence identity (~25% between the major subtypes) demonstrates early divergence, implicating 5-HT receptors as one of the oldest receptor systems.¹²¹

The relationship between 5-HT receptors was first determined through testing of LSD **3**. While hallucinogenic compounds like **3** (Fig. 8) have been shown to target multiple 5-HT receptors, the 5-HT_{2A} receptor is most commonly associated with the majority of psychotropic effects.¹²³ Previously, structure-activity relationship studies between 5-HT_{2A} and numerous psychoactive compound scaffolds have demonstrated that hallucinogenic potency is not necessarily a function of affinity, likely due to more nuanced mechanisms of functional selectivity.¹²⁴ However, a recent crystal structure of **3** complexed with 5-HT_{2B} (a model system for 5-HT_{2A}) was reported and combined with molecular dynamic simulations, identified a molecular basis for the particular potency of **3**.¹²⁵ The authors demonstrate that the diethylamide side chain of **3** adopts a restrictive conformation when bound to 5-HT_{2B} that increases residence time and improves β -arrestin translocation to the cell membrane. This enhanced β -arrestin translocation results in desensitization of the cell to stimuli by uncoupling G-proteins from receptors and could explain the long duration of action of **3**.

2.2 *N,N*-Dimethyltryptamine

N,N-dimethyltryptamine (DMT) **29** (Fig. 9) is likely the most pervasive psychoactive compound across species and is found in dozens of plant and animal species, including humans.¹²⁶ Root, bark, and leaf preparations from plants such as *Psychotria viridis*, containing DMT and its structural analogs (Fig. 9) have been used in shamanic ritual practices for at least 1000 years.¹²⁷ Interestingly, in addition to plants, structural analogs 5-methoxy-*N,N*-dimethyltryptamine **39** and bufotenin **40**, are also found in the toxin of the Colorado River toad *Incilius alvarius*, formerly known as *Bufo alvarius*, whose remains have been found as a part of Olmec ritual ceremonies dating back to pre-Columbian Mesoamerica (Fig. 10).^{128,129} Referred to colloquially as the “Psychedelic Toad of the Sonoran Desert,” exudates from the amphibian’s specialized glands may contain up to fifteen percentage dry weight **39**, representing the most notable example of a psychoactive natural product of

animal origin.¹³⁰ DMT **29** was first isolated from the shrub *Mimosa tenuiflora* in 1946 by Oswaldo Gonçalves de Lima,¹³¹ but its hallucinogenic effects were not discovered for another decade.¹³² **29**, like all L-tryptophan derived hallucinogens, is a serotonin receptor agonist. While the functional selectivity of **29** towards the 5HT_{2A} receptor is believed to be necessary for its effects, **29** can bind to many serotonin receptors that may also contribute to its psychoactivity.¹²⁶

While the precise role of endogenous **29** in humans has yet to be ascertained,¹³³ one study speculates it may have a role in protecting from hypoxia.¹³⁴ Further, **29** has shown promise as a therapeutic anti-depressive agent and is known to promote neural plasticity.^{135,136} Interestingly, brominated forms of DMT such as, 5-bromo-*N,N*-dimethyltryptamine **41**, have been isolated from the marine sponges^{137,138} and show particular promise as anti-depressives.¹³⁹ Finally, **29** has limited neurotoxicity and only exhibits cardiovascular effects when taken intravenously in large doses, furthering its therapeutic potential.¹²⁶

2.2.1 Biosynthesis of DMT—The biosynthesis of DMT **29** is the shortest pathway described in this review, requiring just two enzymes. Biogenesis begins with the decarboxylation of the proteinogenic amino acid L-tryptophan **11** to form tryptamine **14** by an aromatic amino acid decarboxylase (AADC) (Fig. 11, and Fig. 2).¹⁴⁰ The PLP-dependent AADCs in most species display a broad substrate scope, operating on multiple aromatic amino acids and derivatives.¹⁴⁰ Tryptamine **14** is then methylated sequentially by an iterative *N*-methyltransferase (INMT) to first form the secondary amine, then **29**, using SAM (Fig. 2B) as a methyl donor.^{141,142}

2.3 Psilocybin

Psilocybin (4-phosphoryloxy-*N,N*-dimethyltryptamine) **1**, one of the major natural products from hallucinogenic *Psilocybe sp.* (“magic mushrooms”), was first isolated from *Psilocybe mexicana* by Albert Hofmann in 1958 (Fig. 12).¹⁴³ The description of “magic mushrooms” in scientific literature and the subsequent isolation and characterization of their psychoactive metabolites was the culmination of decades of effort to identify the sacred mushroom that the South American Aztecs referred to as *teonanacatl*, meaning “god’s flesh.”¹⁴⁴ Psilocybin **1** itself is not psychoactive, but rather exists as a prodrug. After ingestion, psilocybin **1** is metabolized through dephosphorylation and becomes psilocin (4-hydroxy-*N,N*-dimethyltryptamine) **42**, a potent psychotropic 5HT_{2A} receptor agonist.^{145,146} In addition to its psychoactivity, **1** has shown some promise as a therapeutic for treating depression, anxiety and tobacco addiction.^{147–149}

2.3.1 Biosynthesis of psilocybin—A biosynthetic pathway for psilocybin was proposed based on isotope feeding studies as early as 1968.¹⁵⁰ Agurell *et al.* hypothesized that following decarboxylation, L-tryptophan **11**, now tryptamine **14**, would be methylated iteratively to form the psychoactive dimethyltryptamine **29**. This was a reasonable hypothesis because indolethylamine(tryptamine)-*N*-methyltransferases were a popular enzyme for study at the time following their discovery rat, rabbit, and human tissues.

Recently, a psilocybin biosynthetic cluster from *Psilocybe cubensis* and *Psilocybe cyanescens* was identified and characterized by Fricke *et al.* (Fig. 13).¹⁵¹ The authors first sequenced the genomes of both *Psilocybe sp.* Then, using a combination of a methyltransferase, a hydroxylase, and a kinase as queries, a putative biosynthetic cluster present in both species was identified and characterized. Fricke *et al.* determined that the iterative *N*-methylation was the terminal step of psilocybin biosynthesis by enzymatic action of PsiM whose sequence is unrelated to the well-characterized mammalian indolethylamine-*N*-methyltransferases, and thus revised the hypothesis that DMT **29** is an intermediate in psilocybin biosynthesis. Starting from *L*-tryptophan **11**, PsiD catalyzes a decarboxylation reaction to yield **14**. The amino acid sequence for PsiD diverges from the more common PLP-dependent aromatic amino acid decarboxylases and instead shares similarity with the PLP-independent phosphatidylserine decarboxylases. PsiH, a P450 monooxygenase, then hydroxylates the indole C4 to yield 4-hydroxytryptamine **43**.

Next PsiK, a predicted kinase, catalyzes the phosphorylation of 4-hydroxytryptamine **43** into norbaeocystin **44** using ATP as the phosphate donor. Phosphoryltransferase (or kinases) are relatively uncommon in natural product biosynthesis. Recent examples include the biosynthesis of calyculin protoxins and the lasso peptide paeninodin, in which phosphorylation plays a role in self-immunity which could highlight the importance of dedicated kinases.^{152,153} Lastly, PsiM methylates the terminal amine in **44** in an iterative fashion using SAM as a methyl donor to give **1**. PsiM only methylates phosphorylated tryptamine **44**, indicating that psilocybin biosynthesis is nearly linear. In water, **1** undergoes spontaneous hydrolysis of the phosphate group to form **42**, but PsiK accepts psilocin as a substrate and readily phosphorylates to reform psilocybin **1**. As previously mentioned, this hydrolysis results in the psychoactive form, **42**, upon ingestion by vertebrates.

Subsequently, additional psilocybin biosynthetic clusters were found in distant fungal species and provide some evolutionary evidence of the ecological role of psilocybin in influencing mycophagy in animals, which is to reduce their consumption from invertebrate predators.¹⁵⁴ Thus, the bioactivity of **1** may provide a fitness advantage to natural producers over their competitors. Further, a recent preprint presents evidence of a new, diverged psilocybin cluster in *Inocybe corydalina* that contains a second methyltransferase that may produce the trimethylated, quaternary ammonium salt analogue of **1**, aeruginascin.¹⁵⁵

2.3.2 Heterologous production of psilocybin—Since the elucidation of the psilocybin biosynthetic pathway, engineering efforts for high-titer production of psilocybin **1** in various microbial hosts, such as the filamentous fungus *A. nidulans*, Baker's yeast *S. cerevisiae*, and the model bacterium *E. coli* have been reported.^{81,91,94} Hoefgen *et al.* developed a polycistronic expression system in *A. nidulans* and used the psilocybin pathway as a proof-of-concept. They obtained 110 mg/L of **1** at 1.5% dry mycelial weight which is a titer comparable to native psilocybin producers.

Adams *et al.* were able to combine heterologous expression and metabolic engineering strategies to achieve a titer of 1.16 g/L psilocybin **1** in *E. coli* in a 1.5-L bioreactor from 3.05 g/L of gradually supplied 4-hydroxyindole **45** (Fig. 14) over several days. The exogenously supplied **45** is first converted into 4-hydroxy-*L*-tryptophan **46** by TrpB, an endogenous

bacterial enzyme in the L-tryptophan biosynthetic pathway that catalyzes the condensation of indole with serine to form **46**. PsiD, PsiK, and PsiM from *P. cubensis* were heterologously expressed under a single T7 promoter on a high copy plasmid, which facilitated the conversion of **44** formed *in situ* into psilocybin **1**. Endogenous levels of serine and SAM, required by TrpB and PsiM, respectively, were not sufficient for high-titer production and thus the media was supplemented with excess amounts of serine and methionine. The native *E. coli* enzyme MetK is able to anabolize the exogenous methionine into SAM while the *E. coli* enzymes Mtn, LuxS, and MetE are able to recycle the by-product S-adenosylhomocysteine (SAH) into more methionine.

Engineered de novo production of psilocybin **1** was recently reported in a fully integrated *S. cerevisiae* strain with a titer of 627 ± 140 mg/L of psilocybin **1** and 580 ± 276 mg/L of psilocin **1** from 1L scale fed-batch fermentation over ~9 days (Fig. 15). Psilocybin pathway genes from *P. cubensis* were expressed under strong, constitutive promoters. Instead of expressing the pathway decarboxylase PsiD, Milne *et al.* expressed a tryptophan decarboxylase from *Catharanthus roseus*, CrTDC, which was previously shown to have high catalytic efficiency when expressed in yeast.⁷⁶ Additionally, the authors expressed a cytochrome P450 reductase (CPR) from *P. cubensis* to improve activity of PsiH. Matching a P450 with its cognate reductase partner has been demonstrated to be important for functional heterologous expression and is an effective technique to improve heterologous expression of P450 enzymes.^{106,156} To increase endogenous L-tryptophan levels, the authors overexpressed ARO1 and ARO2, which are involved in combining erythrose 4-phosphate **47** and phosphoenolpyruvic acid **48** to form chorismic acid **49** in the shikimate pathway leading to L-tryptophan biosynthesis. This, combined with knockout of a shikimate pathway regulator, RIC1, were effective towards elevating L-tryptophan supply.

2.4 Ayahuasca

Most hallucinogens are rapidly metabolized *in vivo* following ingestion by the action of monoamine oxidases (MAO) for eventual renal elimination, resulting in many hallucinogens being orally inactive. MAOs, as the name suggest, catalyze the oxidative deamination of neurotransmitters and structurally similar compounds.¹⁵⁷ It follows that ingestion of MAO inhibitors (MAOIs) concurrently with hallucinogens can increase their bioavailability. This synergy is best demonstrated by ayahuasca, a psychoactive decoction commonly prepared from the vine *Banisteriopsis caapi*, containing MAO inhibiting harmala alkaloids, and some DMT **29** containing species such as the shrub *Psychotria viridis*.^{158,159} Ayahuasca, derived from a Quechua term meaning “vine of the soul,” has been used as a spiritual medicine by indigenous groups in South America’s Amazon basin for at least one thousand years.¹²⁷ During a ceremony in which the brew is ingested, practitioners experience several stages of visual and purgative experiences in order to heal physical, emotional, and spiritual imbalances.¹⁶⁰ While there are no currently approved therapeutic uses for ayahuasca or its active metabolites, harmala alkaloids have shown promise as an antidepressant through brain plasticity modulation.¹⁶¹

The harmala alkaloids are compounds that contain a β -carboline scaffold with various methyl or methoxy substitutions and different degrees of unsaturation. The β -carboline

scaffold itself is characterized by a pyridine ring *ortho*-fused to indole resulting in a 6-5-6 tricycle with possible substitutions at the *ortho* position to the pyridine nitrogen. The major harmala alkaloids that contribute to the MAOI activity are harmine **23**, harmaline **50**, and tetrahydroharmine **51**. These compounds are abundant at ~ 0.05 – 0.1% of dried plant material in *B. caapi* (Fig. 16).¹⁶² Thorough pharmacokinetic data is scarce, but psychotropic action of harmala alkaloids is expected to occur around 20–50 mg with a typical 100 mL ayahuasca brew containing between ~300–600 mg of harmala alkaloids and 20–60 mg of **29**.¹⁶³

Another example of a MAOI natural product cocktail is the recent isolation of **23** and related β -carbolines from numerous hallucinogen-producing *Psilocybe sp.* as known as “magic mushrooms”.¹⁶⁴ This serves as an interesting example of a single organism with diverged secondary metabolite scaffolds, where the biosynthetic pathways of both compounds diverge at tryptamine **14** but contribute to the same psychoactive effect.

2.4.1 Biosynthesis of harmala alkaloids—Initial feeding studies with radioactively labelled substrates into seedlings of the known harmala alkaloid producer, *Peganum harmala*, demonstrated that L-tryptophan and L-methionine are precursors in biosynthesis of harmala alkaloids.¹⁶⁵ A later study demonstrated that radiolabeled **26** could be converted into its dehydrogenated form, **50**, and that harmala alkaloid biosynthesis is likely compartmentalized across different tissues.¹⁶⁶

While the complete set of biosynthetic genes implicated in harmala alkaloid formation have yet to be determined, one proposal¹⁶⁷ postulates the sequence shown in Fig. 17. As in the case of the other indole containing compounds described, **11** is first decarboxylated to form **14** (Fig. 17). Next, pyruvic acid **22** is incorporated by a Mannich or Pictet-Spengler type reaction to form the β -carboline carboxylic acid **52** (also see Fig. 2). To determine the biosynthetic origin of the C-1 β -carboline methyl, radiolabeled feeding of acetic acid and pyruvic acid was performed.¹⁶⁵ Stolle *et al.* observed specific incorporation of the radiolabeled C-2 and C-3 carbons of pyruvic acid **22** into the pyridine ring of the β -carboline scaffold, while radiolabeled acetic acid carbons were non-specifically incorporated throughout as a result of primary metabolism. 1-methyl β -carboline **53** is then formed by oxidative decarboxylation, followed by subsequent hydroxylation and *O*-methylation reactions to form harmaline **50**. Formation of harmine **23** or tetrahydroharmine **51** takes places through either oxidation, or reduction of **50**, respectively.

2.5 Lysergic acid and LSD

Lysergic acid diethylamide (LSD) **3** was first synthesized from lysergic acid **54** by Albert Hofmann in 1938. Like other 5HT_{2A} receptor agonists, ingestion of **3** results in altered states of consciousness and visual hallucinations.¹⁶⁸ While **3** has not been observed to occur naturally, its precursor, **54**, is a natural product belonging to a class of diverse molecules broadly known as ergot alkaloids. **54** is isolated from many fungi with the ergot fungus, *Claviceps purpurea* (Fig. 18) being the most notable.^{169,170} Ergot alkaloids are commonly associated with the disease ergotism, known colloquially as Saint Anthony’s Fire, caused by eating rye or other cereal crops contaminated with ergot fungi.¹⁷¹ In addition to the

vasoconstrictive and convulsive symptoms of the disease, mania and psychosis have been observed, underlining the psychoactivity of ergot alkaloids.¹⁷¹

Ergot alkaloids, derived from L-tryptophan **11**, are characterized by a unique tetracyclic ergoline skeleton where the indole comprises the A and B rings. The C and D rings of the ergoline scaffold are derived from a cyclization of dimethylallyl pyrophosphate with the L-tryptophan amino group.¹⁷² There are three main ergot alkaloid classes, clavines, ergoamides (lysergamides), and ergopeptides, with **3** belonging to the ergoamide class.¹⁷³ Ergoamides contain a C8-amide linkage on the D ring of the ergoline scaffold and is a common point of derivatization for drug development.¹⁷⁴ Modifications on the amide can greatly affect bioactivity and in the case of **3**, the diethylamide moiety is crucial for its prolonged psychoactivity.¹²⁵

2.5.1 Biosynthesis of lysergic acid—Isotope labeling studies during the 1950s and 1960s determined that a mevalonate acid-derived isoprenoid, a methionine-derived methyl group and L-tryptophan **11** were key precursors to ergot alkaloid biosynthesis.¹⁷⁵ The first enzymatic study in *Claviceps sp.* was the purification and characterization of 4-dimethylallyl-L-tryptophan synthetase (DMATS) that catalyzes the first committed step in ergot alkaloid biosynthesis: C-prenylation of L-tryptophan **11** with dimethylallylpyrophosphate at the indole C4 position to form 4-dimethylallyl-L-tryptophan **55** (Fig. 19, also see Fig. 4D).¹⁷⁶ Recently, many laboratories have focused on characterizing prenyltransferases, of which DMATS is the original member of a new superfamily of prenyltransferase enzymes. Since the discovery of the DMATS, prenyltransferases that can regioselectively transfer allylic prenyl groups to almost every position on the indole ring have been identified.^{48,177–181} Members of the DMATS superfamily also have broad substrate scopes while maintaining regioselectivity which has aided in their development as tools for chemoenzymatic syntheses of natural and unnatural prenylated compounds, including the cannabinoid family (see 4.2.2).^{47,53,182,183}

Chromosome walking using the gene encoding DMATS as a step-off point led to the identification of an ergot alkaloid biosynthetic gene cluster in the fungus *C. purpurea*.^{184,185} Sequence alignment revealed an N-methyltransferase, EasF which was proposed to convert 4-dimethylallyl-L-tryptophan **55** into 4-dimethylallyl-L-abrine **56** using SAM as a methyl donor. Thorough characterization of a homologous enzyme in an *Aspergillus fumigatus* ergot gene cluster, FgaMT, supported this hypothesis.¹⁸⁶

Conversion of **56** into the cyclized chanoclavine-I **57** is facilitated by the FAD-linked oxidoreductase EasE and EasC, which was initially annotated as a catalase. Knock-out studies in both *C. purpurea* and the homologous cluster in *A. fumigatus* confirmed that both enzymes are necessary for production of **57**.^{187,188} Subsequent pathway reconstitution studies in *Aspergillus nidulans* and *Saccharomyces cerevisiae* further supported the essential roles of EasE and EasC in biosynthesis.^{189,190} Until recently, however, the precise mechanisms of EasE and EasC were not resolved. Lorenz *et al.* initially postulated that EasE catalyzes the oxidative diene formation from **56** followed by decarboxylation through an epoxide intermediate to yield chanoclavine-I **57**, with EasC serving as a scavenger of hydrogen peroxide generated from EasE.¹⁸⁸ A recent pathway reconstitution in *A. nidulans*

enabled isolation of the a previously unknown intermediate, pre-chanoclavine diene **58**, which verified the diene formation activity of EasE.^{191,192} Subsequent incubation of **58** with EasC recombinantly purified from *E. coli* led to the formation of **57** via a proposed radical addition mechanism using O₂ as an oxidant.¹⁹² Hence, EasC is an essential redox enzyme in the main pathway to **54**.

A short-chain reductase (SDR), FgaDH, was identified in an *A. fumigatus* gene cluster that produces a related ergot alkaloid fumigaclavine C.¹⁹³ *In vitro* assays using recombinantly expressed enzyme determined that FgaDH catalyzes the oxidation of the allylic alcohol on **57** to an aldehyde to form chanoclavine-I aldehyde **59**, strictly using NAD⁺ as the electron acceptor.¹⁹³ A homologous SDR was subsequently identified in the lysergic acid biosynthetic gene cluster in *C. purpurea* and named EasD.¹⁹⁴

The next steps in the pathway represent a branching point for ergot alkaloids. Functional differences in a conserved flavin-dependent old yellow enzyme known as EasA (an isomerase) from *C. purpurea* and FgaOx3 (a reductase) from *A. fumigatus* and *P. commune* represent a mechanistic branching point in D-ring formation.^{195–197} Here we will focus on the formation of agroclavine **61** from **59** towards the psychoactive lysergic acid amides in *C. purpurea*. EasA performs a hydride mediated isomerization of the α,β -unsaturated carbonyl from the *E*-alkene geometry to the *Z*-configuration through an enolate intermediate.¹⁹⁶ This rearrangement positions the carbonyl for an intramolecular cyclization with the secondary amine resulting in the formation of the D-ring.¹⁹⁶ Following ring closure, the iminium intermediate agroclavinium **60** then undergoes NADPH-dependent reduction by the oxidoreductase EasG to form **61**.¹⁹⁸

Assays of microsomal fractions from *C. purpurea* determined that **61** undergoes a 2-electron oxidation of the methyl group to an alcohol to form elymoclavine **62** by an unidentified cytochrome P450 monooxygenase.¹⁹⁹ The only P450 enzyme in the biosynthetic gene cluster, CloA, does not catalyze this transformation and instead performs the 4-electron oxidation of **62** to paspalic acid **63** as suggested from two knock-out studies.^{200,201} In *cloA* mutants, **62** was still detected and supports the likelihood of an additional P450 enzyme in the host that can perform the first 2-electron oxidation. Finally, allylic isomerization of **63** forms the product lysergic acid **54**. This transformation can occur spontaneously, but it remains possible that that an unidentified isomerase can catalyze this reaction as enzyme-catalyzed allylic rearrangements have been observed in other pathways.^{202,203}

54 itself serves as a branching point for the formation of many ergopeptines or ergoamides. These derivatives are formed by a non-ribosomal peptide synthase (NRPS) enzyme complex of two synthetases, LPS1 and LPS2.¹⁷³ One of these lysergic acid derivatives from *Ipomoea purpurea* (Morning Glory), ergine **64** (lysergic acid amide, LSA) is psychoactive. The pathway leading to formation of **64**, while unconfirmed, could involve amidation by an NRPS or degradation of another NRPS product.²⁰⁴

2.6 Peyote

Peoples indigenous to North America have consumed the cactus, peyote, for over one thousand years as a part of their religious practices.²⁰⁵ Peyote, *Lophophora williamsii* (Fig.

20), is a small, spineless cactus with a crown consisting of round buttons that, among other cacti species, contain the hallucinogen, mescaline **65**.²⁰⁵ The psychoactive effects have been described to be similar to LSD, but with a significantly lower potency at a ratio of about 1:2500 mescaline:LSD.¹¹⁷ Despite peyote's status as a Schedule I controlled substance in the United States, it remains legal as an important part of religious practices by the Native American Church and other religious organizations who are protected by the American Indian Religious Freedom Act.

The natural products, elemicin **66** and myristicin **67** (Fig. 8) from nutmeg, or *Myristica fragrans*, are tetrasubstituted benzenes and structurally related to **65**. Despite not being psychoactive, **66** and **67** are believed to be prodrugs as they are metabolized in the liver into 3-methoxy-4,5-methylenedioxyamphetamine, also known as MDMA.^{206,207} MDMA and its analogs were first synthesized from **65** by Alexander Shulgin, and similar to **65**, MDMA is a 5HT_{2A} receptor agonist, but with almost double the potency.²⁰⁸ Shulgin would later detail his extensive clandestine investigations into the syntheses and effects of substituted phenethylamines and tryptamines, earning him the title “godfather of psychedelics.”^{209,210}

2.6.1 Biosynthesis of mescaline—Before the discovery of the mammalian iterative methyltransferase that catalyzes *N*-methylation of tryptamine **14** and serotonin **38** into hallucinogenic compounds,¹⁴¹ Axelrod and Tomchick identified another neurotransmitter methyltransferase, catechol *O*-methyltransferase (COMT).²¹¹ COMT, along with monoamine oxidase, modified the L-tyrosine-derived catecholamine neurotransmitter dopamine **17** (Fig. 21) for excretion in the urine.²¹² In the years following, similar to the case of endogenous DMT biosynthesis, several studies identified enzymes in mammalian tissues that could catalyze the chemical transformations of dopamine-related metabolites 3-methoxytyramine **68** into 3-methoxy-5-hydroxytyramine **69** and 3,5-dimethoxytyramine **70** into **65**, although no endogenous **65** could be identified from mammalian organisms.^{213,214} Several mechanisms for **65** biosynthesis in peyote and related cacti have been proposed by metabolite isolation and radiolabeled feeding studies.^{215–219} One proposed pathway by Lundström is shown in Fig. 21.²¹⁹

The proposed biosynthesis begins with hydroxylation of L-tyrosine **12** to 3-hydroxy-L-tyrosine (L-DOPA, **71**) by tyrosine hydroxylase (TH), followed by decarboxylation catalyzed by DOPA decarboxylase (DDC) to yield **17**. Alternatively, **12** may also be converted to tyramine **15** through a decarboxylation catalyzed by tyrosine decarboxylase (TyrDC), followed by aromatic hydroxylation to **17** by an unknown enzyme. From either route, **17** can be converted into 3-methoxytyramine **68**, which has been isolated from mescaline producing plants, by the enzyme catechol *O*-methyltransferase (COMT) using SAM as the methyl donor. The final intermediates towards mescaline production 3-methoxy-5-hydroxytyramine **69** and 3,5-dimethoxytyramine **70** have been determined to be naturally occurring in mescaline producing plants by inverse isotope dilution, but neither have been isolated from plants. These are likely to be on pathway intermediates since they are incorporated into mescaline to a greater extent than other possible intermediates.²¹⁹

While the biosynthesis of **65** in peyote has yet to be elucidated, Ibarra-Laclette *et al.* recently generated two cDNA libraries of the *L. williamsii* transcriptome, one for button and one for

root, using RNA-seq.²²⁰ From this data set, the authors identified putative genes that may encode biosynthetic enzymes for mescaline production including DOPA decarboxylases, hydroxylases, and O-methyltransferases based on phylogenetic analysis.²²⁰ Careful *in vitro* experiments will be required to finally ascertain the mescaline biosynthetic pathway.

2.7 Fly agaric

Ibotenic acid **72**, a nonproteinogenic amino acid with a hydroxylated isoxazole ring, and its decarboxylated form, muscimol **73**, are the main psychoactive constituents of the toadstool, *Amanita muscaria*, commonly known as fly agaric (Fig. 22).¹⁶⁴ Similar to *Psilocybe sp.*, recreational consumption of *Amanita sp.* rose in popularity in the 1960s. However, contrary to other fungal psychoactives that target the serotonin receptor, these compounds are γ -aminobutyric acid type A (GABA_A) receptor agonists.²²² GABA_A receptors are found in multiple regions of the brain and thus **72** and **73** can alter the activity of the cerebral cortex and cerebellum leading to alterations in sensory processing and motor function, respectively.²²³ *A. muscaria* is classified as poisonous, which can in part be attributed to the neurotoxicity of **72**. Its structural similarity to L-glutamic acid **36** allows **72** to act as an agonist towards the N-methyl-D-aspartate (NMDA) receptor resulting in electrolytic lesions in the brain.²²⁴

72 and **73** naturally occur in low concentrations (~100 – 1000 ppm) in the cap and stem of *A. muscaria*.²²⁵ Minimal dosage for psychedelic effects are estimated as low as 6 mg for **46** and 30–60 mg for **72**.²²⁶ Interestingly, *A. muscaria* and its constituents are not regulated by the United States federal government, in contrast to **1** and **42** from *Psilocybe sp.*

While **72** was first isolated over 50 years ago, its biosynthesis remained elusive.²²⁷ Recently, Obermaier and Muller identified a gene cluster encoding **72** and **73** biosynthesis in *A. muscaria*.²²⁸ The key to locating this cluster was the identification of a glutamate hydroxylase, an enzyme first implicated in **72** biosynthesis over 50 years ago, but never found. This enzyme, a nonheme, iron and α -ketoglutarate-dependent dioxygenase named IboH, hydroxylates L-glutamate **36** at the C3 position resulting in the formation of 3-hydroxy-L-glutamic acid **74**.

2.7.1 Biosynthesis of ibotenic acid—Obermaier and Muller proposed two pathways (A and B) for ibotenic acid biosynthesis diverging from **74** (Fig. 23). One proposal (Pathway A) is that **74** undergoes a condensation reaction catalyzed by IboA, an adenylating enzyme, with ammonia from an unidentified donor to form 3-hydroxyglutamine **75**. A likely amine source is glutamine which is the amine donor in various metabolic reactions. IboF, a flavin-dependent monooxygenase, would then catalyze N-oxidation of the terminal amide to form 3-hydroxyglutamine hydroxamic acid **76**. Next, either IboG1 or IboG2, PLP-dependent paralogs found in the biosynthetic gene cluster, catalyzes the intramolecular cyclization of the hydroxamic acid with the hydroxyl group at the C3 position to form the five-membered heterocycle tricholomic acid **77**. Alternatively, Pathway B involves N–O bond formation between an unidentified, hydroxylamine **78** with the C3 hydroxyl group on **74** by IboG1/G2 to form a 3-hydroxy-L-glutamic acid derivative **79**. In this pathway, the external hydroxylamine could derive from hydroxylation of an external amine **80** catalyzed by IboF.

IboA would then facilitate cyclization of the hydroxylamine with the C-5 carbonyl of the 3-hydroxy-L-glutamic acid derivative **79** to form **50**. From tricholomic acid **77**, IboC, a cytochrome P450, catalyzes the desaturation of the 3-oxoisoxazolidine ring to form ibotenic acid **72**. IboD, a PLP-dependent decarboxylase can catalyze the further decarboxylation of **72** to form the other major psychoactive compound, muscimol **73**.

2.8 Iboga alkaloids

Root and bark from the iboga tree, *Tabernanthe iboga*, has been used for both therapeutic and spiritual ritual purposes in West Central Africa for hundreds of years.²²⁹ *T. iboga* is rich in L-tryptophan derived-monoterpene indole alkaloids (MIAs), an expansive class of over 3000 plant natural products starting from the universal MIA precursor, strictosidine **25**.^{230,231} Many molecules of this class have broad bioactivities that include anti-cancer²²¹, anti-malarial²³², anti-addiction²³³ and more.²³⁴ The potent MIA cancer therapeutics vincristine and vinblastine from *Catharanthus roseus* are listed on the World Health Organization's List of Essential Medicines, underlining the value of MIAs as human therapeutics. One of the MIAs from iboga roots is the psychedelic (–)-ibogaine **2** that has multiple neurotransmitter interactions including the κ - and μ -opioid receptors and the serotonin transporter, which collectively results in a feeling of a dream-like state of consciousness.²²⁹ Additionally, **2** and some of its derivatives have shown promise as anti-addictive agents.^{233,235}

The iboga alkaloid scaffold is characterized by a 6-5-7 ring system comprised of indole and tetrahydroazepine fused to an isoquinuclidine ring to form a pentacyclic skeleton with a tertiary amine serving as the bridgehead (Fig. 24). The addition of a C5 methoxy group on the indole ring within the iboga scaffold provides **3**. Variable substitutions on the indole ring and the presence of a carbomethoxy group at the indoloazepine-isoquinuclidine junction lead to different family members within this class. Interestingly, **2** is the only known compound with the iboga scaffold to have hallucinogenic properties, which raises questions about the structure-activity relationship between **2** and 5-HT receptors. According to a recent study, iboga scaffolds lacking the isoquinuclidine ring resulting in an indole-tetrahydroazepine tricycle lost their hallucinogenic properties but maintained their ability to promote neural plasticity, the mechanism that may be the key to its anti-addiction properties.²⁶

2.8.1 Biosynthesis of iboga alkaloids—Given that strictosidine **25** is the central metabolite in the MIA biosynthetic pathways in plants, there has been intense efforts to understand how nature transforms the simple geranyl (C10) precursor that combines with tryptamine **14** to yield the complex **25**. These efforts from different labs have fully elucidated the pathway to **25**. In recent years, further efforts have led to the complete mapping of the downstream enzymatic transformation to vinblastine in *C. roseus*, which comprise of over 30 enzymes starting from primary metabolites.^{45,236–243} Shortly after, the (–)-ibogaine biosynthetic pathway from **25** was also elucidated, as well as other complex MIA compounds.²⁴⁴

The first committed step in the seco-iridoid pathway towards the monoterpene scaffold in **25** is the formation of geraniol **81** (Fig. 25). While it was predicted that **81** was hydrolyzed from the mevalonate pathway intermediate, geranyl pyrophosphate (GPP) **82**,^{245,246} the enzymatic basis of its formation was unknown until the discovery of geraniol synthase (GES) from sweet basil (*Ocimum basilicum*) decades later.¹⁹³ Since then, many GES homologs have been discovered from various plants. The activity of GES, which is to hydrolyze **82** to **81**, represents a divergence point between primary and secondary terpene metabolism in plants. In primary metabolism, GPP is further elongated to farnesyl pyrophosphate (FPP), which is central towards the synthesis of steroids and coenzyme Q. By hydrolyzing the pyrophosphate in GPP, GES commits the geraniol group for MIA biosynthesis and siphons GPP away from primary metabolism. In the MIA pathway, geraniol **81** is then hydroxylated by the P450 enzyme geraniol 8-hydroxylase (G8H) to form 8-hydroxygeraniol **83**.²⁴⁷

The next four biosynthetic steps were all discovered from analysis of the *C. roseus* transcriptome.⁴⁵ 8-hydroxygeraniol oxidoreductase (GOR) iteratively oxidizes the two alcohols in **83** to yield 8-oxogeraniol **84**, a dialdehyde that is poised for intramolecular cyclization. It was initially believed that iridoid synthase (ISY) was an NAD(P)H-dependent cyclase.²⁴⁸ However, a recent report demonstrated that ISY is a reductase that can reduce **84** to an enol intermediate.²⁴⁹ A previously undiscovered cyclase, major latex protein-like (MLPL), then facilitates the cyclization of the reduced enol to form *cis-trans* nepetalactol **85** in a non-cofactor dependent mechanism.²⁴³ **85** is the first molecule in the pathway that has the iridoid structure. In plants such as *Nepeta*, **85** can be oxidized to nepetalactone, which is the cat attractant produced by these plants.²⁴⁹ In the MIA pathway **85** undergoes a 4-electron oxidation catalyzed by the P450 iridoid oxidase (IO) to install an α,β -unsaturated carboxylic acid in 7-deoxyloganetic acid **30**. The next step is glucosylation by 7-deoxyloganetic acid glucosyl transferase (7DLGT) with UDP-glucose to form 7-deoxyloganic acid **31** (See Fig. 3C). Glucosylation of the hemiacetal presumably stabilizes the compound and prevents spontaneous ring opening. The third P450 in the pathway, 7-deoxyloganic acid hydroxylase (7DLH), catalyzes hydroxylation of the cyclopentane ring in **31** to form loganic acid **86**.

Expression data revealed that the next two genes in the seco-iridoid pathway encoding for loganic acid *O*-methyltransferase (LAMT) and secologanin synthase (SLS) are part of a separate regulon from the early pathway.^{250,251} The seco-iridoid pathway is also spatially segmented between the internal phloem associated parenchyma (IPAP) cells for iridoid production and leaf epidermis cells for the remaining steps towards production of strictosidine **25**.²⁵² **86** is first transported from the cytosol of the IPAP cells into the cytosol of epidermic cells by a nitrate/peptide family (NPF) transporter.²⁵³ The cytosolic LAMT subsequently converts **86** into loganin **34**.²⁵⁰ The fourth P450 in the pathway, SLS then catalyzes oxidative cleavage of the cyclopentanol ring of **34** to unveil the reactive aldehyde handle in secologanin **24** (See Fig. 5A).⁵⁶

To form strictosidine **25**, **24** and **14** are condensed through a stereospecific Pictet-Spengler reaction catalyzed by strictosidine synthase (STR) (Fig. 26, and see Fig. 3).²⁵⁴ This mechanism had been long proposed before the discovery of STR, modeled after the formation of *L*-benzylisoquinolines alkaloids.²⁵⁵ Considering the synthetic challenges

associated with accessing **25**, STR has become an attractive enzyme for the chemoenzymatic and biotransformative syntheses of analogs of **25**.^{256–258} The regulation and complexity of MIA biosynthesis is further highlighted by the transient sub-cellular compartmentalization of **25** formation in the vacuole of epidermis cells followed by immediate export towards the nucleus.²⁵⁹ It is believed that the spatial isolation of STR and its substrates prevents accumulation of the highly-reactive strictosidine aglycone intermediate, 4,21-dehydrogeissoschizine **87** (*vide infra*), a dialdehyde which leads to toxic protein cross-linking.²⁶⁰ It is hypothesized that this is a plant defense mechanism from herbivores mirroring the activation of the related phenolic secoiridoid glycoside, oleuropein, from the privet tree, *Ligustrum obtusifolium* following tissue damage.²⁶¹

From **25**, different branches of the MIA family can be accessed. The first step is the deglycosylation of **25** by the enzyme strictosidine-*O*- β -glucosidase (SGD).²⁶² Whereas **25** is relatively stable and benign to the host, removal of the glucose group which essentially serves to mask the hemiacetal, leads to the dialdehyde 4,21-dehydrogeissoschizine **87** that is prone to cross-linking. **87** can exist in equilibrium with the more stable epimers cathenamine and epicathenamine.²⁶³ Each of these aglycone intermediates represents a divergence point towards different terminal alkaloids.^{241,264} From **87**, the next two transformations to form 19(*E*)-geissoschizine **88** and preakuammicine **89** catalyzed by geissoschizine synthase (GS) and geissoschizine oxidase (GO), respectively, were characterized by Tatsis *et al.*²⁴² **87** is converted into **88** through iminium reduction catalyzed by GS.²⁴¹ **88** then undergoes an oxidative rearrangement catalyzed by the P450 GO to yield an unstable intermediate, preakuammicine **89**, which can undergo spontaneous rearrangement and tandem enzyme-catalyzed reductions to form the stable stemmadenine **90**. Reactive intermediates that form between **88** and **90** exist transiently and can spontaneously undergo chemical transformations that diverge towards different MIAs including corynanthean, strychnos, iboga, and aspidosperma skeletons.²³⁶ From **90**, stemmadenine *O*-acetyltransferase (SAT) catalyzed acetylation forms stemmadenine acetate **91**.

A series of redox transformations and divergent cycloaddition reactions take place to transform **91** into catharanthine, tabersonine, and (–)-coronaridine **92**. Catharanthine and tabersonine are both on-pathway intermediates to vinblastine, while **92** has essentially the same carbon skeleton as ibogaine **2**. These transformations have recently been characterized through analysis of transcriptome datasets from *T. iboga* and subsequent biochemical characterizations.^{244,265} First, a tandem amine oxidation-iminium reduction cascade catalyzed by precondylocarpine acetate (PAS) and dihydroprecondylocarpine acetate synthase (DPAS), respectively, would generate the enamine dihydroprecondylocarpine acetate **93**. The net outcome from **92** to **93** is migration of the olefin to set up the subsequent [4 + 2]-Diels–Alder reactions.²³⁷ In ibogaine biosynthesis, TiDPAS would promote the deacetoxylation with concomitant carbon-carbon bond cleavage, and NADPH-dependent tautomerization to generate the iminium dehydrosecodine **94**. The enzyme coronaridine synthase (CS) would then catalyze a formal [4 + 2]-Diels–Alder to form (–)-coronaridine **92**. In the biosynthesis of catharanthine and tabersonine, a corresponding pair of DPAS and cyclization enzyme (catharanthine synthase and tabersonine synthase, respectively) are involved to forge the different connectivities via cycloadditions. A recent study by the

O'Connor group reports the structural basis for the divergence in regio- and stereo-selectivity of the Diels-Alderase found in iboga and aspidosperma alkaloid biosynthesis.²⁶⁶ From **92**, the P450 enzyme ibogaine 10-hydroxylase (I10H) catalyzes hydroxylation at the C-5 position of the indole ring, followed by noribogaine 10-*O*-methyltransferase (N10OMT)-catalyzed *O*-methylation to yield (–)-voacangine **95**.²⁶⁵ Both **92** and **95** have shown promise as acetylcholinesterase inhibitors.²⁶⁷ In the last step, **92** undergoes decarboxylation to form (–)-ibogaine **2**. This process can occur nonenzymatically under heat, but it is likely there is an unidentified decarboxylase that facilitates this step *in planta*.

2.8.2 Heterologous production of iboga alkaloids—*De novo* production of strictosidine **25** in *S. cerevisiae* was demonstrated by Brown *et al.* in a landmark achievement of synthetic biology in 2015 (Fig. 27). The authors' engineered yeast strain comprised of twenty-one genome integrated genes, three genome-deletions and expression of a high-copy plasmid encoding a codon-optimized G8H gene. The host produced ~ 0.5 mg/L of extracellular strictosidine after 6 days. Since simple expression of the required pathway genes did not result in detectable production of pathway intermediates, the authors employed a series of metabolic engineering steps to boost precursor titers, reduce nonproductive shunt product formation, and increase P450 activity.

Towards increasing precursor titers, a truncated yeast 3-hydroxy-3-methylglutaryl-CoA reductase (tHMGR) was expressed to increase the reduction of 3-hydroxy-3-methylglutaryl-CoA **96** to form mevalonate **97**. Since GPP **82** is not a native yeast metabolite, expression of a GPP synthase (AgGPPS1) from *Abies grandis* combined with expression of a mutated farnesyl pyrophosphate synthase (mFPS144) with partial GPP synthase activity from the avian *Gallus gallus* resulted in **82** biosynthesis. Maintaining some level of essential yeast metabolite farnesyl pyrophosphate (FPP) biosynthesis with mFPS144 was required since yeast FPP synthase, ERG20, was knocked-out to shift mevalonate pathway flux from FPP to **82**. Balancing concentrations of isomers isopentenyl pyrophosphate **98** and dimethylallyl pyrophosphate **99** required for **82** formation was achieved through expression of a second copy of yeast isomerase IDI1. To further increase **81** titers, the authors overexpressed MAF1, a negative tRNA biosynthesis regulator, which reduced the amount of **98** utilized for tRNA formation.

Geraniol **81** can be rapidly metabolized by yeast enzymes to form esterified and reduced shunt products.²⁶⁸ ATF1, an alcohol acetyltransferase, and OYE2, an NADPH-dependent oxidoreductase, were knocked-out to reduce nonproductive shunt product formation. A later study by Billingsley *et al.* identified more yeast enzymes that when knocked-out, further attenuate shunt product formation from 8-hydroxygeraniol **83** and channel additional flux of **83** towards iridoid biosynthesis.⁸²

The strictosidine biosynthetic pathway contains four P450 enzymes which require reductase partners to facilitate the electron shuttling during catalysis. The *C. roseus* P450 reductase partners, cytochrome P450 reductase (CPR) and cytochrome b5 (CYB5), were expressed in yeast along with a putative alcohol dehydrogenase that was identified from MIA biosynthesis coexpression profiles (CYPADH) to increase P450 activity. Since these P450s also all require NADPH as an electron donor, ZWF1 which is yeast glucose-6-phosphate

dehydrogenase, was overexpressed to increase intracellular NADPH concentrations. SAM2, yeast SAM synthetase, was also overexpressed to increase SAM availability for LAMT.

Overall, the metabolic engineering and synthetic biology strategies employed to create this yeast platform illustrates the possibility of an alternative pipeline for MIA production. Biotransformation of **25** into ibogaine **2** is another twelve enzymatic steps. While a *de novo* ibogaine biosynthesis yeast platform has yet to be published, many of the enzymes downstream of **53** biosynthesis have been demonstrated to be functional in yeast which is promising for providing sustainable access to **2** and potential derivatives.^{236,244}

2.9 Salvia

Salvia divinorum colloquially known as the “sage of the diviners” was introduced to western academics by the indigenous people of the Sierra Mazateca in Mexico. While the botanical history of this plant has remained elusive, the hallucinogenic properties of salvia are currently employed by Mazatec shamans to facilitate visions of curing and divination. The active constituent, salvorin A **37**, was first isolated by Ortega and coworkers in 1982 and further characterized by Valdes *et al.* two years later (Fig. 28).^{269,270} The potent hallucinogenic properties of the isolated **37** were confirmed by ethnobotanist Daniel Siebert, who noted that a dose of 200 µg could produce effects identical to that of whole herb ingestion.²⁷¹ Unlike other known hallucinogenic natural products, salvia does not function as a serotonin receptor agonist. Instead, **37** is a selective opioid agonist, binding strongly to κ-opioid receptors (KORs), and was identified as the first non-nitrogenous opioid receptor ligand.^{22,272} Given these unique properties, numerous therapeutic uses for salvinorins have been proposed, including anti-inflammatory, analgesic, and anti-addiction treatments.^{273,274} Salvia is consumed primarily as a recreational drug inducing powerful, sometimes disorienting hallucinations and has a legal status that is highly contested.

2.9.1 Biosynthesis of salvinorins—**37** is a modified neo-clerodane type diterpenoid featuring a unique furyl-δ-lactone fragment. Structural-activities relationship studies of **37** analogues with modifications to the furanyl group, as well as molecular modelling have implicated the furan ring in selective KOR binding.²⁷⁵ In 2015, Gupta *et al.* reported collybolide, a fungal sesquiterpene bearing a similar furyl-δ-lactone, exhibiting KOR agonism similar to salvorin.²⁷⁶ Investigations into the biosynthetic route to **37** are still in their infancy. Produced and stored in the leaf trichomes,²⁷⁷ tissue culture of *S. divinorum* grown on isotopically labelled substrate confirmed that the diterpene core of salvinorins arises via the deoxyxylulose phosphate (DXP) pathway.²⁷⁸ This information aided the trichome-specific transcriptomics studies that investigators have used to identify pathway genes. In 2016, two research groups simultaneously identified and characterized the first enzyme involved in biosynthesis of **37**, the (–)-kolavenyl diphosphate synthase (KPS) (Fig. 29). KPS is a class II diterpene synthase, performing cycloisomerization of geranylgeranyl pyrophosphate **100** through a carbocation intermediate to form (–)-kolavenyl pyrophosphate **101**.^{279,280} Hardwickic acid **102** has been proposed as an on-pathway intermediate based on co-localization and structural similarity to the salvinorins. Based on more than a dozen salvorin-like molecules that have been isolated, a hypothetical downstream biosynthetic pathway has been proposed.²⁷⁹ However, the exact series of oxidative decorations and

cyclizations leading formation of the rare furyl- δ -lactone moiety will be of interest to biosynthetic chemists and metabolic engineers alike.

3. Alkaloidal Stimulants

Alkaloidal stimulants may be regarded as the most culturally pervasive secondary metabolites; consumption of plants containing the alkaloidal stimulant caffeine **4** may have occurred as early as 2500 BC in China. By the 1600s, alkaloid containing plants were distributed as luxury commodities along every major trade route. Alkaloid consumption was a key driver of the Euro-American slave trade, which occurred from the 16th to the 19th centuries and enabled early efforts to characterize active constituents.²⁸¹ Indeed, the alkaloid caffeine is currently world's most widely consumed psychoactive drug; although global consumption statistics have been difficult to estimate, more than 85% of adults in the U.S. regularly consume caffeine at an average rate of 0.2 grams per person per day.²⁸ While an exhaustive list of natural product stimulants would encompass molecules that are of diverse biosynthetic origins, the well-known members covered in this review fall within three major categories – the purine alkaloids, pyridine alkaloids, and tropane alkaloids. In addition to these alkaloids for which the biosynthesis has been well-studied, stimulants from a number of other plants including khat, areca, and ephedra are increasing in notoriety. Investigations into the biosynthesis, safety, and efficacy of these alkaloidal stimulants remain in their infancy.

3.1 Catecholamine neurotransmitters

Generally speaking, a stimulant may be defined as a substance that increases the activity of the central nervous system (CNS). Most stimulants function by increasing the synaptic concentrations of catecholamine neurotransmitters – namely dopamine **17**, epinephrine **103**, and norepinephrine **104**.²⁸² Produced by adrenal glands, catecholamines act as signaling molecules to activate the sympathetic nervous system. Increases in synaptic catecholamine levels are primarily achieved via blocking their reuptake or stimulating their efflux, however there are notable examples of stimulants with more indirect modes of CNS activation. As a result, a description of the physiological targets of natural products described in this section is provided alongside the individual stimulant. Despite disparate mechanisms of achieving their effects, all known natural product stimulants are alkaloidal in nature (Fig. 30).

Alkaloids are commonly defined as molecules possessing one or more basic nitrogen atoms; this chemical property facilitated early isolation via acid–base extraction, making alkaloidal stimulants some of the first natural products to undergo biosynthetic investigation.

3.2 Caffeine

In addition to early reports of human consumption of caffeine **4** in the Yunnan Province of China, caffeine containing plants were independently discovered in Africa and South America, where they were consumed for their energizing, anti-fatigue effects. Caffeine belongs to the purine alkaloid (PuA) family of natural products, which are defined by their 3,7-dihydropurine-2,6-dione core. Despite their structural simplicity, at least 80 plant species in 13 orders of the kingdom are known to produce PuAs, indicating important biological function.²⁸³ Bitter in taste PuAs are primarily involved in plant defense as an

antifeedant, comprising between 1–3 percent dry weight in most producing organisms.^{284,60} Additional research suggests that caffeine may function as an allelopathic signaling molecule,²⁸⁵ or even a conditioning molecule to train plant pollinators.²⁸⁶ In humans, PuAs work as antagonists of adenosine A_{2A}G protein-coupled receptors. During the course of the day, adenosine **77** accumulates in the neuronal synapse; subsequent binding results a negative regulation of CNS activity causing drowsiness. As structural analogues of adenosine, PuAs bind tightly (caffeine K_D = 2.4 μM) but do not activate adenosine receptors.²⁸⁷ The resulting activation of specific regions of the brain causes accumulation of stimulatory dopamine **17** and acetylcholine **106**, facilitating wakefulness. Other purine alkaloids with varying methylation patterns of the purine heterocycle exhibit variable potencies and include theobromine **107**, theophylline **108**, and xanthine **109**.

3.2.1 Biosynthesis of purine alkaloids—Caffeine **4** was first isolated in 1819 by the German chemist Friedlieb Ferdinand Runge.²⁸⁸ By the end of the century, Fisher devised a synthesis from theobromine **107** (Fig. 32) which employed methyl iodide for base-catalyzed *N*-alkylation, thus establishing caffeine's structure and formula.²⁸⁹ Given the widespread occurrence of caffeine across the plant kingdom, the biosynthesis of caffeine and related PuAs has been of interest from both a secondary metabolism and evolutionary perspectives. The biosynthesis has been studied primarily in *Camellia sinensis* (tea plant) and *Coffea arabica* (coffee plant). As early as 1962, the feeding of ¹⁴C-labeled precursors confirmed that PuAs originate from the primary purine metabolite xanthosine in *Coffea*.²⁹⁰ Direct evidence for the conversion of xanthosine **110** to 7-methylxanthosine **111** was first shown by Negishi *et al.* using plant extracts.²⁹¹ Elucidation of the subsequent hydrolysis step by a nonspecific *N*-methyl nucleosidase was frustrated by contaminating nucleosidase activity in crude enzyme extracts, but eventually confirmed using advanced chromatography methods.²⁹² Finally, tedious preparation of tea leaf enzymatic extracts in 1975 provided direct evidence for the transfer of methyl groups from SAM in the conversion of 7-methylxanthine **111** via theobromine **107** to caffeine **4**.²⁹³ Development of methods for recombinant protein production enabled Ashihara, Fujimura, and others to provide conclusive *in vitro* evidence for the biosynthetic route from xanthosine shown in Fig. 32A, with the genes encoding the responsible enzymes identified in both coffee and tea.^{294,295}

Several routes to the primary metabolite xanthosine **110** have been elucidated, however efficient incorporation of adenine **113** implicated adenosine monophosphate (AMP) **114** as a prominent source of purine equivalents.²⁹⁶ Caffeine production from AMP **114** begins with deamination to inosine monophosphate **115**, oxidation to xanthosine monophosphate **116**, and hydrolysis to xanthosine **110** by AMP deaminase (AMPD), IMP dehydrogenase (IMPDH), and 5'-nucleotidase (XMPN), respectively.²⁹⁷ The resulting xanthosine **110** is methylated by a xanthosine methyltransferase (XMT) and hydrolyzed by *N*-methylnucleosidase (NS) to give 7-methylxanthine **112**. Iterative methylation of **112** in tea has been confirmed by isolation of a caffeine synthase (*CsTCS1*) exhibiting both N3 and N1 methylation activity.²⁹⁴ Orthologous genes in coffee have been identified which exhibit either theobromine synthase (*CaMXMT1*) or caffeine synthase (*CaDXMT1*) activity, using **112** and **107** as a substrates.^{298,299}

In addition to the major pathway described above, caffeine biosynthesis evolved independently at least five times during flowering plant history, a striking example of convergent evolution towards a secondary metabolite.³⁰⁰ Analysis of the enzymes recruited by distantly related plants to carry out identical reactions has provided strong evidence for the “patchwork hypothesis” as a model to describe pathway evolution. Additional studies aimed at unravelling pathway regulation in the plant have given further insight into the “provider pathways” used by plants to increase xanthosine **110** pools. In 2001, Koshiishi *et al.* unexpectedly observed incorporation of SAM-derived adenosine **105** into the purine ring using cell free extracts of tea leaves.³⁰¹ As shown in Fig. 32B, SAH-equivalents released upon substrate methylation with SAM could be funneled into purine metabolism, providing an alternative pathway to the well-established *de novo* adenosine production routes. Alternative guanosine recycling pathways have also been identified via incorporation of [8-¹⁴C]guanosine.²⁹⁷ Sub-cellular localization of the caffeine biosynthetic pathway has also been examined. Like many plant secondary metabolites, caffeine accumulates in the vacuole,³⁰² whereas several enzymes involved in the biosynthesis associate with the chloroplasts³⁰³ or cytosol.³⁰¹

3.2.2 Heterologous production of purine alkaloids—Extensive biosynthetic investigations provided a foundation for numerous efforts in plant and microbial engineering, facilitating the creation of caffeine (and caffeine-free) biotechnologies. Knockdown of the *CaMXMT1* encoding theobromine synthase using RNA interference resulted in a 70% reduction of caffeine content, highlighting the possibility to circumvent costly decaffeination protocols using genetic engineering of *Coffea*.³⁰⁴ Recent efforts in microbial engineering for *de novo* production of xanthine alkaloids have also garnered moderate success, with benchmark titers of 0.27 mg/L and 21 mg/L in *S. cerevisiae* and *E. coli* respectively.^{92,89} In both studies, low levels of endogenous xanthosine represented a key hurdle that was approached using two different methods. McKeague *et al.* devised a xanthine **109** salvage pathway in yeast, using xanthine phosphoribosyltransferase (XPT) to revert flux towards **116** (Fig. 32C). A combination of genomic integration and low copy expression of the biosynthetic and salvage pathways using strong constitutive promoters provided maximum caffeine titers of 0.031 mg/L following 6 days of culture. In the same study, a key observation was made that xanthine could be accepted by caffeine synthase, which enabled construction of a theophylline production strain. Bench scale fermentations of customized strains permitted improved production titers of caffeine **4** (0.27 mg/L), theophylline **108** (0.06 mg/L), and 3-methylxanthine **117** (3.71 mg/L).

In *E. coli*, a xanthosine-to-caffeine conversion pathway was leveraged, taking advantage of background xanthine methylation activity exhibited by the *CsTCS1* (Fig. 32D). Li *et al.* employed plasmid-based expression using inducible promoters to enhance xanthine and SAM biosynthesis.⁸⁹ Following bioprospecting, codon optimization, and media optimization, a 4-day shake flask culture enabled production of caffeine at 21 mg/L. Despite these efforts, microbes lack the optimized flavor profiles and titers of caffeine plant products. In each of these studies, however, accumulation of monomethylated xanthines was observed, indicating the potential for metabolic engineers to produce valuable pathway intermediates of low natural abundance.

3.3 Nicotine

The pyridine alkaloids (PyAs) are comprised of the highly-addictive stimulant nicotine **5**, along with the structurally related anabasine **118** and nornicotine **119** (Fig. 33 and 34). Nicotine **5** is produced by numerous members of the Solanaceae (nightshade) family of flowering plants, and like the xanthine alkaloids, pyridine alkaloids are bitter antifeedants. In fact, the nicotine scaffold served as inspiration for the controversial neonicotinoid insecticides, the use of which has been linked to honey-bee health and colony collapse disorder.^{305,306} Most of the nightshades, including potatoes, tomatoes, and eggplant, produce PyAs in trace amounts (~0.00001 percent dry weight);³⁰⁷ selective breeding has been used to generate tobacco cultivars containing up to 3.0 percent dry weight nicotine.³⁰⁸ Discovered by the native people of Mesoamerica and South America, tobacco was traditionally used in spiritual ceremonies as well as for its medicinal properties, owing to its analgesic effects when smoked.¹²⁸ Binding of nicotine to nicotinic acetylcholine receptors results in activation of the mesolimbic pathway and subsequent release of dopamine; at higher concentrations, the activity shifts from stimulant to sedative via dampening of neural activity.³⁰⁹ Recent evidence suggests that cotinine, a metabolic degradation product of **5**, is responsible for at least some of tobacco's psychoactive effects.³¹⁰

3.3.1 Biosynthesis of pyridine alkaloids—Initially isolated as tobacco's active constituent in 1828, nicotine was structurally characterized in 1893 and synthesized by Pictet in 1904.³¹¹ Efforts to isolate nicotine and oxidation products by Weidel also led to the discovery of an aspartic acid **120**-derived nicotinic acid (niacin, **121**), precursor to the universal cellular redox currency nicotinamide adenine dinucleotide cofactors.³¹² Investigations into the biosynthesis commenced rapidly in the late 1950s with the discovery that metabolic precursors could be incorporated into nicotine via sterile root cultures. Tandem feeding studies by Byerrum *et al.* indicated that 2-¹⁴C-labeled L-glutamic acid³¹³ **36** and L-ornithine³¹⁴ **13** were incorporated into two different positions of nicotine **5**, sparking interest in a proposed "symmetrical intermediate." Leete was the first to propose the diamine putrescine **16**, derived via L-ornithine decarboxylation, as a pyridine alkaloid precursor.³¹⁵ Later studies confirmed incorporation of putrescine **16**,³¹⁶ N-methylputrescine **18**,³¹⁷ and N-methylpyrrolinium **20**.³¹⁸ Tamaki and coworkers subsequently identified putrescine N-methyltransferase³¹⁹ and N-methylputrescine oxidase³²⁰ activity in tobacco roots, confirming the pathway to **20** shown in Fig. 34.

Genes in tobacco encoding the responsible enzymes were later identified by comparison to a low-nicotine mutant and cloned into *E. coli* for functional characterization.³²¹ L-Glutamic acid **36** derived L-ornithine **13** is first decarboxylated by an ornithine decarboxylase (ODC), which is subsequently methylated by putrescine N-methyltransferase (PMT). Sequence analysis indicates that PMTs are closely related to spermidine synthases (SPDSs), which utilize decarboxylated SAM as the coenzyme to transfer an aminopropyl group onto putrescine. PMTs likely evolved via gene duplication and neofunctionalization, as mutational studies indicated that changing only a few amino acids resulted in the generation of PMT activity in SPDS proteins.³²² Next, oxidative deamination of N-methyl putrescine **18** to N-methylaminobutanal **19** is carried out by N-methylputrescine oxidase (NMO), which was functionally verified using *E. coli* expression.³²³ NMO belongs to the superfamily of

copper-containing amine oxidases, which employ a covalently bound topaquinone (TPQ) cofactor generated via autooxidation of a conserved tyrosine residue. (Fig. 34A) The Cu-TPQ complex enables radical-based oxidative deamination consisting of two steps. Following formation of a Schiff base between the TPQ and substrate amine, proton abstraction and hydrolysis result in aldehyde release. Then, reduced TPQ is reoxidized with molecular oxygen through two sequential single electron transfers via a Cu(I)-semiquinone radical intermediate, releasing H₂O₂ and NH₄⁺. A homodimer, NMO exhibits 7-fold greater catalytic efficiency towards **18** compared to **16**, achieved via a substantial decrease in K_M. The NMO product *N*-methylaminobutanal **19** spontaneously cyclizes to give the Schiff base *N*-methylpyrrolinium cation, **20**.

Surprisingly, the identity of the final stereospecific enzyme in the pathway, nicotine synthase, has yet to be elucidated. Little progress has been made since Frieson and Leete demonstrated formation of nicotine from *N*-methylpyrrolinium cation **20** and [2-³H]-labeled-**121** using crude extracts.³²⁴ The loss of the C-6 hydrogen suggested a hydride mediated formation of the 3,6-dihydronicotinic acid, which would readily decarboxylate to give the 1,2-dihydropyridine **122** (Fig. 34B). Hashimoto and coworkers utilized RNAi knockdown of the A622 gene in tobacco (belonging to the PIP family of NADPH-dependent reductases), which resulted in the decrease in the formation of nicotine and accumulation of nicotinic acid *N*-glucoside **123**, a presumed detoxification product.³²⁵ While additional studies have confirmed the involvement of A622 in nicotine biosynthesis, more biochemical evidence is needed to ascertain its catalytic function.

Following reduction of aspartic acid **120** derived niacin **121**, a proposed nucleophilic attack of *N*-methylpyrrolinium **20** by **122** is believed to occur either spontaneously or enzymatically in a Mannich-like reaction, providing the dihydropyridine precursor to the final product nicotine **5**. Subsequent RNAi targeting of a vacuolar berberine bridge enzyme-like (BBL) protein resulted in accumulation of a new nicotine-related metabolite, dihydrometanicotine **124** (Fig. 34C).³²⁶ Direct conversion of the ring-open **124** by the BBL protein would explain the enantiomeric purity of (*S*)-nicotine **5** (whereas the (*R*)-enantiomer only accounts for just 0.2% of the total nicotine). However, in experiments using recombinant BBL protein as well as crude tobacco cell extracts, oxidative conversion of **124** was not observed. Enantioselective demethylation of (*R*)-nicotine **125** by several P450s (CYP82E4, CYP82E5v2, and CYP82E10) has been postulated to explain how tobacco maintains the (*S*)-nicotine **5** and (*R*)-nornicotine **119** pools. Further studies are required in order to definitively establish the identity and mechanism of nicotine synthase, as well as the predicted anabasine **118** synthase.

3.3.2 Heterologous production of pyridine alkaloids—Complete reconstitution of the nicotine pathway in a heterologous host has not been possible due to missing steps in the biosynthesis. However, identification of genes involved in nicotine precursor formation have been used in genome mining and *N*-methylpyrrolinium platform engineering. Complete pathway elucidation will enable the use of such chassis strains for the production of rare or unnatural pyridine alkaloids. Now an undisputed model organism and biotechnological chassis, *Nicotiana* plants have been extensively engineered for applications ranging from

production of biopharmaceuticals to heterologous natural product biosynthesis.^{327,328} Synthetic biology tools analogous to those developed for microbial engineering have been extended to *N. tabacum* and *N. benthamiana*; the future of such *Nicotiana* “plant biofactories” has been recently reviewed.³²⁹ Identification and silencing of the nicotine *N*-demethylase using RNAi led to suppression of P450-mediated conversion of (*R*)-nicotine **125** to the carcinogenic nornicotine **119**.³³⁰ Recently, the CRISPR-mediated simultaneous knockout of the BBL-family protein and five additional isoforms was shown to reduce the amount of nicotine produced in tobacco by >99%, providing additional evidence for the involvement of this BBL protein in nicotine formation.³³¹ Optimizing the alkaloid profiles of “nonfood” industrial crops such as tobacco expands the capabilities of an additional chassis for industrial chemical manufacture.

3.4 Cocaine

Tropane alkaloids encompass the third class of nitrogen-containing stimulants discussed, and are defined by their characteristic 8-methyl-8-azabicyclo(3.2.1)octane (“tropane”) ring system. While just a few tropane alkaloids are known to be psychoactive, this family of molecules includes the well-known illicit stimulant cocaine **6**. Named for *Erythroxylum coca* (endogenous to South America, Mexico, Indonesia, and the West Indies), cocaine use can be traced to indigenous populations in the Andes. As early as 1000 BC, the leaves of coca were chewed for religious and medicinal purposes. At present, Columbia is the largest producer of cocaine; hundreds of metric tons are extracted and exported annually.³³² The product may be refined and distributed as the cocaine hydrochloride salt, or neutralized and distributed as the inhalable free base, a subtle difference which has resulted in extreme sentencing discrepancies.³³³ Despite its current Schedule II status in the United States, a myriad of medicinal uses for cocaine have been described, and in 2020 a cocaine hydrochloride formulation was approved for use as a topical anesthetic. The principal mechanism of action is to block monoamine transporters, resulting in the accumulation of dopamine **17** in the synaptic cleft and strong sympathomimetic effect.³³⁴ In addition to cocaine, the tropane alkaloids include the hallucinogenic scopolamine **126** as well as catuabines and calystegines.

3.4.1 Biosynthesis of tropane alkaloids—Tropane structure and biosynthesis has been a topic of intense investigation for over a century. Structural confirmation of the tropane core in cocaine accompanied Willstätter’s lengthy synthesis, which warranted a 1915 Nobel Prize in Chemistry.³³⁵ Two years later, Robinson published a one-pot tropinone formation by the addition of succinaldehyde to an acetone-dicarboxylic equivalent, which is widely regarded as the first biomimetic synthesis.¹³ This elegant method stimulated Robinson’s 1955 proposal of an analogous biosynthesis involving condensation of a pyrrolidine ring with an “acetone equivalent.” Indeed, work by Leete confirmed incorporation of L-ornithine **13** into tropanes,³³⁶ establishing a pathway identical to the *N*-methylpyrrolinium **20** formation described in nicotine biosynthesis. Feeding of labeled acetate and advanced intermediates hinted that condensation of **20** with malonate units occurs via a polyketide synthase (PKS).³³⁷ Subsequent advancements in molecular biology and genomics have rapidly facilitated the near complete pathway elucidation and engineering of tropane alkaloids.

Using differential transcriptomics of plant tissues, Bedewitz *et al.* identified a type III PKS (AbPYKS) expressed in the roots of *Atropa belladonna*, confirming its involvement in tropinone biosynthesis using virus-induced gene silencing.³³⁸ Recombinant expression of AbPYKS in *E. coli* indicated direct use of the *N*-methylpyrrolinium cation **20** as a starter substrate prior to incorporation of two malonyl-CoA **105** units, forming 4-(1-methyl-2-pyrrolidinyl)-3-oxobutanoic acid **106** (Fig. 36). Subsequently, Huang and coworkers proposed an alternative route to **106** following additional crystallographic and mechanistic studies.³³⁹ In the absence of **20**, AbPYKS was shown to produce 3-oxo-glutaric acid **21**; this compound undergoes non-enzymatic condensation with **20** via an intermolecular Mannich reaction, the kinetics of which were unaffected by the presence of AbPYKS.³³⁹ The resulting racemic **128** is thought to be the divergence point between the tropinone **129** pathway (leading to scopolamine – resolved, Fig. 37) and methylecognone **130** pathway (leading to cocaine – unresolved, Fig. 38).

Bedewitz *et al.* also hypothesized that a P450 may be responsible for the cyclization of nascent **128** via amine oxidation. Pathway reconstitution of candidate P450s identified via transcriptomics indicated that AbCYP82M3 encodes a tropinone synthase (TS), which was directly confirmed by conversion of **128** to **129** using yeast microsomes.³³⁸ The proposed mechanism involves hydroxylation and dehydration of the pyrrolidinyl to generate the pyrrolinium intermediate. Oxidation of **128** sets up the intramolecular Mannich cyclization to produce ecgonone **131**, establishing the tropane skeleton; subsequent nonenzymatic decarboxylation produces **129**. As discussed in Section 1.2.2, iminium formation and intramolecular Mannich-cyclization is a common cascade observed in the biogenesis of diverse plant alkaloid scaffolds.³⁴⁰ Two different tropinone reductases (TPI and TPII) were identified in *Datura stramonium* of high sequence identity (64% identity), each performing stereospecific reduction of **129** to either tropine **132** (TPI) or pseudotropine **133** (TPII), the precursor to the calystegines.³⁴¹

The phenylacetate unit required for littorine **134** biosynthesis is derived from phenylalanine **135**, which is transaminated by an aromatic amino acid aminotransferase (AT4)³⁴² and reduced by a phenylpyruvic acid reductase (PPAR)³⁴³ to provide phenyllactic acid **136**. This compound is subsequently glucosylated by phenyllactate UDP-glycosyltransferase (UGT1).³⁴⁴ The resulting phenylacetylglucose **137** is then used by littorine synthase (LS) to acylate **132**, forming littorine.³⁴⁴ The longstanding mystery around rearrangement of littorine was solved in 2006, wherein **134** was converted into hyoscamine aldehyde **138** by CYP80F1 via a benzylic carbocation intermediate.^{345,346} A recently identified hyoscyamine dehydrogenase (HDH) then reduces **138** to hyoscamine **139** followed by epoxidation catalyzed by an α -ketoglutarate-dependent hydroxylase/dioxygenase (Dsh6H) to complete the biosynthetic pathway to scopolamine **126**.⁷³

The majority of the pathway towards cocaine **6** has been established, with the exception of the enzymes responsible for production of the precursor methylecognone **130**. Evidence suggests a sequence analogous to tropinone **129** formation starting from a PKS product. During tropinone **129** biogenesis, the spontaneous decarboxylation following cyclization permits the use of either stereoisomer of **128**. The retention of the carboxymethyl in the

methylecognone **130** scaffold, however, necessitates incorporation of the (*S*)-enantiomer. The decarboxylation product of **128**, hygrine **140**, is known to racemize rapidly at physiological conditions. The proposed mechanism involves a retro-aza-Michael addition (Fig. 38A). Stereospecific incorporation of (*S*)-**128** into cocaine may involve selective methylation and cyclization, facilitated by spontaneous or enzyme catalyzed stereoinversion of (*R*)-**128**. A proposed methylation of (*S*)-**128** followed by a P450-mediated Mannich-cyclization by an enzyme homologous to tropinone synthase would yield the confirmed on pathway metabolite methylecognone **130**. Product methylation is believed to take place before cyclization, otherwise rapid decarboxylation of the putative β -keto acid would occur. This hypothesis is supported by a feeding study in which a low but observable amount of the methyl ester of **128** painted on coca leaves was incorporated into cocaine.³⁴⁷ Following cyclization, methylecognine **141** is formed via methylecognine reductase (MecgoR).³⁴⁸ MecgoR belongs to the aldo-keto reductase family of enzymes, indicating tropine ester formation evolved independently in *E. coca* and *A. belladonna*. The final enzyme, cocaine synthase, is a BAHD acyltransferase which condenses methylecognine with activated benzoyl-CoA **142**.³⁴⁹

3.4.2 Heterologous production of tropane alkaloids—Extensive engineering efforts by Srinivasan and Smolke allowed for the first reported *de novo* production of hyoscyamine **139** (10.3 $\mu\text{g/L}$) and scopolamine **126** (0.87 $\mu\text{g/L}$) in yeast (Fig. 35).⁷³ This synthetic biology achievement builds upon previous works to reconstitute segments of the tropane alkaloid biosynthetic pathway in *E. coli* and yeast.^{108,350,351} The fully integrated yeast strain contains 26 additional genes from yeast, *E. coli* and five different plants along with disruption of 8 native yeast genes for a total of 34 chromosomal modifications (Fig. 39). The authors organized the biosynthetic pathway with five modules, each comprised of a distinct pathway segment.

Module I is dedicated to putrescine **16** production and contains heterologous plant (AsADC) and bacterial (SpeB) putrescine pathway genes as well as additional copies of native yeast putrescine biosynthesis genes (Arg2, Fms1, Car1, Spe1) to maximize putrescine **16** accumulation. The authors also disrupted two yeast genes *MEU1* and *OAZ1* involved in off-pathway polyamine formation that reduce putrescine **16** accumulation. Module II then contains the genes encoding for the enzymes required to transform putrescine **16** into tropine **132** along with disruptions of five endogenous aldehyde dehydrogenases (Ald2–5 and Hfd1) that were previously determined to decrease *N*-methylaminobutanal **19** titers.¹⁰⁸ These two modules were a part of the platform strain from previous work by Srinivasan et al. that were leveraged to produce the non-canonical tropane alkaloid, cinnamoyltropine, from the acyl donor cinnamoyl-CoA.³⁵¹ This acyl donor is also used in the biogenesis of the polyketide-derived kavalactones, which are the anxiolytic sedatives found in the kava plant, *Piper methysticum*.⁹⁸

The next module, Module III, contains the genes required for biotransformation of phenylalanine **135** into the acyl donor, phenylacetyl glucose **137**. The pathway intermediate phenyllactic acid **136** is likely produced non-specifically by action of an endogenous yeast lactate dehydrogenase. However, the authors determined that expression of a phenylpyruvic

acid reductase from the fungus *Wickerhamia fluorescens* increased phenyllactic acid **136** titers by nearly 80-fold. Yeast glucosidase Egh1 was disrupted to prevent hydrolysis of the heterologous glucoside, phenylacetyl glucose **137**.

Module IV contains the genes encoding for enzymes to transform the TA scaffold into medicinal alkaloids, hyoscyamine **139** and scopolamine **126**, including a newly identified hyoscyamine dehydrogenase (HDH) that was discovered by manually screening 12 putative HDHs genome mined from available *A. belladonna* transcriptome datasets. The final module, Module V, contains genes that encode for the vacuole transporter NtJAT1 and an engineered, chimeric AbLS to form littorine **134** in the yeast vacuole. Initial expression of AbLS resulted in growth defects and no activity *in vivo* which the authors attributed to difficulties in post-translational processing stemming from differences in glycosylation pattern recognition and transport factors between yeast and plants. Srinivasan et al. determined AbLS may be stalled in the secretion pathway upstream of the *trans*-Golgi network based on an *N*-terminal signal peptide and designed a chimera with DsRed linked to the *N*-terminus of AbLS to mask said signal peptide. This modification allowed the chimeric AbLS to be properly sorted to the yeast vacuole and restored activity *in vivo*. To allow ample supply of tropine **132** and phenyllactic acid glucoside **137** into the vacuole to access the sorted AbLS, several vacuole transporters from plants were tested and expression of the transporter NtJAT1 resulted in the highest titers of the AbLS product, littorine **134**.

Like heterologous production of iboga alkaloids, a yeast-based platform for medicinal tropane alkaloids demonstrates the potential of a more sustainable and reliable pipeline for production. While titers on the microgram scale do not make this platform competitive to current processes for obtaining tropane alkaloids, further host engineering combined with fermentation optimization could result in an economically viable strain. In recent years, sub-cellular localization has been a popular method to greatly improve product titers and cellular fitness via forming enzymatic cascades, accessing rich chemical environments, and sequestering toxic intermediates.^{105,352,353} Here, the recapitulation of the endogenous plant vacuole sorting and intermediate transport system in yeast is an innovative approach to sub-cellular localization that is a promising strategy that may benefit other yeast systems heterologously expressing complex, spatially-organized plant pathways.

3. Cannabinoids

Cannabis indica, *C. sativa* (Fig. 40), and *C. ruderalis* are traditional plants that have been used as medicine, recreationally, and as a fiber for all of recorded history.³⁵⁴ This plant treats epilepsy,³⁵⁵ inflammatory bowel disorder,³⁵⁶ fibromyalgia³⁵⁷ and holds promise in treating cancer,³⁵⁸ psychiatric disorders,³⁵⁹ multiple sclerosis,³⁶⁰ basal ganglia disorders,³⁶¹ and others.³⁶² Despite this lengthy history and myriad of medicinal applications, the usage of this plant has remained controversial.³⁶³ For example, in the 1930s, Harry Anslinger demonized usage of *Cannabis* for his own political benefit and reshaped the American consensus on the plant.³⁶³ Because of this, today, previous colloquialisms such as ‘marijuana’ are currently being depopularized, as the term was used to purposely force negative associations with the Latino community. This is reestablishing the scientific name and “pot,” “weed,” or “bud” as common names.

Arguably, the *Cannabis* plant is unparalleled in morphological and biochemical diversity as well as its gamut of bioactive compounds – producing more than 80 biologically active compounds.^{354,365} Cannabinoids covered in this section are psychoactive *Cannabis* plant-based hybrid meroterpenoid natural products, containing terpene and polyketide fragments. These structures all contain a 5-pentylbenzene-1,3-diol (olivetol) substituted with a dimethyl octadiene chain (geranyl) (Fig. 41). The geranyl diene arm undergoes various intramolecular reactions with the polyketide core to form classic cannabinoid tetrahydrobenzochromene, vinyl biphenyl, and related chromene scaffolds.

Tetrahydrocannabinol (THC, **7**) is the major psychoactive cannabinoid and is metabolized to cannabinol (CBN, **143**) (Fig. 41).³⁶⁶ **7** and **143** define the classic cannabinoid benzochromene skeleton. Typically, *Cannabis* plants contain, depending on variety, between 5–16% **7** content, but in some cases can be as high as 18% with a theoretical maximum of 54%.³⁵⁴

Cannabidiol (CBD, **8**) has a vinyl biphenyl skeleton and is a non-euphoric compound that is produced in a 1:1 ratio with **7** in *C. indica*.³⁶⁷ Fascinatingly, **8** is reported to act against adverse effects of **7**.³⁶⁸ Some reports refer to **8** as non-psychoactive as it is not intoxicating nor euphoric, but this compound does alter brain behavior^{369–371} and therefore referred to herein as psychoactive. The pharmacology of **8** is complex as it interacts with many types of receptors and enzymes.^{372–374}

Cannabichromene (CBC, **144**) is a natural chromene racemate that functions through non-cannabinoid receptor mechanisms activating the ankyrin transient receptor potential channels 1 (TRPA1).³⁷⁵ **144** has also been reported to modulate **7** activity.³⁷⁶ Cannabicyclol (CBL, **145**) is the photochemical formal [2+2] cycloadduct of **144** – this process is nonenzymatic and dependent on storing the plant material in light.³⁷⁷ Formation of **145** likely occurs during medicinal and recreational smoking of the *Cannabis* plant. However, there is no published pharmacological data on **145**.

Natural products **7**, **8**, and **143–145** all derive from cannabigerolic acid (CBGA) **33** and cannabinerolic acid (CBNA) **146**. This pathway was originally hypothesized in 1964 upon isolation of the decarboxylated product cannabigerol (CBG, **147**).³⁷⁸ Until recently, **147** has not been studied, and like **8**, was believed to be non-psychoactive despite modulating multiple receptors.^{369,379}

Previously, the cannabinoid natural product scaffolds were thought to be exclusively produced by the *Cannabis* plant. With an increase in interest in such compounds and modern characterization techniques, related scaffolds have been discovered in rhododendrons (*Rhododendron dauricum*), liverworts (*Radula perrottetii*), indigo bushes (*Amphora fruticosa*), and even fungi (*Cylindrocarpon olidum*) (Fig. 42).^{380–383} The key difference in many of these scaffolds is the alkyl chain substituent changing from an alkyl to an aralkyl (**148**, **149**) or β -aralkyl substituent (**150**). In other cases, this alkyl chain is truncated (**151**). Intriguingly, some of these compounds were shown to exhibit similar bioactivities to classical cannabinoids.³⁸¹

4.1 Cannabinoid Receptors

Isolation of **7**, **8**, and **143** and then chemical synthesis of **7** facilitated the discovery and characterization of the G protein-coupled receptors (GPCR) named the cannabinoid receptor type 1 and 2 (CB1 and CB2).^{384–386} CB1 and CB2 cooperatively function with heterotrimeric G protein alpha subunits ($G_{i/o}$) to inhibit adenylyl cyclase activity and activate mitogen-activated protein kinase (MAPK).³⁸⁷ The CB1 and CB2 receptors are involved in achieving homeostasis after exposure to physical or mental stimuli, and therefore are attractive as therapeutic targets to treat various pathologies.³⁸⁸ The CB1 receptor is primarily found in the central nervous system at the terminals of central and peripheral neurons. The location of the CB1 correlates receptor activation with effects on motor function, cognition and memory, and analgesia. The CB2 is found in the immune system cells and affect immune cell migration. These GPCR receptors share 44% sequence homology overall, and 68% homology between transmembrane domains.³⁸⁵ The functional equivalence of CB1 and CB2 is evident in cannabinoids half maximal inhibitory concentration (IC_{50}), where typically these small molecules inhibit the receptors at near similar concentrations (Fig. 43). Synthetic analogues and some natural cannabinoids have been found to selectively potentiate the cannabinoid receptors (Fig. 43).

Over the years, the structure-activity relationships between cannabinoids and receptors have been established. A key discovery was that molecule potency is proportional to the C3 chain length.³⁸⁹ Cannabinoid analogues have been isolated and synthesized with C3 alkyl chain lengths ranging from 1–7 carbons; the CB1 and CB2 inhibitory activities of propyl and heptyl-substituted analogs are highlighted in Fig. 44. The propyl-substituted THC and CBD derivatives, tetrahydrocannabivarin (THCV, **152**) and cannabidivarin (CBDV, **153**), have weaker inhibitory activities as the alkyl chain cannot adequately fill the hydrophobic channel of CB1 and CB2.^{390–392} This means that THCV and CBDV have a more subtle or even no psychoactive effect, giving these molecules other therapeutic potentials.^{393,394} Recently, tetrahydrocannabiphorol (THCP, **154**) and cannabidiphorol (CBDP, **155**) were isolated from *C. sativa* L. that feature a C3 heptyl-substituent and are currently the most potent natural CB1 and CB2 modulators.³⁹⁵

Shortly after the discovery of CB1 and CB2 as targets of cannabinoids, Mechoulam *et al.* discovered the entourage effect.^{396,397} When biologically inactive compounds are administered with THC (**7**), these ‘entourage’ compounds modulate the observed psychoactivity. This effect is observed *in vivo* with fatty acid amides, terpenes, cannabinoids, and other compounds.^{396,398} Before naming this effect, other researchers have noted similar properties, for example a *Cannabis* extract produced a psychoactive effect two to four fold of pure **7**.³⁹⁹ The entourage effect could explain why consumers of *Cannabis* might prefer to smoke or vaporize the plant material versus taking single, purified compounds.

4.2 Biosynthesis of cannabinoids

Cannabinoid biosynthesis begins with the Claisen and aldol condensations of malonyl- and hexanoyl-CoA (**127** and **156**) – which is produced by the acyl activating enzyme (AAE1)⁴⁰⁰ – to form the polyketide olivetolic acid **32** (Fig. 40). Taura *et al.* discovered a type III

polyketide synthase (tetraketide synthase, TKS) and proposed its function in cannabinoid biosynthesis, but at the time were unable to produce olivetolic acid *in vitro*.⁴⁰¹ Later, Page *et al.* showed that this TKS enzyme cooperatively functions with olivetolic acid cyclase (OAC) to form **32** – this marked the first example of type III PKS and polyketide cyclase acting in concert to form cyclic polyketides *in planta*.⁴⁰² The biosynthesis starts with incorporation of the hexanoyl unit as the starter unit for TKS, followed by three rounds of decarboxylative chain extension with malonyl-CoA to form a tetraketide. OAC then catalyzes the Claisen-like cyclization to form the dihydroxybenzene ring, followed by hydrolytic release of **32**.

The next step in cannabinoid biosynthesis is the electrophilic addition of a terpene unit to C6 of **32** (also see Fig. 4D). The aromatic prenyltransferase (APT) enzyme⁴⁰³ selectively prenylates C6 of **32** to form either CBGA (**33**) or cannabimerolic acid (CBMRA, **157**).⁴⁰⁴ These molecules **33** and **157** are (*E*) and (*Z*) isomers and are derived from geranyl or neryl pyrophosphate (**82** or **158**), respectively. The activity of APT is dependent on the carboxylic acid of **32**⁴⁰⁴ as the reaction does not occur with a decarboxylated olivetol substrate. This indicates that the decarboxylation to form cannabigerol **147** and cannabimerol **159** occurs after prenylation. Despite this C2 substituent requirement, APT is actually quite promiscuous and able to accommodate varying alkyl-chains at the neighboring C3 position.
75

The diverse psychoactive cannabinoid skeletons all diverge from **33** and **157** as shown in Fig. 41. The aptly named tetrahydrocannabinolic acid synthase (THCAS),⁴⁰⁵ cannabidiolic acid synthase (CBDAS),⁴⁰⁶ and cannabichromenic acid synthase (CBCAS)⁴⁰⁷ catalyze the oxidative cyclizations to form tetrahydrocannabinolic acid (**160**), cannabidiolic acid (**161**), and cannabichromenic acid (**162**) respectively. These compounds can transform nonenzymatically to further generate structural diversity, either at elevated temperatures or in sunlight. Subsequent modifications can lead to the decarboxylated **7**, **8** and **144**, aromatized **143** and cannabinodiol (CBND, **163**), and further cyclized products **145**, cannabielsoin (CBE, **164**), and isotetrahydrocannabinol (ITHC, **165**). There are other known, further functionalized cannabinoid skeletons, but all of them – including **145**, **164**, and **165** – are proposed to form nonenzymatically due to environmental stimuli. However, many of these molecules have no published pharmacological data. Despite our chemical interest in these structures, we do not speculate on the potential herein.

Biochemical characterization and crystal structures of the cyclization enzymes have revealed the likely mechanism through which **33** is modified into the more advanced cannabinoids.^{407–409} These transformations are catalyzed by FAD-dependent berberine bridge enzymes (BBEs). Data indicates that upon binding of **33**, oxidation likely occurs by an active site tyrosine-484 deprotonating the resorcinol C5 proton followed by FAD-catalyzed dehydrogenation of the exocyclic methylene to form a key quinone methide intermediate **166** (Fig. 47A). Interestingly, enzyme activity likely requires the C2 carboxylic acid to be present in the substrate **33**, as cyclization of the decarboxylated **147** has not been observed.⁴⁰⁸ The carboxylic acid is likely an electronic requirement for reactivity with FAD, as when the acid is protonated the pKa of the C5 phenolic hydrogen will decrease and when deprotonated the electron density at C6 will increase. In either protonation state, the carboxylic acid makes the FAD-catalyzed dehydrogenation more facile.

From this key quinone methide intermediate **166**, all three cannabinoid scaffolds (**160**, **161**, and **162**) can be formed by hetero-Diels–Alder, Alder-ene, or electrocyclization reactions, respectively (Fig. 47A, B). This proposed mechanism indicates that these enzymes THCAS, CBDAS, and CBCAS can be considered as multifunctional pericyclases – enzymes that catalyze pericyclic reactions.⁴¹⁰ Very recently, the plant BBE MaDa that shares 45% identity with THCAS has been characterized to catalyze the Diels–Alder reaction.⁴¹¹ Our laboratory has also shown enzymes groups that share >70% homology catalyze stereoselective dehydrations and concomitant pericyclic reactions – either hetero-Diels–Alder or Alder-ene.⁴¹² These findings point us back to the THCAS, CBDAS, and CBCAS enzymes and led us to ask: are these reactions pericyclic? Another aspect of this transformation that warrants further investigation is the **33** substrate 8,9-alkene configuration. **33** is in the (*E*) configuration, but the products of THCAS, CBDAS, and CBCAS are all in the (*Z*) configuration. Authors have shown that THCAS can convert either cannabigerolic acid (**33**) or cannabinerolic acid (**157**) into **160**.⁴⁰⁷ This implies that the enzyme facilitates isomerization upon quinone methide formation and before cyclization, but there is no evidence for the mechanism of isomerization. Further research needs to be conducted in order to fully understand the mechanism in which the psychoactive cannabinoid skeletons are forged.

4.3 Heterologous production of cannabinoids

Keasling and coworkers realized heterologous production of **160** and **161** in *Saccharomyces cerevisiae* from galactose (Fig. 48).⁷⁵ In order to produce cannabinoids in yeast, it was crucial to optimize the flux of geranyl pyrophosphate (**82**) and hexanoyl-CoA (**156**) by introducing an upregulated mevalonate pathway, a mutant (F96W, N127W) of the endogenous farnesyl pyrophosphate synthase (ERG20), and incorporation of an acyl activating enzyme from *Cannabis sativa* to form hexanoyl-CoA (**156**). The use of the mutant ERG20 is to attenuate the conversion of GPP to FPP, as discussed in Section 2.8 in strictosidine biosynthesis. Despite efforts to incorporate APT and catalyze the electrophilic prenylation to form **33**, no activity could be observed when expressed in yeast. The authors searched *Cannabis* transcriptomes for enzymes that share homology with the well-functioning soluble aromatic prenyl transferase, NphB (*vide infra*), of *Streptomyces sp.* and discovered the enzyme CsPT4 – which not only efficiently catalyzes the reaction, but is clustered with other prenyltransferases in *Cannabis*. Incorporation of all genes above led to a 1.4 mg·L⁻¹ titer of **33**. To functionally reconstitute the final oxidative cyclization by THCAS or CBDAS in yeast, the *N*-terminal domain of THCAS and CBDAS were replaced with a vacuolar localization tag. In total, integrating all genes into a single strain and culturing with galactose yielded titers of 8.0 mg·L⁻¹ **160** or 4.2 μg·L⁻¹ **161**.

Due to the substrate promiscuity of OAC, Keasling *et al.* also used this platform to produce cannabinoid C3 alkyl chain derivatives. Starting from various fatty acids, **32**, **33** and **160** could be produced with a propyl, butyl, pentenyl, 3-methylpentyl, hexyl, and hexynyl C3 substituents. This heterologous expression showcases the feasibility of complete cannabinoid and cannabinoid derivative production in yeast. Improvements to this method for microbial cannabinoid production methods are currently being pursued by different synthetic biology startup companies.

Cell-free platforms for cannabinoid production have also garnered much interest and success. As geranyl pyrophosphate (**82**) levels are challenging to optimize in cells, cell-free methods circumvent inherent issues of forming prenylated natural products in large quantities. The Bowie laboratory has successfully used cell-free platforms to produce CBGA (**33**) with a $1.25 \text{ g}\cdot\text{L}^{-1}$ titer⁵³ and, most recently, using a far simpler and more cost-effective system were able to realize a $0.48 \pm 0.12 \text{ g}\cdot\text{L}^{-1}$ titer.¹⁰²

Perhaps a more important discovery than this titer improvement was the implementation and engineering promiscuous bacterial prenyltransferases to catalyze the electrophilic addition of a geranyl pyrophosphate to **32** and **32** derivatives.^{53,413,414} This strategy avoids the native integral membrane bound *Cannabis* prenyltransferase that is intrinsically difficult to work with both *in vivo* and in cell-free systems.⁴⁰³ Previous work by Kuzuyama and coworkers showed that the enzyme NphB could prenylate a wide variety of substrates including olivetol to form **148**.^{413,415,416} Wild type NphB prenylates olivetolic acid nonspecifically generating a mixture of the desired cannabigerolic acid **33** and undesired *O*-prenylated product with a very low k_{cat} (0.002 min^{-1}). Bowie and coworkers expanded on this work by using Rosetta to computationally redesign NphB.⁵³ The endpoint was a soluble, easy-to-work-with enzyme – named M23 – that was highly selective for the desired electrophilic prenylation of C6 to form **33** and exhibited 1,000-fold increase in k_{cat} from the wild-type enzyme. A variant (M31) was also designed to function with divarinic acid **167** (the C3 propyl derivative of olivetolic acid **32**). Now, NphB and its variants can be expressed heterologously or used in cell-free systems to produce **33** and derivatives thereof.

Cell-free systems for divarinic and olivetolic acid (**32** and **163**) production are becoming fairly effective in producing large titers. Recently, Bowie and coworkers used a six-enzyme system to produce **32** and **163** (Fig. 49A) as well as further develop their platform for geranyl pyrophosphate production (Fig. 49B). These methods are generalizable and applicable to many molecules. The authors build off of a previously discovered route^{417,418} in order to minimize the number of expensive adenosine triphosphate (ATP) and coenzyme A (CoA) molecules required for cell-free synthesis. As shown Fig. 49A, first acetic acid is phosphorylated by AckA and then thioesterified to form acetyl-CoA. The CoA group of acetyl-CoA is then transferred to malonic acid to form malonyl-CoA **127** which continues on the canonical pathway to form olivetolic acid **32**. The authors used ThiM to phosphorylate isoprenol and then a subsequent phosphorylation by IPK.^{417,418} Typically ThiM, a hydroxyethylthiazole kinase, phosphorylates 2-hydroxyethyl thiazoles. Here they have used this enzyme to catalyze the same reaction on a simpler acyclic starting material. The following steps to form geranyl pyrophosphate were reported previously¹⁰¹ using typical isopentyl-diphosphate delta-isomerase (IDI) and a modified farnesyl pyrophosphate synthase (FPPS) enzyme that generates the C10 dimethylallyl derived geranyl pyrophosphate. Ultimately, this strategy is a highly modular method to make various malonyl-CoA products and useful for making high-titers of geranylated natural products.

5. Opioids

Western medicine was born from the poppy plant *Papaver somniferum*. Opium has been scraped from the *P. somniferum* bulb and used both recreationally and medicinally for all of

written history.^{419,420} For example, in the 16th century, people used the botanical tincture laudanum,⁴²¹ which is mixture of ambergris, musk, alcohol and opium, for the promise of good health. In the 1800s, morphine (**9**), the major component of opium, was isolated and sold as the first single-molecule drug (Fig. 50).⁴²² This began the contemporary 150-year medicinal tradition of prescribing single-molecule drugs versus botanical tinctures.

5.1 Opioid receptors

There are four class A GPCR opioid receptors, μ , δ , K , and N.⁴²⁴ The μ opioid receptor (MOP) is named for binding morphine. The δ opioid receptor (DOP) is named for being expressed in the *vas deferens*. The K opioid receptor (KOP) is named for binding the synthetic ligand ketocyclazocine. The N opioid receptor (NOP) is named after the endogenous mammalian peptide nociceptin. These names are not truly informative and have been subject to debate. Opioid receptors are distributed throughout the central nervous system and partially in the *vas deferens*, joints, and immune system. MOP, DOP, and KOP are sometimes referred to as classical opioid receptors. Whereas NOP is ‘less’ classical; NOP was discovered later and now is considered an opioid receptor as well. As the ligand was not originally known for NOP, the receptor is sometimes still referred to as an opioid-like receptor or an orphan receptor. Other opioid-like receptors have been identified based on binding, however these are not *bona fide* opioid receptors. The σ receptor (named for binding SKF10047) binds opioids as well as other drugs of abuse like phenylcyclidine. Other receptors that do exhibit related pharmacology to MOP, DOP, KOP, or NOP have been identified but are not fully characterized; for example, the ζ receptor is an opioid growth factor receptor, and the χ receptor and ϵ binding site have been proposed in β -endorphin binding.

The structure function relationship of opioid receptors is relatively well understood.^{425–427} MOP, DOP, KOP, and NOP share ~ 60% homology with highly conserved fingerprints of class A GPCRs and a homologous binding cavity. The small molecule ligands like morphine bind to the conserved receptor residues in the homologous binding cavities.

5.2 Opium alkaloids

The morphinan alkaloids are the most colloquial family of opium alkaloids as morphine (**9**) is the flagship molecule of the family. This family features a tetracyclic phenanthrene fused piperidine core, a so-called morphinan scaffold (Fig. 51). In early 1800s, Friedrich Sertürner isolated **9** (Fig. 51) from *Papaver somniferum*.⁴²⁸ In the following years, Pierre-Jean Robiquet isolated the *O*-methylated morphine derivative, codeine **168** (Fig. 51).⁴²⁹ These discoveries led chemists to develop related compounds, i.e. heroin **169**, that were more potent, safer (minimizes hypoventilation), and touted as “free from abuse liability.”⁴¹⁹ This claim marked the first falsification of opioids being safe to use without risk of addiction, which were most recently repeated by the Sacklers at Purdue Pharma. The morphinan alkaloids are potent analgesics that have been used for thousands of years as opium mixtures and now as isolated pure compounds.⁴²⁴ Natural products oripavine (**170**) and thebaine (**171**) do not exhibit safe pharmacology, but are highly useful morphinan alkaloids as synthetic building blocks for derivatization.

The reticulines are key early pathway intermediates that many families of opioid scaffolds diverge from. These structures are simple benzyloquinolines (Fig. 52). (*S*)-reticuline (**172**) can epimerize to (*R*)-reticuline (**28**) and continue to morphinan biosynthesis or directly undergo a C–C coupling reaction and lead to the phthalide isoquinolines and protoberberines families of opioids. (*S*)-norcoclaurine (**27**) is formed from dopamine **17** and 4-hydroxyphenylacetaldehyde **26** by a Pictet-Spenglerase and marks the first dedicated step in opioid biosynthesis (also see Fig. 3). Though these compounds are not known to be psychoactive, they are the building blocks to form many psychoactive natural products. Of note, the oxidation of the isoquinoline to form papaverine (**173**) alters the pharmacological properties as **173** is an approved antispasmodic drug.

The phthalide isoquinolines class of opioids encompass two general structures in which the isoquinoline is either intact or open as a dimethyl amino sidechain, as exemplified by noscapine (**174**) and narceine (**175**). **174** and **175** are non-narcotic, antitussives with minor hypnotic, euphoric, and analgesic properties. **174** has a lengthy history as a pharmaceutical with its isolation in 1817 and first use as an anti-malarial drug until 1930.⁴³⁰ Now, many are rediscovering **174** as an anti-cancer drug candidate.^{431,432} Such compounds are produced by many species of the *Papaveraceae* poppy plant.

Aporphine opioids are C–C phenol coupled benzyloquinolines that feature a functionalized aporphine structure (Fig. 54). These natural products have a range of activity from anticonvulsant (corytuberine, **176**) to antinociceptive ((*S*)-glaucine, **177**). The unnatural (*R*)-isomer of glaucine **178** is known to be a potent hallucinogen that modulates the 5-HT_{2A} receptor and is sometimes used recreationally. Such compounds can be isolated from a variety of *Papaveraceae* species such as *Glaucium flavum* and *Corydalis yanhusuo*.

Lastly, the berberine opioids are pentacycles with a dibenzoquinizolium core. These molecules are quaternary ammonium salts. Berberine (**179**) is a traditional natural yellow dye and sanguinarine (**180**) is an escharotic toxin that also causes epidemic dropsy. The berberine opioids have been isolated from *Papaver somniferum* and *Macleaya cordata*.

5.2.1 Biosynthesis of opium alkaloids—Biosynthesis of morphinan opioids requires more than 10 enzymatic steps starting from dopamine **17** and 4-hydroxyphenylacetaldehyde **26**. The elucidation of this route has taken more than 30 years of research and is condensed into a single figure, Fig. 56. The first dedicated step in opioid biosynthesis is a Pictet-Spengler reaction catalyzed by norcoclaurine synthase (NCS) to forge the tetrahydroisoquinoline core of (*S*)-norcoclaurine (**27**) – which is a simple example of the benzyloquinoline alkaloid natural product family.^{433,434} There has been many mechanistic studies of this enzyme that are not discussed herein (also see Fig. 3).^{43,435,436}

(*S*)-reticuline (**172**) is formed from **27** by two hydroxylations, an *N*-methylation, and an *O*-methylation by the enzymes norcoclaurine 6-*O*-methyltransferase (6OMT), coclaurine *N*-methyltransferase (CNMT), *N*-methylcoclaurine 3'-hydroxylase (NMCH CYP80B1), and 3'-hydroxy-*N*-methylcoclaurine 4'-*O*-methyltransferase (4'OMT), respectively.^{437–440} These steps can occur in a variety of orders with similar efficiencies and are drawn above in a typical order in Fig. 56. **172** is a key branch point in opioid biosynthesis from which many

benzylisoquinoline scaffolds can form. Recently, the epimerase enzymes STORR reticuline epimerase (REPI) and 1,2-dehydroreticuline synthase-1,2-dehydroreticuline reductase (DRS-DRR) were discovered to convert (*S*)- to (*R*)-reticuline by dehydrogenation at C1 to form an iminium cation which is hydrated from the opposing face.^{441,442} In order to discover these genes, laboratories turned to RNA interface mediated silencing of the codeinone reductase (COR) gene. Silencing COR, which operates several steps downstream from the epimerization of reticuline, results in accumulation of (*S*)-reticuline versus the substrate codeinone **181**. This could occur due to off-target co-silencing of related oxidoreductases that catalyze the epimerization of (*S*) to (*R*) reticuline. Using this strategy, a fusion protein REPI and DRS-DRR was identified that was able to catalyze the crucial epimerization reaction.

In order to discover the enzyme without access to the opium poppy, the Smolke lab searched the 1000 Plants Project and PhytoMetaSyn databases for COR-like enzymes in *Papaver* species. This revealed several genes that encoded for a two-domain enzyme with P450 82Y1-like and COR-like domains. From these two domains it was reasonable to hypothesize that the (*S*)-reticuline **172** could be oxidized to an isoquinilium (P450) and then reduced to (*R*)-reticuline **28** by the COR domain. One of the gene candidates from *P. somniferum*, named DRS-DRR was cultured with P450 reductases, CNMT, 6OMT and 1 mM norlaudanosoline **182**, a desmethoxy derivative of reticuline, for 72 hours, and >50% conversion to (*R*)-reticuline **28** was observed.

(*R*)-reticuline (**28**) is the substrate for the salutaridine synthase (SalSyn) CYP8719B1-catalyzed oxidative phenol coupling reaction that forms a carbon-carbon bond between C2' and C4 α yielding salutaridine (**183**).^{58,443} This reaction is proposed to occur by the iron oxo heme compound I abstracting the hydrogen from the C3' hydroxyl of **28** to generate compound II, which then abstracts the remaining phenol hydrogen to facilitate the cyclization (also see Fig. 5B).⁵⁸ The direct di-keto product readily enolizes to form **183**.

Salutaridine (**183**) is converted to thebaine (**171**) in three enzymatic steps. First, salutaridine reductase (SalR) reduces the quinone ketone to form salutaridinol **184** which is then acylated by the acyl transferase enzyme salutaridinol 7-*O*-acetyltransferase (SalAT) and was believed to slowly cyclize nonenzymatically to form thebaine (**171**).⁴⁴⁴⁻⁴⁴⁶ Recently, thebaine synthase (THS) was discovered and isolated in *Papaver somniferum* opium poppy latex and found to accelerate this cyclization to form the morphine skeleton of **171**.⁴⁴⁷

The final four enzymatic steps in morphine (**9**) biosynthesis are two *O*-demethylations, an isomerization and ketone reduction that are catalyzed by codeine *O*-demethylase (CODM), thebaine 6-*O*-demethylase (T6ODM), neopinone isomerase (NISO), and codeinone reductase (COR), respectively.^{74,448,449} There are two established paths that differ in the first *O*-demethylation, which can lead to either oripavine **170** or codeinone **181**. In 2018, the crystal structure for T6ODM was solved, but the mechanism for the *O*-demethylation is still unknown.⁴⁵⁰ Further *O*-demethylation and isomerization (a formal 1,5-hydrogen shift) produces morphinone **185** which is, finally, reduced to form morphine **9**.

In 2012, a 10-gene cluster responsible for noscapine (**174**) biosynthesis was discovered.⁴⁵¹ Noscapine (**174**) biosynthesis diverges from **9** biosynthesis after (*S*)-reticuline (**172**) formation (Fig. 57). First, **172** is transformed to (*S*)-scoulerine **186** by a berberine bridge enzyme (BBE).^{452,453} This BBE catalyzes an FAD-dependent dehydrogenation of the *N*-methyl group to form a methylene isoquinolinium. This reactive intermediate then undergoes C–C bond formation between the methylene and C2' that is facilitated by glutamate sidechain hydrogen bonding to the C3' phenolic hydrogen. Mechanistic studies have proposed that complete proton transfer is not required,⁴⁵² but the C3' hydroxyl – which increases the nucleophilicity of C2' – is required for catalysis.⁴⁵⁴ Multiple alkaloid classes derive from **186**; for example, the protoberbines, benzophenanthridines, protopines, and the phthalideisoquinolines.

(*S*)-canadine **187**, an antioxidant, is formed by subsequent *O*-methylation and etherification of (*S*)-scoulerine **186** by the scoulerine 9-*O*-methyltransferase (S9OMT) and canadine synthase (CAS) enzymes, respectively.^{455,456} **187** undergoes *N*-methylation by tetrahydroprotoberberine *N*-methyltransferase (TNMT) to form the isoquinolinium core of (*S*)-*N*-methylcanadine **188** that can undergo dihydroxylation by CYP82Y1 to form (*S*)-1,13-dihydroxy-*N*-methylcanadine **189**.^{457–459}

The noscapine core is formed by the oxidative ring opening and cyclization to yield narcotoline hemiacetal **190**. These transformations begin with acetylation of (*S*)-1,13-dihydroxy-*N*-methylcanadine (**189**) to form (*S*)-1-hydroxy-13-*O*-acetyl-*N*-canadine **191** by the acetyltransferase AT1 (see Fig. 4B).⁴⁶⁰ This enzymatically-installed acetyl group is essential for CYP82X1 hydroxylation activity and has been proposed to function as a protecting group to alleviate from precocious hemiacetalization.⁴⁶⁰ Following acetylation, a CYP82X1 installs a hydroxyl *ortho* to the nitrogen that facilitates a spontaneous oxidative ring opening to form (*S*)-4'-*O*-desmethyl-3-*O*-acetylpapaveroxine **192**.

(*S*)-4'-*O*-desmethyl-3-*O*-acetylpapaveroxine (**192**) undergoes three final enzymatic transformations to form noscapine (**174**): hemiacetalization, oxidation and *O*-methylation. The enzyme CXE1 catalyzes the hemiacetalization to form the phthalideisoquinoline core of narcotoline hemiacetal (**190**) which is then oxidized to the lactone (narcotoline, **193**) by the enzyme SDR1.^{460,461} Lastly, noscapine **170** is formed by the *O*-methylation by N4'OMT.⁴⁵⁵ Of note, these last two steps can occur in either order; N4'OMT *O*-methylation can preclude SDR1 lactonization.

5.2.2 Heterologous production of opium alkaloids—There have been many efforts in heterologous production of opioids.^{109,462–467} These pathways, at the time, were the longest biosynthetic pathways reconstituted in yeast.⁴⁶⁶ However, almost all studies stopped at (*S*)-reticuline **172** or begin at highly functionalized opioids, like thebaine **171**. This had to do with the fact that the crucial epimerase that forms (*R*)-reticuline **28** was not characterized until 2015. At this time, Smolke's laboratory had already realized heterologous production of thebaine **171** and hydrocodone **194** in yeast (Fig. 58).⁷⁷ To complete biosynthetic reconstitution, the laboratory had to overcome two main challenges: (1) discover an enzyme that racemizes (*S*)-reticuline **172** to (*R*)-reticuline **28**; and (2) engineer the aryl coupling P450 SalSyn to be fully functional when expressed in yeast. A further challenge was implicit

in the task; simply expressing >20 genes and obtaining high efficiency with each enzymatic transformation. In spite of these challenges, Galanie *et al.* engineered a fully integrated yeast strain that produced $6.4 \pm 0.3 \mu\text{g/L}$ of thebaine **171** and with additional downstream enzymes, $\sim 0.3 \mu\text{g/L}$ of hydrocodone **194** in a culmination of decades of research.^{78,109}

The engineered strain contained 19 heterologously expressed mammalian, bacterial, and plant enzymes, two modified yeast enzymes, two overexpressed native yeast enzymes and one inactivated enzyme for a total of 24 chromosomal modifications. These modifications were split between seven modules for both pathway and chromosomal organization.

Module I consists of overexpression of two modified shikimate pathway enzymes and two native yeast genes. The Q166K point mutation in Aro4p, which catalyzes the aldol condensation of erythrose 4-phosphate **47** and phosphoenolpyruvic acid **48** to form 3-deoxy-D-arabino-2-heptulosonic acid 7-phosphate **195**, renders the enzyme feedback inhibition resistant. Similarly, the T226I mutation in Aro7p, which is one of the enzymes involved in the biotransformation of **195** into 4-hydroxyphenolpyruvic acid **196**, makes the enzyme feedback resistant. Overexpression of Aro10p and Tkl1 resulted in shifting metabolic flux towards the pathway.

The next module (II) focuses on producing and recycling the mammalian redox cofactor, tetrahydrobiopterin (BH_4). This cofactor is essential for the selective C3 hydroxylation of L-tyrosine **12** to form L-DOPA **71** catalyzed by mammalian tyrosine hydroxylase (TyrH) and is not native to yeast. 6-pyruvoyl-tetrahydropterin (PTPS) and sepiapterin reductase (SepR) are used to produce BH_4 from dihydroneopterin, a yeast metabolite. Quinonoid dihydropteridine reductase (QDHPR) and pterin carbinolamine dehydratase (PCD) are then used to recycle BH_4 back to its active form.

Module III uses bacterial, plant, and mammalian enzymes to catalyze formation of the first BIA scaffold. Dihydrofolate reductase (DHFR) is another BH_4 salvage enzyme that works with TyrH^{WT}, a mutant that is more inhibition resistant. Following hydroxylation, L-DOPA **71** undergoes decarboxylation catalyzed by DOPA decarboxylase (DoDC) to form dopamine **17** followed by a Pictet-Spengler reaction between 4-hydroxyphenylacetaldehyde **26** and **17** by norcoclaurine synthase (NCS) to form (*S*)-norcoclaurine **27**.

The remaining modules consists of the biosynthetic pathway enzymes towards thebaine **171** and hydrocodone **194** and the discovered enzyme for (*S*)-reticuline epimerization. The native P450 enzyme SalSyn had low activity when initially expressed in yeast. This was hypothesized to be due to incorrect translocation of nascent SalSyn to the endoplasmic reticulum (ER) lumen as opposed to correct anchoring to the outer ER membrane based on nonnative *N*-glycosylation patterns. Mistranslocation could stem from a poorly recognized *N*-terminus and thus the authors replaced the *N*-terminus portion of SalSyn with that from a homologous, non-glycosylated P450, Cheilanthifoline synthase, that shares 61% identity and exhibits high activity in yeast.⁴⁶⁸ The engineered chimeric SalSyn enzyme exhibited nearly 6-fold improvement in conversion of (*R*)-reticuline **28** to salutaridine **183** compared to the wild type enzyme.

After establishing ~6 µg/L thebaine **171** production with their platform, the authors sought to introduce downstream enzymes towards hydrocodone **194** production. Upon coexpression of two more enzymes, MorB and T6ODM and supplementation with 50 mM oxoglutarate, the strain produced 0.3 µg·L⁻¹ **194**. The Smolke lab previously used MorB, an NADH-dependent morphinone reductase from a bacteria *Pseudomonas putida* M10 that was originally discovered in an opium poppy processing factory, for production of natural and semi-synthetic opioids.^{465,469} Expression of such a long pathway required careful codon-optimization of multiple enzymes and led to proof-of-concept titers that highlight the potential of chassis species for pharmaceutical production.

In 2018, the Smolke lab modified this pathway to produce noscapine **174**.⁴⁷⁰ The new work branches at (*S*)-reticuline **172**, using the BBE to produce (*S*)-scoulerine **186**. Therein, more than 30 enzymes were heterologously expressed, including five plant P450s which are notoriously difficult to express in yeast. To overcome challenges in P450 activity and other pathway bottlenecks, the authors (i) deleted the first 24 amino acids of NCS corresponding to an *N*-terminal signal vacuole translocation peptide to avoid detrimental sorting of the nascent peptide,⁴⁷¹ (ii) codon optimized the TyrH R37E, R38E, W166Y (TyrH^{WR}), (iii) incorporated an NADPH regenerating system, (iv) and lastly, optimized media and fermentation conditions which led to the largest gain (~300-fold) in production. Overall, the combined strategies resulted in a noscapine **174** titer of 2.21 mg·L⁻¹ in 72 h. Finally, Li *et al.* demonstrated the versatility of their yeast platform by generating halogenated BIA derivatives through feeding modified L-tyrosines.

5.3 Kratom

In addition to the opium alkaloids, more than 50 kratom alkaloids have been isolated from the *Mitragyna speciosa* plant, several of which exhibit opioid-like properties.⁴⁷² Native to Southeast Asia, kratom (*Mitragyna speciosa*) has been used in traditional Thai medicine for centuries. The use in the United States has increased rapidly since early 2000s, both recreationally and to relieve chronic pain or opioid withdrawal symptoms. Compared to conventional opium alkaloids, kratom alkaloids exhibit “unique binding and functional profiles” suggesting that plant extracts may be effective alternative to the benzyloisoquinoline-based pain treatments.⁴⁷³ However, similar to opium alkaloids, repeated use of kratom may lead to addiction, and the FDA has not approved kratom for any medical use; as a result, the DEA lists kratom as a Drug of Concern. The first reported and most abundant kratom alkaloid is mitragynine **10**, comprising up to 66% of the alkaloid content in Thai cultivars.⁴⁷⁴ The less abundant 7-hydroxymitragynine **197** and its rearrangement product mitragynine pseudoindoxyl **198** are potent partial agonists of human µ-opioid receptors at nanomolar concentrations.^{27,475}

5.3.1 Biosynthesis of mitragynine—Kratom alkaloids belong to the MIA family, and are presumed to be derived from the universal MIA precursor strictosidine. The 12-step pathway leading to the formation of strictosidine **25** from primary the primary metabolites L-tryptophan **11** and isopentenyl pyrophosphate **98** has been elucidated in *C. roseus* and is discussed in Section 2.8. While the remaining biosynthetic steps leading to the formation of mitragynine are currently unknown, we have proposed the pathway shown in Fig. 60 based

on a number of biochemical observations. It is known that following deglycosylation of **25** by strictosidine-*O*- β -glucosidase (SGD) and subsequent rearrangement, a reductase converts the reactive aglycone **87** isomer into a more stable pathway intermediate.⁴⁷⁶ Examples from literature include tetrahydroalstonine synthase, geissoschizine synthase, and vitrosamine synthase, which are all NADPH-dependent reductases.^{242,477,478} Moreover, O'Connor and coworkers recently identified a dihydrocorynantheine aldehyde synthase (CpDCS) from *Cinchona pubescens* involved in quinine biosynthesis.⁴⁷⁹ CpDCS performs iterative reduction of geissoschizine **87** to provide a demethylcorynantheidine **200** isomer. The authors identified an orthologue in *Mitragyna speciosa* named MsDCS, postulating that following deglycosylation of **25**, two successive reductions of the conjugated iminium **87** would provide the stable demethylcorynantheidine **199**. Reduction of conjugated iminiums has also been demonstrated in the formation of other late stage MIAs including tabersonine and catharanthine.^{236,237} Additionally, production of **199** has been reported in *Uncaria rhynchophylla*, which like kratom belongs to the family Rubiaceae.⁴⁸⁰ Methylation of the putative **199** would provide corynantheidine **200**, which has been isolated from *Mitragyna* and differs from mitragynine by one methoxy group.⁴⁷² Following aromatic hydroxylation and methylation, mitragynine **10** is likely further hydroxylated to 7-hydroxymitragynine **197**. The P450-mediated conversion of **10** to **197** has been demonstrated in both mouse and human liver preparations.²³⁸ A semi-pinacol rearrangement to provide the mitragynine pseudoindoxyl **198** may occur either spontaneously or enzymatically⁴⁸¹ as has been described in analogous transformations by FAD-dependent oxidases in fungal alkaloid pathways.^{482,483} Identification of the *M. speciosa* biosynthetic enzymes will provide biocatalytic tools necessary for heterologous production of kratom alkaloids in existing seco-iridoid producing yeast platforms.⁷⁶

6. Conclusions and perspective

The natural products described in this review run the gamut of metabolic origin, psychoactive effect, and biological source. While most of the compounds discussed have been isolated from plants, we have highlighted several well-known psychoactive natural products produced by fungi and one of animal origin. Given the immense structural diversity exhibited by such molecules, the wide array of psychoactivities is not surprising. We have noted that the majority of the compounds originate from amino acid metabolism, however prominent examples of compound biogenesis via terpenoid and polyketide metabolism have been provided. Moreover, we have featured a number of remarkable enzymatic transformations that not only provide inspiration for biomimetic syntheses, but have been directly used in chemoenzymatic applications; these include completely stereoselective nucleophilic additions, tightly controlled scaffold rearrangements, and regioselective group transfer reactions on deprotected substrates. We have also chosen to outline biosynthetic pathways ranging from fully elucidated to almost entirely incomplete. Ongoing efforts towards total pathway elucidation are necessitated by the multitude of synthetic biology applications that benefit from a complete set of biosynthetic information. Given the rapid expansion of molecular biology techniques and prominent early successes in pathway refactoring, such synthetic biology technologies will very likely play a role in 21st century

biomanufacturing. Major questions around the cost, ethics, and legality of synthetic-biology-based production of psychoactive substances must be answered in the very near future.

At present, the natural products covered in this review are either regulated or unregulated, however this legal binary is currently being traversed by *Cannabis* products. Popular culture and the media have sensationalized cannabinoid research. Despite the wide interest in cannabinoids, the research is still highly controversial and difficult to fund. This is rapidly changing as the World realizes there is ‘money in cannabinoids.’ Western medicine prefers pure, single molecule therapeutics to botanical extracts. In 1996, California legalized botanical cannabis for medicinal use.⁴⁸⁴ This goes against the western medicine doctrine and begs the question: as pharmacology, chemistry, and biochemistry all advance, will western medicine move towards curated complex mixtures of small molecules that emulate botanical tinctures? Perhaps, the cannabinoids will represent a case study that other scheduled substances will follow. Evidentiary developments indicate that *Cannabis* components such as **8** modulate adverse effects of **7**, a phenomenon commonly described as the entourage effect.^{396,397} However the majority of cannabinoid compounds do not have published pharmacological data. And, the molecules that are well-studied are still controlled substances. For example, **8** is a non-euphoric compound with a safe pharmacokinetic profile, yet it is a controlled substance. As Di Marzo and coworkers say, “This anomaly makes clear that, despite considerable scientific evidence, talks about legalization, and the many industrial and medical uses of the plant, stigma around cannabis still hinders the conclusive assessment of the therapeutic potential of the plant’s most abundant components. Further education is needed to reduce the negative impact of these factors on research.”⁴⁸⁵

Undoubtedly, this paradigm extends beyond cannabinoids, as immense untapped therapeutic potential exists in regards to the other compounds described. As Western medicine has long cannibalized indigenous discoveries, however, we must prioritize the rights of practitioners of traditional medicine as we unpack the potential applications of these natural products. Ironically, the same reductionist vision of single molecule therapeutics has resulted in a persistent rejection of holistic approaches to medicine. However, the tides are changing, and practitioners of science are more readily acknowledging the limitations of reductionist frameworks. In the same way that we have reduced the extraordinary complexity of metabolic networks into linear biosynthetic pathways, reductionism should be used to complement holism. From this perspective, medicine, culture, and technology can all be beneficiaries of a comprehensive understanding of Nature’s biosynthetic routes to psychoactive natural products.

Acknowledgements

Related work in the Tang lab is supported by NIH 1R01AT010001. C.S. Jamieson is grateful for additional funding from the Saul Winstein fellowship, the Foote fellowship, and a UCLA Dissertation Year Fellowship. J. Misa is supported by NIGMS-funded predoctoral fellowship T32 GM136614. The authors wish to acknowledge the indigenous peoples whose immense knowledge of the natural world has facilitated the study of psychoactive natural products. We recognize that many of the scientific discoveries described in this review would not be possible were it not for the expert observations of indigenous people of the Sierra Mazateca, indigenous groups in the Amazon basin, indigenous populations in the Andes, indigenous Bwiti practitioners in Gabon, and countless others to whom we pay our respects.

Biographies



Cooper S. Jamieson was born in New York, NY and raised in San Luis Obispo, CA. In 2016, he received a B.A. in Chemistry and a B.A. in Art from Lewis & Clark College in Portland, OR. He moved to far-West Marfa, Texas and worked in art conservation at the Chinati Foundation. Now, Cooper has returned to academia and is in Los Angeles, CA finishing his Ph.D. under the direction of Prof. K. N. Houk and Prof. Yi Tang at UCLA on pericyclases and pericyclic reactions in nature.



Joshua Misa was born and raised in Riverside, CA. He received his B.S. in Chemical Engineering with an emphasis in Biochemical Engineering from the University of California, Riverside (UCR) in 2018, graduating *magna cum laude*. At UCR he worked in Prof. Ian Wheeldon's lab on the development of CRISPR tools for engineering non-conventional yeasts as a Chancellor's Research Fellow. Joshua is currently a Ph.D. candidate working under Prof. Yi Tang on developing yeast-based platforms for production of plant natural products and new, biosynthetic analogues.



Yi Tang received his undergraduate degree in Chemical Engineering and Material Science from Penn State University. He received his Ph.D. in Chemical Engineering from California Institute of Technology in 2002. After NIH postdoctoral training in Chemical Biology at Stanford University, he started his independent career at the University of California Los Angeles in 2004. He is currently Professor in the Department of Chemical and Biomolecular Engineering at UCLA, and holds joint appointments in the Department of Chemistry and Biochemistry; and Department of Bioengineering. His lab is interested in natural product biosynthesis, biocatalysis and protein engineering.



John M. Billingsley grew up in Cambria, NY, and attended the University at Buffalo pursuing a B.S. in Chemical Engineering. There, John developed a budding interest in natural product biosynthesis during an internship in Prof. Andrew Gulick's lab at the Hauptmann-Woodward Medical Research Institute. John received a Ph.D. in Chemical Engineering from UCLA in 2019 under the guidance of Yi Tang, where they investigated and engineered the biosynthesis of plant and fungal alkaloids. John currently lives in West Hollywood, is a Visiting Scientist at UCLA and Principal Scientist at Invizyne Technologies in Monrovia, CA.

9 References

1. Merlin MD, *Econ. Bot.*, 2003, 57, 295–323.
2. Guerra-Doce E, *Time Mind*, 2015, 8, 91–112.
3. Buenz EJ, Verpoorte R and Bauer BA, *Annu. Rev. Pharmacol. Toxicol.*, 2018, 58, 509–530. [PubMed: 29077533]
4. Efferth T, Banerjee M, Paul NW, Abdelfatah S, Arend J, Elhassan G, Hamdoun S, Hamm R, Hong C, Kadioglu O, Naß J, Ochwangi D, Ooko E, Ozenver N, Saeed MEM, Schneider M, Seo EJ, Wu CF, Yan G, Zeino M, Zhao Q, Abu-Darwish MS, Andersch K, Alexie G, Bessarab D, Bhakta-Guha D, Bolzani V, Dapat E, Donenko FV, Efferth M, Greten HJ, Gunatilaka L, Hussein AA, Karadeniz A, Khalid HE, Kuete V, Lee IS, Liu L, Midiwo J, Mora R, Nakagawa H, Ngassapa O, Noysang C, Omosa LK, Roland FH, Shahat AA, Saab A, Saeed EM, Shan L and Titinchi SJJ, *Phytomedicine*, 2016, 23, 166–173. [PubMed: 26926178]
5. George JR, Michaels TI, Sevelius J and Williams MT, *J. Psychedelic Stud.*, 2019, 4, 4–15.
6. Gootenberg P, *Am. Anthropol.*, 2005, 107, 152–153.
7. Kean S, *Science (80-.)*, 2019, 364, 16–20.
8. Provine DM, *Annu. Rev. Law Soc. Sci.*, 2011, 7, 41–60.
9. Sullivan RJ and Hagen EH, *Addiction*, 2002, 97, 389–400. [PubMed: 11964056]
10. Martini A, *J. Wine Res.*, 1993, 4, 165–176.
11. Brito GSL, *Cad. Saude Publica*, 1994, 10, 403–405.
12. Dias DA, Urban S and Roessner U, *Metabolites*, 2012, 2, 303–336. [PubMed: 24957513]
13. Robinson R, *J. Chem. Soc. Trans.*, 1917, 111, 762–768.
14. Kornfeld EC, Fornefeld EJ, Bruce Kline G, Mann MJ, Morrison DE, Jones RG and Woodward RB, *J. Am. Chem. Soc.*, 1956, 78, 3087–3114.
15. Walsh CT and Tang Y, *Natural Product Biosynthesis: Chemical and Enzymatic Logic*, Royal Society of Chemistry, 2017.
16. Pluskal T and Weng JK, *Chem. Soc. Rev.*, 2018, 47, 1592–1637. [PubMed: 28933478]
17. Valenstein ES, *Brain Cogn.*, 2002, 49, 73–95. [PubMed: 12027394]
18. Murnane KS, in *Progress in Brain Research*, 2018, vol. 242, pp. 25–67. [PubMed: 30471682]
19. Nadim F and Bucher D, *Curr. Opin. Neurobiol.*, 2014, 29, 48–56. [PubMed: 24907657]
20. Bracco L and Kearsley J, *Trends Biotechnol.*, 2003, 21, 346–353. [PubMed: 12902171]
21. Contet C, Kieffer BL and Befort K, *Curr. Opin. Neurobiol.*, 2004, 14, 370–378. [PubMed: 15194118]
22. Roth BL, Baner K, Westkaemper R, Siebert D, Rice KC, Steinberg SA, Ernsberger P and Rothman RB, *Proc. Natl. Acad. Sci. U. S. A.*, 2002, 99, 11934–11939. [PubMed: 12192085]

23. Nutt D, PLOS Biol., 2015, 13, e1002047. [PubMed: 25625189]
24. Carhart-Harris RL, Bolstridge M, Day CMJ, Rucker J, Watts R, Erritzoe DE, Kaelen M, Giribaldi B, Bloomfield M, Pilling S, Rickard JA, Forbes B, Feilding A, Taylor D, Curran HV and Nutt DJ, Psychopharmacology (Berl)., 2018, 235, 399–408. [PubMed: 29119217]
25. Carhart-Harris RL, Leech R, Williams TM, Erritzoe D, Abbasi N, Bargiotas T, Hobden P, Sharp DJ, Evans J, Feilding A, Wise RG and Nutt DJ, Br. J. Psychiatry, 2012, 200, 238–244. [PubMed: 22282432]
26. Cameron LP, Tombari RJ, Lu J, Pell AJ, Hurley ZQ, Ehinger Y, Vargas MV, McCarroll MN, Taylor JC, Myers-Turnbull D, Liu T, Yaghoobi B, Laskowski LJ, Anderson EI, Zhang G, Viswanathan J, Brown BM, Tjia M, Dunlap LE, Rabow ZT, Fiehn O, Wulff H, McCorvy JD, Lein PJ, Kokel D, Ron D, Peters J, Zuo Y and Olson DE, Nature, 2021, 589, 474–479. [PubMed: 33299186]
27. Salim V, Yu F, Altarejos J and De Luca V, Plant J., 2013, 76, 754–765. [PubMed: 24103035]
28. Barone JJ and Roberts HR, Food Chem. Toxicol, 1996, 34, 119–129. [PubMed: 8603790]
29. Fiore MC, Smith SS, Jorenby DE and Baker TB, JAMA J. Am. Med. Assoc, 1994, 271, 1940–1947.
30. Grinspoon L and Bakalar JB, J. Ethnopharmacol, 1981, 3, 149–159. [PubMed: 7017287]
31. Amin MR and Ali DW, in Advances in Experimental Medicine and Biology, 2019, vol. 1162, pp. 151–165. [PubMed: 31332738]
32. Rosenblum A, Marsch LA, Joseph H and Portenoy RK, Exp. Clin. Psychopharmacol, 2008, 16, 405–416. [PubMed: 18837637]
33. Iijima Y, Gang DR, Fridman E, Lewinsohn E and Pichersky E, Plant Physiol., 2004, 134, 370–379. [PubMed: 14657409]
34. Tang M-C, Zou Y, Watanabe K, Walsh CT and Tang Y, Chem. Rev, 2017, 117, 5226–5333. [PubMed: 27936626]
35. Walsh CT and Moore BS, Angew. Chemie Int. Ed, 2019, 58, 6846–6879.
36. Lin C-I, McCarty RM and Liu H, Angew. Chemie Int. Ed, 2017, 56, 3446–3489.
37. Walsh CT and Tang Y, The Chemical Biology of Human Vitamins, Royal Society of Chemistry, 2018.
38. Blicke FF, Org. React, 2011, 303–341.
39. Leete E, Planta Med, 1990, 56, 339–352. [PubMed: 2236285]
40. Kohnen-Johannsen K and Kayser O, Molecules, 2019, 24, 796.
41. Allen JRF and Holmstedt BR, Phytochemistry, 1980, 19, 1573–1582.
42. Maresh JJ, Giddings L-A, Friedrich A, Loris EA, Panjekar S, Trout BL, Stöckigt J, Peters B and O'Connor SE, J. Am. Chem. Soc, 2008, 130, 710–723. [PubMed: 18081287]
43. Ilari A, Franceschini S, Bonamore A, Arengi F, Botta B, Macone A, Pasquo A, Bellucci L and Boffi A, J. Biol. Chem, 2009, 284, 897–904. [PubMed: 19004827]
44. Walsh CT, Tu BP and Tang Y, Chem. Rev, 2018, 118, 1460–1494. [PubMed: 29272116]
45. Miettinen K, Dong L, Navrot N, Schneider T, Burlat V, Pollier J, Woittiez L, Van Der Krol S, Luga R, Ilc T, Verpoorte R, Oksman-Caldentey KM, Martinoia E, Bouwmeester H, Goossens A, Memelink J and Werck-Reichhart D, Nat. Commun, 2014, 5, 1–12.
46. Metzger U, Schall C, Zoicher G, Unsöld I, Stec E, Li S-M, Heide L and Stehle T, Proc. Natl. Acad. Sci, 2009, 106, 14309 LP–14314. [PubMed: 19706516]
47. Tanner ME, Nat. Prod. Rep, 2015, 32, 88–101. [PubMed: 25270661]
48. Grundmann A and Li SM, Microbiology, 2005, 151, 2199–2207. [PubMed: 16000710]
49. Kato H, Yoshida T, Tokue T, Nojiri Y, Hirota H, Ohta T, Williams RM and Tsukamoto S, Angew. Chemie - Int. Ed, 2007, 46, 2254–2256.
50. Li SM, Nat. Prod. Rep, 2010, 27, 57–78. [PubMed: 20024094]
51. Walsh CT, ACS Chem. Biol, 2014, 9, 2718–2728. [PubMed: 25303280]
52. Lin HC, Chiou G, Chooi YH, McMahon TC, Xu W, Garg NK and Tang Y, Angew. Chemie - Int. Ed, 2015, 54, 3004–3007.
53. Valliere MA, Korman TP, Woodall NB, Khitrov GA, Taylor RE, Baker D and Bowie JU, Nat. Commun, 2019, 10, 565. [PubMed: 30718485]

54. Walsh CT and Wencewicz TA, *Nat. Prod. Rep.*, 2013, 30, 175–200. [PubMed: 23051833]
55. Yamamoto H, Katano N, Ooi A and Inoue K, *Phytochemistry*, 2000, 53, 7–12. [PubMed: 10656401]
56. Irmeler S, Schröder G, St-Pierre B, Crouch NP, Hotze M, Schmidt J, Strack D, Matern U and Schröder J, *Plant J.*, 2000, 24, 797–804. [PubMed: 11135113]
57. Kishimoto S, Sato M, Tsunematsu Y and Watanabe K, *Mol.*, 2016, 21.
58. Gesell A, Rolf M, Ziegler J, Chávez MLD, Huang FC and Kutchan TM, *J. Biol. Chem.*, 2009, 284, 24432–24442. [PubMed: 19567876]
59. Shipkowski KA, Betz JM, Birnbaum LS, Bucher JR, Coates PM, Hopp DC, MacKay D, Oketch-Rabah H, Walker NJ, Welch C and Rider CV, *Food Chem. Toxicol.*, 2018, 118, 963–971. [PubMed: 29626579]
60. Hollingsworth RG, Armstrong JW and Campbell E, *Ann. Appl. Biol.*, 2003, 142, 91–97.
61. Leonard E, Runguphan W, O'Connor S and Prather KJ, *Nat. Chem. Biol.*, 2009, 5, 292–300. [PubMed: 19377455]
62. Cravens A, Payne J and Smolke CD, *Nat. Commun.*, 2019, 10, 2142. [PubMed: 31086174]
63. Gibson DG, Young L, Chuang RY, Venter JC, Hutchison CA and Smith HO, *Nat. Methods*, 2009, 6, 343–345. [PubMed: 19363495]
64. Gresham D, Dunham MJ and Botstein D, *Nat. Rev. Genet.*, 2008, 9, 291–302. [PubMed: 18347592]
65. Urnov FD, Rebar EJ, Holmes MC, Zhang HS and Gregory PD, *Nat. Rev. Genet.*, 2010, 11, 636–646. [PubMed: 20717154]
66. Kosuri S and Church GM, *Nat. Methods*, 2014, 11, 499–507. [PubMed: 24781323]
67. Wang Z, Gerstein M and Snyder M, *Nat. Rev. Genet.*, 2009, 10, 57–63. [PubMed: 19015660]
68. Hsu PD, Lander ES and Zhang F, *Cell*, 2014, 157, 1262–1278. [PubMed: 24906146]
69. Khalil AS and Collins JJ, *Nat. Rev. Genet.*, 2010, 11, 367–379. [PubMed: 20395970]
70. Osbourn A, *Plant Physiol.*, 2010, 154, 531–535. [PubMed: 20921179]
71. Field B, Fiston-Lavier AS, Kemen A, Geisler K, Quesneville H and Osbourn AE, *Proc. Natl. Acad. Sci. U. S. A.*, 2011, 108, 16116–16121. [PubMed: 21876149]
72. Liu Z, Cheema J, Vigouroux M, Hill L, Reed J, Paajanen P, Yant L and Osbourn A, *Nat. Commun.*, 2020, 11, 5354. [PubMed: 33097700]
73. Srinivasan P and Smolke CD, *Nature*, 2020, 585, 614–619. [PubMed: 32879484]
74. Dastmalchi M, Chen X, Hagel JM, Chang L, Chen R, Ramasamy S, Yeaman S and Facchini PJ, *Nat. Chem. Biol.*, 2019, 15, 384–390. [PubMed: 30886433]
75. Luo X, Reiter MA, d’Espaux L, Wong J, Denby CM, Lechner A, Zhang Y, Grzybowski AT, Harth S, Lin W, Lee H, Yu C, Shin J, Deng K, Benites VT, Wang G, Baidoo EEK, Chen Y, Dev I, Petzold CJ and Keasling JD, *Nature*, 2019, 567, 123–126. [PubMed: 30814733]
76. Brown S, Clastre M, Courdavault V and O'Connor SE, *Proc. Natl. Acad. Sci. U. S. A.*, 2015, 112, 3205–3210. [PubMed: 25675512]
77. Galanie S, Thodey K, Trenchard IJ, Interrante MF and Smolke CD, *Science (80-.)*, 2015, 349, 1095–1100.
78. Deloache WC, Russ ZN, Narcross L, Gonzales AM, Martin VJJ and Dueber JE, *Nat. Chem. Biol.*, 2015, 11, 465–471. [PubMed: 25984720]
79. Packer MS and Liu DR, *Nat. Rev. Genet.*, 2015, 16, 379–394. [PubMed: 26055155]
80. Liu N, Santala S and Stephanopoulos G, *Curr. Opin. Biotechnol.*, 2020, 62, 15–21. [PubMed: 31513988]
81. Adams AM, Kaplan NA, Wei Z, Brinton JD, Monnier CS, Enacopol AL, Ramelot TA and Jones JA, *Metab. Eng.*, 2019, 56, 111–119. [PubMed: 31550507]
82. Billingsley JM, DeNicola AB, Barber JS, Tang MC, Horecka J, Chu A, Garg NK and Tang Y, *Metab. Eng.*, 2017, 44, 117–125. [PubMed: 28939278]
83. Copeland WB, Bartley BA, Chandran D, Galdzicki M, Kim KH, Sleight SC, Maranas CD and Sauro HM, *Metab. Eng.*, 2012, 14, 270–280. [PubMed: 22629572]
84. Finnigan W, Hepworth LJ, Flitsch SL and Turner NJ, *Nat. Catal.*, 2021, 4, 98–104. [PubMed: 33604511]

85. Sheppard MJ, Kunjapur AM, Wenck SJ and Prather KLJ, *Nat. Commun*, 2014, 5, 5031. [PubMed: 25248664]
86. Bachmann BO, *Nat. Chem. Biol*, 2010, 6, 390–393. [PubMed: 20479744]
87. Casini A, Chang FY, Eluere R, King AM, Young EM, Dudley QM, Karim A, Pratt K, Bristol C, Forget A, Ghodasara A, Warden-Rothman R, Gan R, Cristofaro A, Borujeni AE, Ryu MH, Li J, Kwon YC, Wang H, Tatsis E, Rodriguez-Lopez C, O'Connor S, Medema MH, Fischbach MA, Jewett MC, Voigt C and Gordon DB, *J. Am. Chem. Soc.*, 2018, 140, 4302–4316. [PubMed: 29480720]
88. Carbonell P, Le Feuvre R, Takano E and Scrutton NS, *Synth. Biol*, 2020, 5, ysaa020.
89. Li M, Sun Y, Pan SA, Deng WW, Yu O and Zhang Z, *RSC Adv.*, 2017, 7, 56382–56389.
90. Nakagawa A, Matsumura E, Koyanagi T, Katayama T, Kawano N, Yoshimatsu K, Yamamoto K, Kumagai H, Sato F and Minami H, *Nat. Commun*, 2016, 7, 10390. [PubMed: 26847395]
91. Milne N, Thomsen P, Mølgaard Knudsen N, Rubaszka P, Kristensen M and Borodina I, *Metab. Eng.*, 2020, 60, 25–36. [PubMed: 32224264]
92. McKeague M, Wang YH, Cravens A, Win MN and Smolke CD, *Metab. Eng.*, 2016, 38, 191–203. [PubMed: 27519552]
93. Skellam E, *Trends Biotechnol.*, 2019, 37, 416–427. [PubMed: 30316556]
94. Hoefgen S, Lin J, Fricke J, Stroe MC, Mattern DJ, Kufs JE, Hortschansky P, Brakhage AA, Hoffmeister D and Valiante V, *Metab. Eng.*, 2018, 48, 44–51. [PubMed: 29842926]
95. Ohashi M, Liu F, Hai Y, Chen M, Tang M, Yang Z, Sato M, Watanabe K, Houk KN and Tang Y, *Nature*, 2017, 549, 502. [PubMed: 28902839]
96. Reed J, Stephenson MJ, Miettinen K, Brouwer B, Leveau A, Brett P, Goss RJM, Goossens A, O'Connell MA and Osbourn A, *Metab. Eng.*, 2017, 42, 185–193. [PubMed: 28687337]
97. Lau W and Sattely ES, *Science (80-.)*, 2015, 349, 1224–1228.
98. Pluskal T, Torrens-Spence MP, Fallon TR, De Abreu A, Shi CH and Weng JK, *Nat. Plants*, 2019, 5, 867–878. [PubMed: 31332312]
99. Nett RS, Lau W and Sattely ES, *Nature*, 2020, 584, 148–153. [PubMed: 32699417]
100. Opgenorth PH, Korman TP and Bowie JU, *Nat. Chem. Biol*, 2016, 12, 393–395. [PubMed: 27065234]
101. Korman TP, Opgenorth PH and Bowie JU, *Nat. Commun*, 2017, 8, 15526. [PubMed: 28537253]
102. Valliere MA, Korman TP, Arbing MA and Bowie JU, *Nat. Chem. Biol*, 2020, 16, 1427–1433. [PubMed: 32839605]
103. Roze LV, Chanda A and Linz JE, *Fungal Genet. Biol*, 2011, 48, 35–48. [PubMed: 20519149]
104. Dueber JE, Wu GC, Malmirchegini GR, Moon TS, Petzold CJ, Ullal AV, Prather KLJ and Keasling JD, *Nat. Biotechnol.*, 2009, 27, 753–759. [PubMed: 19648908]
105. Hammer SK and Avalos JL, *Nat. Chem. Biol*, 2017, 13, 823–832. [PubMed: 28853733]
106. Renault H, Bassard JE, Hamberger B and Werck-Reichhart D, *Curr. Opin. Plant Biol*, 2014, 19, 27–34. [PubMed: 24709279]
107. Leonard E and Koffas MAG, *Appl. Environ. Microbiol.*, 2007, 73, 7246–7251. [PubMed: 17905887]
108. Ping Y, Li X, Xu B, Wei W, Kai G, Zhou Z and Xiao Y, *ACS Synth. Biol*, 2019, 8, 257–263. [PubMed: 30691267]
109. Hawkins KM and Smolke CD, *Nat. Chem. Biol*, 2008, 4, 564–573. [PubMed: 18690217]
110. Bowie JU, Sherkhanov S, Korman TP, Valliere MA, Opgenorth PH and Liu H, *Trends Biotechnol.*, 2020, 38, 766–778. [PubMed: 31983463]
111. Clomburg JM, Crumbley AM and Gonzalez R, *Science (80-.)*, 2017, 355, aag0804.
112. Kumar V, Bhalla A and Rathore AS, *Biotechnol. Prog.*, 2014, 30, 86–99. [PubMed: 24123959]
113. Gilman J, Walls L, Bandiera L and Menolascina F, *ACS Synth. Biol*, 2021, 10, 1–18. [PubMed: 33406821]
114. Xia P-F, Ling H, Foo JL and Chang MW, *Biotechnol. Adv.*, 2019, 37, 107393. [PubMed: 31051208]

115. Win MN, Klein JS and Smolke CD, *Nucleic Acids Res.*, 2006, 34, 5670–5682. [PubMed: 17038331]
116. Portnoy VA, Bezdán D and Zengler K, *Curr. Opin. Biotechnol.*, 2011, 22, 590–594. [PubMed: 21497080]
117. Nichols DE, *Pharmacol. Rev.*, 2016, 68, 264–355. [PubMed: 26841800]
118. O’Neill-Dee C, Spiller HA, Casavant MJ, Kistangari S, Chounthirath T, Smith GA, O’Neill-Dee C, Spiller HA, Casavant MJ, Kistangari S, Chounthirath T and Smith GA, *Clin. Toxicol.*, 2020, 58, 813–820.
119. Tyš F, Pálení ek T and Horá ek J, *Eur. Neuropsychopharmacol.*, 2014, 24, 342–356. [PubMed: 24444771]
120. Halberstadt AL, *Behav. Brain Res.*, 2015, 277, 99–120. [PubMed: 25036425]
121. Nichols DE and Nichols CD, *Chem. Rev.*, 2008, 108, 1614–1641. [PubMed: 18476671]
122. Beliveau V, Ganz M, Feng L, Ozenne B, Højgaard L, Fisher PM, Svarer C, Greve DN and Knudsen GM, *J. Neurosci.*, 2017, 37, 120–128. [PubMed: 28053035]
123. López-Giménez JF and González-Maeso J, in *Current Topics in Behavioral Neurosciences*, Springer Verlag, 2017, vol. 36, pp. 45–73.
124. Nichols DE, *Wiley Interdiscip. Rev. Membr. Transp. Signal.*, 2012, 1, 559–579.
125. Wacker D, Wang S, McCorvy JD, Betz RM, Venkatakrishnan AJ, Levit A, Lansu K, Schools ZL, Che T, Nichols DE, Shoichet BK, Dror RO and Roth BL, *Cell*, 2017, 168, 377–389.e12. [PubMed: 28129538]
126. Carbonaro TM and Gatch MB, *Brain Res. Bull.*, 2016, 126, 74–88. [PubMed: 27126737]
127. Miller MJ, Albarracín-Jordan J, Moore C and Capriles JM, *Proc. Natl. Acad. Sci. U. S. A.*, 2019, 166, 11207–11212.
128. Carod-Artal FJ, *Neurol. (English Ed)*, 2015, 30, 42–49.
129. Weil AT and Davis W, *J. Ethnopharmacol.*, 1994, 41, 1–8. [PubMed: 8170151]
130. Most A, *Bufo alvarius: the psychedelic toad of the Sonoran Desert*, Venom Press, 1984.
131. de Lima OG, *Arq. do Inst. Pesqui. Agronômicas*, 1946, 4, 45–80.
132. Szára S, *Experientia*, 1956, 12, 441–442. [PubMed: 13384414]
133. Barker SA, *Front. Neurosci.*, 2018, 12, 536. [PubMed: 30127713]
134. Szabo A, Kovacs A, Riba J, Djurovic S, Rajnavolgyi E and Frecska E, *Front. Neurosci.*, 2016, 10, 423. [PubMed: 27683542]
135. Cameron LP, Benson CJ, Dunlap LE and Olson DE, *ACS Chem. Neurosci.*, 2018, 9, 1582–1590. [PubMed: 29664276]
136. Ly C, Greb AC, Cameron LP, Wong JM, Barragan EV, Wilson PC, Burbach KF, Soltanzadeh Zarandi S, Sood A, Paddy MR, Duim WC, Dennis MY, McAllister AK, Ori-McKenney KM, Gray JA and Olson DE, *Cell Rep.*, 2018, 23, 3170–3182. [PubMed: 29898390]
137. Djura P, Stierle DB, Sullivan B, Faulkner DJ, Arnold E and Clardy J, *J. Org. Chem.*, 1980, 45, 1435–1441.
138. Longeon A, Copp BR, Quévrain E, Roué M, Kientz B, Cresteil T, Petek S, Debitus C and Bourguet-Kondracki ML, *Mar. Drugs*, 2011, 9, 879–888. [PubMed: 21673896]
139. Kochanowska AJ, Rao KV, Childress S, El-Alfy A, Matsumoto RR, Kelly M, Stewart GS, Sufka KJ and Hamann MT, *J. Nat. Prod.*, 2008, 71, 186–189. [PubMed: 18217716]
140. LOVENBERG W, WEISSBACH H and UDENFRIEND S, *J. Biol. Chem.*, 1962, 237, 89–93. [PubMed: 14466899]
141. Axelrod J, *Science (80-.)*, 1961, 134, 343–343.
142. Thompson MA and Weinshilboum RM, *J. Biol. Chem.*, 1998, 273, 34502–34510. [PubMed: 9852119]
143. Hofmann A, Heim R, Brack A, Kobel H, Frey A, Ott H, Petrzilka T and Troxler F, *Helv. Chim. Acta*, 1959, 42, 1557–1572.
144. Nichols DE, *J. Antibiot. (Tokyo)*, 2020, 73, 679–686. [PubMed: 32398764]
145. Hasler F, Bourquin D, Brenneisen R and Vollenweider FX, *J. Pharm. Biomed. Anal.*, 2002, 30, 331–339. [PubMed: 12191719]

146. Hasler F, Grimberg U, Benz MA, Huber T and Vollenweider FX, *Psychopharmacology (Berl.)*, 2004, 172, 145–156. [PubMed: 14615876]
147. Mahapatra A and Gupta R, *Ther. Adv. Psychopharmacol.*, 2017, 7, 54–56. [PubMed: 28101325]
148. Grob CS, Danforth AL, Chopra GS, Hagerty M, McKay CR, Halberstad AL and Greer GR, *Arch. Gen. Psychiatry*, 2011, 68, 71–78. [PubMed: 20819978]
149. Johnson MW, Garcia-Romeu A, Cosimano MP and Griffiths RR, *J. Psychopharmacol.*, 2014, 28, 983–992. [PubMed: 25213996]
150. Agurell S and Nilsson JL, *Acta Chem. Scand.*, 1968, 22, 1210–1218. [PubMed: 5750023]
151. Fricke J, Blei F and Hoffmeister D, *Angew. Chemie - Int. Ed.*, 2017, 56, 12352–12355.
152. Wakimoto T, Egami Y, Nakashima Y, Wakimoto Y, Mori T, Awakawa T, Ito T, Kenmoku H, Asakawa Y, Piel J and Abe I, *Nat. Chem. Biol.*, 2014, 10, 648–655. [PubMed: 24974231]
153. Zhu S, Hegemann JD, Fage CD, Zimmermann M, Xie X, Linne U and Marahiel MA, *J. Biol. Chem.*, 2016, 291, 13662–13678. [PubMed: 27151214]
154. Reynolds HT, Vijayakumar V, Gluck-Thaler E, Korotkin HB, Matheny PB and Slot JC, *Evol. Lett.*, 2018, 2, 88–101. [PubMed: 30283667]
155. Awan AR, Winter JM, Turner D, Shaw WM, Suz LM, Bradshaw AJ, Ellis T and Dentinger BTM, *bioRxiv*, 2018, 374199.
156. Paddon CJ, Westfall PJ, Pitera DJ, Benjamin K, Fisher K, McPhee D, Leavell MD, Tai A, Main A, Eng D, Polichuk DR, Teoh KH, Reed DW, Treynor T, Lenihan J, Jiang H, Fleck M, Bajad S, Dang G, Dengrove D, Diola D, Dorin G, Ellens KW, Fickes S, Galazzo J, Gaucher SP, Geistlinger T, Henry R, Hepp M, Horning T, Iqbal T, Kizer L, Lieu B, Melis D, Moss N, Regentin R, Secrest S, Tsuruta H, Vazquez R, Westblade LF, Xu L, Yu M, Zhang Y, Zhao L, Lievens J, Covello PS, Keasling JD, Reiling KK, Renninger NS and Newman JD, *Nature*, 2013, 496, 528–532. [PubMed: 23575629]
157. Osamu S, Katsumata Y and Masakazu O, *Biochem. Pharmacol.*, 1981, 30, 1353–1358. [PubMed: 6791651]
158. McKenna D and Riba J, in *Current Topics in Behavioral Neurosciences*, Springer Verlag, 2018, vol. 36, pp. 283–311. [PubMed: 28401525]
159. Estrella-Parra EA, Almanza-Pérez JC and Alarcón-Aguilar FJ, *Nat. Products Bioprospect*, 2019, 9, 251–265.
160. Ayala Flores F and Lewis WH, *Econ. Bot.*, 1978, 32, 154–156.
161. Morales-García JA, De La Fuente Revenga M, Alonso-Gil S, Rodríguez-Franco MI, Feilding A, Perez-Castillo A and Riba J, *Sci. Rep.*, 2017, 7, 1–13. [PubMed: 28127051]
162. Callaway JC, Brito GS and Neves ES, *J. Psychoactive Drugs*, 2005, 37, 145–150. [PubMed: 16149327]
163. Brito-da-costa AM, Dias-da-silva D, Gomes NGM, Dinis-oliveira RJ and Madureira-carvalho Á, *Pharmaceuticals*, 2020, 13, 1–39.
164. Blei F, Dörner S, Fricke J, Baldeweg F, Trottmann F, Komor A, Meyer F, Hertweck C and Hoffmeister D, *Chem. - A Eur. J.*, 2020, 26, 729–734.
165. Stolle K and Gröger D, *Arch. Pharm. (Weinheim)*, 1968, 301, 561–571.
166. Nettleship L and Slaytor M, *Phytochemistry*, 1974, 13, 735–742.
167. Dewick PM, *Medicinal Natural Products: A Biosynthetic Approach: Third Edition*, Second., 2009.
168. Nichols DE, *Pharmacol. Ther.*, 2004, 101, 131–181. [PubMed: 14761703]
169. Lorenz N, Haarmann T, Pažoutová S, Jung M and Tudzynski P, *Phytochemistry*, 2009, 70, 1822–1832. [PubMed: 19695648]
170. Wallwey C and Li SM, *Nat. Prod. Rep.*, 2011, 28, 496–510. [PubMed: 21186384]
171. van Dongen PWJ and de Groot ANJA, *Eur. J. Obstet. Gynecol. Reprod. Biol.*, 1995, 60, 109–116. [PubMed: 7641960]
172. Jakubczyk D, Cheng JZ and O'Connor SE, *Nat. Prod. Rep.*, 2014, 31, 1328–1338. [PubMed: 25164781]

173. Gerhards N, Neubauer L, Tudzynski P and Li SM, *Toxins (Basel)*, 2014, 6, 3281–3295. [PubMed: 25513893]
174. Sharma N, Sharma V, Manikyam H and Krishna A, *European J. Med. Plants*, 2016, 14, 1–17.
175. Gröcer D and Floss HG, *Alkaloids Chem. Biol*, 1998, 50, 171–218.
176. Lee SL, Floss HG and Heinstein P, *Arch. Biochem. Biophys*, 1976, 177, 84–94. [PubMed: 999297]
177. Yin WB, Grundmann A, Cheng J and Li SM, *J. Biol. Chem*, 2009, 284, 100–109. [PubMed: 19001367]
178. Winkelblech J and Li SM, *ChemBioChem*, 2014, 15, 1030–1039. [PubMed: 24692239]
179. Schultz AW, Lewis CA, Luzung MR, Baran PS and Moore BS, *J. Nat. Prod*, 2010, 73, 373–377. [PubMed: 20055491]
180. Yu X, Liu Y, Xie X, Zheng XD and Li SM, *J. Biol. Chem*, 2012, 287, 1371–1380. [PubMed: 22123822]
181. Fan A, Chen H, Wu R, Xu H and Li SM, *Appl. Microbiol. Biotechnol*, 2014, 98, 10119–10129. [PubMed: 24970457]
182. Li SM, *Appl. Microbiol. Biotechnol*, 2009, 84, 631–639. [PubMed: 19633837]
183. Mori T, *J. Nat. Med*, 2020, 74, 501–512. [PubMed: 32180104]
184. Tudzynski P, Hölter K, Correia T, Arntz C, Grammel N and Keller U, *Mol. Gen. Genet*, 1999, 261, 133–141. [PubMed: 10071219]
185. Haarmann T, Machado C, Lübbe Y, Correia T, Schardl CL, Panaccione DG and Tudzynski P, *Phytochemistry*, 2005, 66, 1312–1320. [PubMed: 15904941]
186. Rigbers O and Li SM, *J. Biol. Chem*, 2008, 283, 26859–26868. [PubMed: 18678866]
187. Goetz KE, Coyle CM, Cheng JZ, O'Connor SE and Panaccione DG, *Curr. Genet*, 2011, 57, 201–211. [PubMed: 21409592]
188. Lorenz N, Olšovská J, Šulc M and Tudzynski P, *Appl. Environ. Microbiol*, 2010, 76, 1822–1830. [PubMed: 20118373]
189. Ryan KL, Moore CT and Panaccione DG, *Toxins (Basel)*, 2013, 5, 445–455. [PubMed: 23435153]
190. Nielsen CA, Folly C, Hatsch A, Molt, Schröder H, O'Connor SE and Naesby, *Microb. Cell Fact*, 2014, 13, 95. [PubMed: 25112180]
191. Chen KL, Lai CY, Pham MT, Chein RJ, Tang Y and Lin HC, *Org. Lett*, 2020, 22, 3302–3306. [PubMed: 32243182]
192. Yao Y, An C, Evans D, Liu W, Wang W, Wei G, Ding N, Houk KN and Gao SS, *J. Am. Chem. Soc*, 2019, 141, 17517–17521. [PubMed: 31621316]
193. Iijima Y, Gang DR, Fridman E, Lewinsohn E and Pichersky E, *Plant Physiol.*, 2004, 134, 370–379. [PubMed: 14657409]
194. Wallwey C, Heddergott C, Xie X, Brakhage AA and Li SM, *Microbiol. (United Kingdom)*, 2012, 158, 1634–1644.
195. Coyle CM, Cheng JZ, O'Connor SE and Panaccione DG, *Appl. Environ. Microbiol*, 2010, 76, 3898–3903. [PubMed: 20435769]
196. Cheng JZ, Coyle CM, Panaccione DG and O'Connor SE, *J. Am. Chem. Soc*, 2010, 132, 12835–12837. [PubMed: 20735127]
197. Jakubczyk D, Caputi L, Hatsch A, Nielsen CAF, Diefenbacher M, Klein J, Molt A, Schröder H, Cheng JZ, Naesby M and O'Connor SE, *Angew. Chemie*, 2015, 127, 5206–5210.
198. Matuschek M, Wallwey C, Xie X and Li SM, *Org. Biomol. Chem*, 2011, 9, 4328–4335. [PubMed: 21494745]
199. Maier W, Schumann B and Gröger D, *J. Basic Microbiol*, 1988, 28, 83–93.
200. Haarmann T, Ortel I, Tudzynski P and Keller U, *ChemBioChem*, 2006, 7, 645–652. [PubMed: 16538694]
201. Robinson SL and Panaccione DG, *Appl. Environ. Microbiol*, 2014, 80, 6465–6472. [PubMed: 25107976]

202. Schardl CL, Panaccione DG and Tudzynski P, *Alkaloids Chem. Biol.*, 2006, 63, 45–86. [PubMed: 17133714]
203. Schwab JM and Henderson BS, *Chem. Rev.*, 1990, 90, 1203–1245.
204. Chen J-JJ, Han M-YY, Gong T, Yang J-LL and Zhu P, *Recent progress in ergot alkaloid research*, Royal Society of Chemistry, 2017, vol. 7.
205. Bruhn JG, Lindgren JE, Holmstedt B and Adovasio JM, *Science* (80-), 1978, 199, 1437–1438.
206. Braun U and Kalbhen D, *Pharmacology*, 1973, 9, 312–316. [PubMed: 4737998]
207. Stein U, Greyer H and Hentschel H, *Forensic Sci. Int.*, 2001, 118, 87–90. [PubMed: 11343860]
208. Shulgin AT, *Nature*, 1964, 201, 1120–1121. [PubMed: 14152788]
209. Shulgin AT and Shulgin A, *Pihkal : a chemical love story*, Transform Press, Berkeley, CA, 1991.
210. Shulgin AT and Shulgin A, *Tihkal : the continuation*, Transform Press, Berkeley, CA, 1997.
211. AXELROD J and TOMCHICK R, *J. Biol. Chem.*, 1958, 233, 702–705. [PubMed: 13575440]
212. Kopin IJ, in *Catecholamines*, Springer Berlin Heidelberg, Berlin, Heidelberg, 1972, pp. 270–282.
213. Benington F and Morin RD, *Experientia*, 1968, 24, 33–34. [PubMed: 5637608]
214. Friedhoff AJ, Schweitzer JW and Miller J, *Nature*, 1972, 237, 454–455. [PubMed: 4557472]
215. Agurell S, Lundström J and Sandberg F, *Tetrahedron Lett.*, 1967, 8, 2433–2435.
216. Kapadia GJ, Vaishnav YN and Fayez MBE, *J. Pharm. Sci.*, 1969, 58, 1157–1159. [PubMed: 5346086]
217. Lundström J and Agurell S, *Tetrahedron Lett.*, 1969, 10, 3371–3374.
218. Lundström J, *Acta Pharm. Suec.*, 1970, 7, 651–666. [PubMed: 5511715]
219. Lundström J, *Acta Chem. Scand.*, 1971, 25, 3489–3499. [PubMed: 5144505]
220. Ibarra-Laclette E, Zamudio-Hernández F, Pérez-Torres CA, Albert VA, Ramírez-Chávez E, Molina-Torres J, Fernández-Cortes A, Calderón-Vázquez C, Olivares-Romero JL, Herrera-Estrella A and Herrera-Estrella L, *BMC Genomics*, 2015, 16, 657. [PubMed: 26330142]
221. Lundström J, *Acta Chem. Scand.*, 1971, 25, 3489–3499. [PubMed: 5144505]
222. Krogsgaard-Larsen P, Hjeds H, Curtis DR, Lodge D and Johnston GAR, *J. Neurochem.*, 1979, 32, 1717–1724. [PubMed: 448364]
223. Chandra D, Halonen LM, Linden AM, Procaccini C, Hellsten K, Homanics GE and Korpi ER, *Neuropsychopharmacology*, 2010, 35, 999–1007. [PubMed: 20032968]
224. Winn P, Tarbuck A and Dunnett SB, *Neuroscience*, 1984, 12, 225–240. [PubMed: 6462446]
225. Tsujikawa K, Kuwayama K, Miyaguchi H, Kanamori T, Iwata Y, Inoue H, Yoshida T and Kishi T, *J. Chromatogr. B Anal. Technol. Biomed. Life Sci.*, 2007, 852, 430–435.
226. Stebelska K, *Ther. Drug Monit.*, 2013, 35, 420–442. [PubMed: 23851905]
227. Takemoto T, Nakajima T, T., and Yokobe, *J. Pharm. Soc. Japan*, 1964, 84, 1232–1233.
228. Obermaier S and Müller M, *Angew. Chemie - Int. Ed.*, 2020, 59, 12432–12435.
229. Alper KR, in *Alkaloids: Chemistry and Biology*, Academic Press, 2001, vol. 56, pp. 1–38. [PubMed: 11705103]
230. O'Connor SE and Maresh JJ, *Nat. Prod. Rep.*, 2006, 23, 532. [PubMed: 16874388]
231. Pan Q, Mustafa NR, Tang K, Choi YH and Verpoorte R, *Phytochem. Rev.*, 2016, 15, 221–250.
232. Chierrito TP, Aguiar AC, De Andrade IM, Ceravolo IP, Gonçalves RA, De Oliveira AJ and Krettli AU, *Malar. J.*, 2014, 13, 142. [PubMed: 24731256]
233. Ma iulaitis R, Kontrimavi iute V, Bressolle FMM and Briedis V, *Hum. Exp. Toxicol.*, 2008, 27, 181–194. [PubMed: 18650249]
234. Li S, Long J, Ma Z, Xu Z, Li J and Zhang Z, *Curr. Med. Res. Opin.*, 2004, 20, 409–415. [PubMed: 15025850]
235. Alper KR, Lotsof HS and Kaplan CD, *J. Ethnopharmacol.*, 2008, 115, 9–24. [PubMed: 18029124]
236. Qu Y, Easson MEAM, Simionescu R, Hajicek J, Thamm AMK, Salim V and De Luca V, *Proc. Natl. Acad. Sci. U. S. A.*, 2018, 115, 3180–3185. [PubMed: 29511102]
237. Caputi L, Franke J, Farrow SC, Chung K, Payne RME, Nguyen TD, Dang TTT, Teto Carqueijeiro IS, Koudounas K, De Bernonville TD, Ameyaw B, Jones DM, Curcino Vieira IJ, Courdavault V and O'Connor SE, *Science* (80-), 2018, 360, 1235–1239.

238. Salim V, Yu F, Altarejos J and De Luca V, *Plant J.*, 2013, 76, 754–765. [PubMed: 24103035]
239. Asada K, Salim V, Masada-Atsumi S, Edmunds E, Nagatoshi M, Terasaka K, Mizukami H and De Luca V, *Plant Cell*, 2013, 25, 4123–4134. [PubMed: 24104568]
240. Qu Y, Easson MLAE, Froese J, Simionescu R, Hudlicky T and DeLuca V, *Proc. Natl. Acad. Sci. U. S. A.*, 2015, 112, 6224–6229. [PubMed: 25918424]
241. Qu Y, Thamm AMK, Czerwinski M, Masada S, Kim KH, Jones G, Liang P and De Luca V, *Planta*, 2018, 247, 625–634. [PubMed: 29147812]
242. Tatsis EC, Carqueijeiro I, Dugé De Bernonville T, Franke J, Dang TTT, Oudin A, Lanoue A, Lafontaine F, Stavrinides AK, Clastre M, Courdavault V and O'Connor SE, *Nat. Commun.*, 2017, 8, 1–10. [PubMed: 28232747]
243. Lichman BR, Godden GT, Hamilton JP, Palmer L, Kamileen MO, Zhao D, Vaillancourt B, Wood JC, Sun M, Kinser TJ, Henry LK, Rodriguez-Lopez C, Dudareva N, Soltis DE, Soltis PS, Robin Buell C and O'Connor SE, *Sci. Adv.*, 2020, 6, eaba0721. [PubMed: 32426505]
244. Farrow SC, Kamileen MO, Caputi L, Bussey K, Mundy JEA, McAtee RC, Stephenson CRJ and O'Connor SE, *J. Am. Chem. Soc.*, 2019, 141, 12979–12983. [PubMed: 31364847]
245. Croteau R, *Chem. Rev.*, 1987, 87, 929–954.
246. Bouwmeester HJ, Gershenson J, Konings MCJM and Croteau R, *Plant Physiol.*, 1998, 117, 901–912. [PubMed: 9662532]
247. Collu G, Unver N, Peltenburg-Looman AMG, Van der Heijden R, Verpoorte R and Memelink J, *FEBS Lett.*, 2001, 508, 215–220. [PubMed: 11718718]
248. Geu-Flores F, Sherden NH, Glenn WS, O'connor SE, Courdavault V, Burlat V, Nims E, Wu C and Cui Y, *Nature*, 2012, 492, 138–142. [PubMed: 23172143]
249. Lichman BR, Kamileen MO, Titchiner GR, Saalbach G, Stevenson CEM, Lawson DM and O'Connor SE, *Nat. Chem. Biol.*, 2019, 15, 71–79. [PubMed: 30531909]
250. Murata J, Roepke J, Gordon H and De Luca V, *Plant Cell*, 2008, 20, 524–542. [PubMed: 18326827]
251. Guirimand G, Guihur A, Ginis O, Poutrain P, Héricourt F, Oudin A, Lanoue A, St-Pierre B, Burlat V and Courdavault V, *FEBS J.*, 2011, 278, 749–763. [PubMed: 21205206]
252. Courdavault V, Papon N, Clastre M, Giglioli-Guivarc'h N, St-Pierre B and Burlat V, *Curr. Opin. Plant Biol.*, 2014, 19, 43–50. [PubMed: 24727073]
253. Larsen B, Fuller VL, Pollier J, Van Moerkercke A, Schweizer F, Payne R, Colinas M, O'Connor SE, Goossens A and Halkier BA, *Plant Cell Physiol.*, 2017, 58, 1507–1518. [PubMed: 28922750]
254. Bracher D and Kutchan TM, *Arch. Biochem. Biophys.*, 1992, 294, 717–723. [PubMed: 1567228]
255. Battersby AR, in *Alkaloids*, 2007, vol. 1, pp. 31–47.
256. McCoy E and O'Connor SE, *J. Am. Chem. Soc.*, 2006, 128, 14276–14277. [PubMed: 17076499]
257. Bernhardt P, McCoy E and O'Connor SE, *Chem. Biol.*, 2007, 14, 888–897. [PubMed: 17719488]
258. Runguphan W, Qu X and O'Connor SE, *Nature*, 2010, 468, 461–467. [PubMed: 21048708]
259. Payne RME, Xu D, Foureau E, Teto Carqueijeiro MIS, Oudin A, De Bernonville TD, Novak V, Burow M, Olsen CE, Jones DM, Tatsis EC, Pendle A, Halkier BA, Geu-Flores F, Courdavault V, Nour-Eldin HH and O'Connor SE, *Nat. Plants*, 2017, 3, 16208. [PubMed: 28085153]
260. Guirimand G, Courdavault V, Lanoue A, Mahroug S, Guihur A, Blanc N, Giglioli-Guivarc'h N, St-Pierre B and Burlat V, *BMC Plant Biol.*, 2010, 10, 182. [PubMed: 20723215]
261. Konno K, Hirayama C, Yasui H and Nakamura M, *Proc. Natl. Acad. Sci. U. S. A.*, 1999, 96, 9159–9164. [PubMed: 10430912]
262. Luijendijk TJC, Stevens LH and Verpoorte R, *Plant Physiol. Biochem.*, 1998, 36, 419–425.
263. Geerlings A, Martinez-Lozano Ibañez M, Memelink J, Van Der Heijden R and Verpoorte R, *J. Biol. Chem.*, 2000, 275, 3051–3056. [PubMed: 10652285]
264. Gerasimenko I, Sheludko Y, Ma X and Stöckigt J, *Eur. J. Biochem.*, 2002, 269, 2204–2213. [PubMed: 11985599]
265. Farrow SC, Kamileen MO, Meades J, Ameyaw B, Xiao Y and O'Connor SE, *J. Biol. Chem.*, 2018, 293, 13821–13833. [PubMed: 30030374]

266. Caputi L, Franke J, Bussey K, Farrow SC, Vieira IJC, Stevenson CEM, Lawson DM and O'Connor SE, *Nat. Chem. Biol.*, 2020, 16, 383–386. [PubMed: 32066966]
267. Zhan ZJ, Yu Q, Wang ZL and Shan WG, *Bioorganic Med. Chem. Lett.*, 2010, 20, 6185–6187.
268. Steyer D, Erny C, Claudel P, Riveill G, Karst F and Legras JL, *Food Microbiol.*, 2013, 33, 228–234. [PubMed: 23200656]
269. Ortega A, Blount JF and Manchand PS, *J. Chem. Soc. Perkin Trans 1*, 1982, 2505.
270. Valdes LJ, Butler WM, Hatfield GM, Paul AG and Koreeda M, *J. Org. Chem.*, 1984, 49, 4716–4720.
271. Siebert DJ, *J. Ethnopharmacol.*, 1994, 43, 53–56. [PubMed: 7526076]
272. Prisinzano TE, *Life Sci.*, 2005, 78, 527–531. [PubMed: 16213533]
273. Coffeen U and Pellicer F, *J. Pain Res.*, 2019, Volume 12, 1069–1076. [PubMed: 30962708]
274. Kivell BM, Ewald AWM and Prisinzano TE, in *Advances in Pharmacology*, 2014, vol. 69, pp. 481–511. [PubMed: 24484985]
275. Yan F, Mosier PD, Westkaemper RB, Stewart J, Zjawiony JK, Vortherms TA, Sheffler DJ and Roth BL, *Biochemistry*, 2005, 44, 8643–8651. [PubMed: 15952771]
276. Gupta A, Gomes I, Bobeck EN, Fakira AK, Massaro NP, Sharma I, Cavé A, Hamm HE, Parello J, Devi LA and Snyder SH, *Proc. Natl. Acad. Sci. U. S. A.*, 2016, 113, 6041–6046. [PubMed: 27162327]
277. Siebert DJ, *Ann. Bot.*, 2004, 93, 763–771. [PubMed: 15087301]
278. Kutrzeba L, Dayan FE, Howell J, Feng J, Giner JL and Zjawiony JK, *Phytochemistry*, 2007, 68, 1872–1881. [PubMed: 17574635]
279. Chen X, Berim A, Dayan FE and Gang DR, *J. Exp. Bot.*, 2017, 68, 1109–1122. [PubMed: 28204567]
280. Pelot KA, Mitchell R, Kwon M, Hagelthorn DM, Wardman JF, Chiang A, Bohlmann J, Ro DK and Zerbe P, *Plant J.*, 2017, 89, 885–897. [PubMed: 27865008]
281. Nunn N and Qian N, *J. Econ. Perspect.*, 2010, 24, 163–188.
282. DeVido JJ, in *Absolute Addiction Psychiatry Review*, 2020, pp. 185–203.
283. Ashihara H and Suzuki T, *Front. Biosci.*, 2004, 9, 1864–1876. [PubMed: 14977593]
284. Nathanson JA, *Science (80-.)*, 1984, 226, 184–187.
285. Chou CH and Waller GR, *J. Chem. Ecol.*, 1980, 6, 643–654.
286. Wright GA, Baker DD, Palmer MJ, Stabler D, Mustard JA, Power EF, Borland AM and Stevenson PC, *Science (80-.)*, 2013, 339, 1202–1204.
287. Carpenter B and Lebon G, *Front. Pharmacol.*, 2017, 8, 898. [PubMed: 29311917]
288. Waldvogel SR, *Angew. Chemie Int. Ed.*, 2003, 42, 604–605.
289. Fischer E, *Berichte der Dtsch. Chem. Gesellschaft*, 1898, 31, 3266–3277.
290. Anderson L and Gibbs M, *J. Biol. Chem.*, 1962, 237, 1941–1944. [PubMed: 13861254]
291. Negishi O, Ozawa T and Imagawa H, *Agric. Biol. Chem.*, 1985, 49, 887–890.
292. Negishi O, Ozawa T and Imagawa H, *Agric. Biol. Chem.*, 1988, 52, 169–175.
293. Kato M, Mizuno K, Fujimura T, Iwama M, Irie M, Crozier A and Ashihara H, *Plant Physiol.*, 1999, 120, 579–586. [PubMed: 10364410]
294. Kato M, Mizuno K, Crozier A, Fujimura T and Ashihara H, *Nature*, 2000, 406, 956–957. [PubMed: 10984041]
295. Mizuno K, Kato M, Irino F, Yoneyama N, Fujimura T and Ashihara H, *FEBS Lett.*, 2003, 547, 56–60. [PubMed: 12860386]
296. Ashihara H, Monteiro AM, Gillies FM and Crozier A, *Plant Physiol.*, 1996, 111, 747–753. [PubMed: 12226327]
297. Negishi O, Ozawa T and Imagawa H, *Biosci. Biotechnol. Biochem.*, 1992, 56, 499–503. [PubMed: 27321000]
298. Mizuno K, Okuda A, Kato M, Yoneyama N, Tanaka H, Ashihara H and Fujimura T, *FEBS Lett.*, 2003, 534, 75–81. [PubMed: 12527364]

299. Ogawa M, Herai Y, Koizumi N, Kusano T and Sano H, *J. Biol. Chem.*, 2001, 276, 8213–8218. [PubMed: 11108716]
300. Huang R, O'Donnell AJ, Barboline JJ and Barkman TJ, *Proc. Natl. Acad. Sci. U. S. A.*, 2016, 113, 10613–10618. [PubMed: 27638206]
301. Koshiishi C, Kato A, Yama S, Crozier A and Ashihara H, *FEBS Lett.*, 2001, 499, 50–54. [PubMed: 11418110]
302. Waldhauser SSM and Baumann TW, *Phytochemistry*, 1996, 42, 985–996.
303. Kato A, Crozier A and Ashihara H, *Phytochemistry*, 1998, 48, 777–779.
304. Ogita S, Uefuji H, Yamaguchi Y, Nozomu K and Sano H, *Nature*, 2003, 423, 823.
305. Lu C, Warchol KM and Callahan RA, *Bull. Insectology*, 2014, 67, 125–130.
306. Tsvetkov N, Samson-Robert O, Sood K, Patel HS, Malena DA, Gajiwala PH, Maciukiewicz P, Fournier V and Zayed A, *Science (80-.)*, 2017, 356, 1395–1397.
307. Siegmund B, Leitner E and Pfannhauser W, *J. Agric. Food Chem.*, 1999, 47, 3113–3120. [PubMed: 10552617]
308. Lewis RS, Drake-Stowe KE, Heim C, Steede T, Smith W and Dewey RE, *Front. Plant Sci.*, 2020, 11, 368. [PubMed: 32318084]
309. Benowitz NL, *Annu. Rev. Pharmacol. Toxicol.*, 2009, 49, 57–71. [PubMed: 18834313]
310. Moran VE, *Front. Pharmacol.*, 2012, 3, 173. [PubMed: 23087643]
311. Pictet A and Rotschy A, *Berichte der Dtsch. Chem. Gesellschaft*, 1904, 37, 1225–1235.
312. Weidel H, *Justus Liebigs Ann. Chem.*, 1873, 165, 328–349.
313. Cheng JZ, Coyle CM, Panaccione DG and O'Connor SE, *J. Am. Chem. Soc.*, 2010, 132, 12835–12837. [PubMed: 20735127]
314. Lamberts BL, Dewey LJ and Byerrum RU, *BBA - Biochim. Biophys. Acta*, 1959, 33, 22–26. [PubMed: 13651178]
315. Leete E, in *Alkaloids: chemical and biological perspectives*, The Society, 1983, vol. 1, pp. 85–151.
316. Walton NJ, Robins RJ and Rhodes MJC, *Plant Sci.*, 1988, 54, 125–131.
317. Leete E and McDonell JA, *J. Am. Chem. Soc.*, 1981, 103, 658–662.
318. Mizusaki S, Kisaki T and Tamaki E, *Plant Physiol.*, 1968, 43, 93–98. [PubMed: 16656744]
319. Mizusaki S, Tanabe Y, Noguchi M and Tamaki E, *Plant Cell Physiol.*, 1971, 12, 633–640.
320. Mizusaki S, Tanabe Y, Noguchi M and Tamaki E, *Phytochemistry*, 1972, 11, 2757–2762.
321. Hibi N, Higashiguchi S, Hashimoto T and Yamada Y, *Plant Cell*, 1994, 6, 723–735. [PubMed: 8038607]
322. Biastoff S, Reinhardt N, Reva V, Brandt W and Dräger B, *FEBS Lett.*, 2009, 583, 3367–3374. [PubMed: 19796640]
323. Moriyama S, Tanaka H, Uwataki M, Muguruma M and Ohta K, *J. Biosci. Bioeng.*, 2003, 96, 324–331. [PubMed: 16233531]
324. Brent Friesen J and Leete E, *Tetrahedron Lett.*, 1990, 31, 6295–6298.
325. Kajikawa M, Hirai N and Hashimoto T, *Plant Mol. Biol.*, 2009, 69, 287–298. [PubMed: 19002761]
326. Kajikawa M, Shoji T, Kato A and Hashimoto T, *Plant Physiol.*, 2011, 155, 2010–2022. [PubMed: 21343426]
327. Goulet M-C, Gaudreau L, Gagné M, Maltais A-M, Laliberté A-C, Éthier G, Bechtold N, Martel M, D'Aoust M-A, Gosselin A, Pepin S and Michaud D, *Front. Plant Sci.*, 2019, 10, 735. [PubMed: 31244869]
328. Romanowski S and Eustáquio AS, *Curr. Opin. Chem. Biol.*, 2020, 58, 137–145. [PubMed: 33130520]
329. Molina-Hidalgo FJ, Vazquez-Vilar M, D'Andrea L, Demurtas OC, Fraser P, Giuliano G, Bock R, Orzáez D and Goossens A, *Trends Biotechnol.*, DOI:10.1016/j.tibtech.2020.11.012.
330. Lewis RS, Jack AM, Morris JW, Robert VJM, Gavilano LB, Siminszky B, Bush LP, Hayes AJ and Dewey RE, *Plant Biotechnol. J.*, 2008, 6, 346–354. [PubMed: 18282175]
331. Schachtsiek J and Stehle F, *Plant Biotechnol. J.*, 2019, 17, 2228–2230. [PubMed: 31206994]

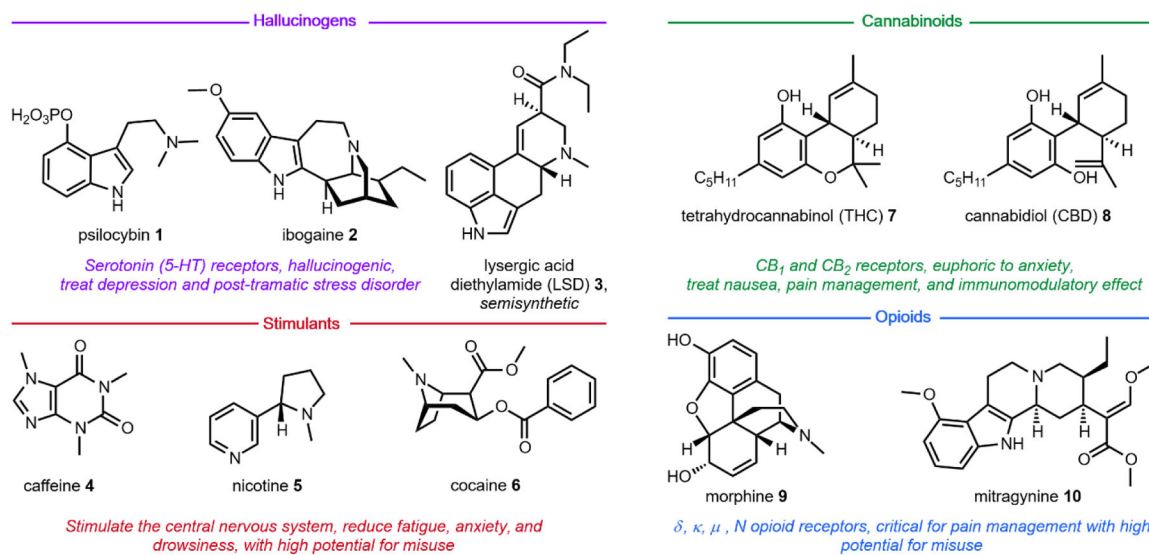
332. United Nations, World Drug Report 2018, 2018.
333. Walker LS and Mezuk B, *BMC Int. Health Hum. Rights*, 2018, 18, 43. [PubMed: 30497476]
334. Nestler E, *Sci. Pract. Perspect*, 2005, 3, 4–10. [PubMed: 18552739]
335. Humphrey AJ and O'Hagan D, *Nat. Prod. Rep*, 2001, 18, 494–502. [PubMed: 11699882]
336. Leete E, Marion L and Spenser ID, *Nature*, 1954, 174, 650–651. [PubMed: 13203600]
337. Duran-Patron R, O'Hagan D, Hamilton JTG and Wong CW, *Phytochemistry*, 2000, 53, 777–784. [PubMed: 10783983]
338. Bedewitz MA, Jones AD, D'Auria JC and Barry CS, *Nat. Commun*, 2018, 9, 5281. [PubMed: 30538251]
339. Huang J-P, Fang C, Ma X, Wang L, Yang J, Luo J, Yan Y, Zhang Y and Huang S-X, *Nat. Commun*, 2019, 10, 4036. [PubMed: 31492848]
340. Lichman BR, *Nat. Prod. Rep*, 2021, 38, 103–129. [PubMed: 32745157]
341. Dräger B, *Phytochemistry*, 2006, 67, 327–337. [PubMed: 16426652]
342. Gonzales-Vigil E, Góngora-Castillo E, Uebler JB, Gonzales-Vigil E, Wiegert-Rininger KE, Childs KL, Hamilton JP, Vaillancourt B, Yeo YS, Chappell J, Della DP, Daniel Jones A, Robin Buell C and Barry CS, *Plant Cell*, 2014, 26, 3745–3762. [PubMed: 25228340]
343. Nichols DE and Nichols CD, *Chem. Rev*, 2008, 108, 1614–1641. [PubMed: 18476671]
344. Qiu F, Zeng J, Wang J, Huang JP, Zhou W, Yang C, Lan X, Chen M, Huang SX, Kai G and Liao Z, *New Phytol.*, 2020, 225, 1906–1914. [PubMed: 31705812]
345. Li R, Reed DW, Liu E, Nowak J, Pelcher LE, Page JE and Covello PS, *Chem. Biol*, 2006, 13, 513–520. [PubMed: 16720272]
346. Nasomjai P, Reed DW, Tozer DJ, Peach MJG, Slawin AMZ, Covello PS and O'Hagan D, *ChemBioChem*, 2009, 10, 2382–2393. [PubMed: 19693762]
347. Leete E, Bjorklund JA, Couladis MM and Kim SH, *J. Am. Chem. Soc*, 1991, 113, 9286–9292.
348. Jirschitzka J, Schmidt GW, Reichelt M, Schneider B, Gershenzon J and D'Auria JC, *Proc. Natl. Acad. Sci. U. S. A.*, 2012, 109, 10304–10309. [PubMed: 22665766]
349. Schmidt GW, Jirschitzka J, Porta T, Reichelt M, Luck K, Torre JCP, Dolke F, Varesio E, Hopfgartner G, Gershenzon J and D'auria JC, *Plant Physiol.*, 2015, 167, 89–101. [PubMed: 25406120]
350. Ping Y, Li X, You W, Li G, Yang M, Wei W, Zhou Z and Xiao Y, *ACS Synth. Biol*, 2019, 8, 1257–1262. [PubMed: 31181154]
351. Srinivasan P and Smolke CD, *Nat. Commun*, 2019, 10, 3634. [PubMed: 31406117]
352. Wheeldon I, Minter SD, Banta S, Barton SC, Atanassov P and Sigman M, *Nat. Chem*, 2016, 8, 299–309. [PubMed: 27001725]
353. DeLoache WC, Russ ZN and Dueber JE, *Nat. Commun*, 2016, 7, 1–11.
354. Russo EB, *Chem. Biodivers*, 2007, 4, 1614–1648. [PubMed: 17712811]
355. Press CA, Knupp KG and Chapman KE, *Epilepsy Behav.*, 2015, 45, 49–52. [PubMed: 25845492]
356. Lal S, Prasad N, Ryan M, Tangri S, Silverberg MS, Gordon A and Steinhart H, *Eur. J. Gastroenterol. Hepatol*, 2011, 23, 891–896. [PubMed: 21795981]
357. Fiz J, Durán M, Capellà D, Carbonell J and Farré M, *PLoS One*, 2011, 6, e18440. [PubMed: 21533029]
358. Abrams DI and Guzman M, *Clin. Pharmacol. Ther*, 2015, 97, 575–586. [PubMed: 25777363]
359. Sarris J, Sinclair J, Karamacoska D, Davidson M and Firth J, *BMC Psychiatry*, 2020, 20, 24. [PubMed: 31948424]
360. Corey-Bloom J, Wolfson T, Gamst A, Jin S, Marcotte TD, Bentley H and Gouaux B, *Can. Med. Assoc. J*, 2012, 184, 1143 LP–1150. [PubMed: 22586334]
361. Müller-Vahl KR, Kolbe H, Schneider U and Emrich HM, *Complement. Med. Res*, 1999, 6(suppl 3), 23–27.
362. Wei D, Dinh D, Lee D, Li D, Anguren A, Moreno-Sanz G, Gall CM and Piomelli D, *Cannabis Cannabinoid Res.*, 2016, 1, 81–89. [PubMed: 28861483]
363. Solomon R, *Cannabis Cannabinoid Res.*, 2020, 5, 2–5. [PubMed: 32322671]
364. Russo EB, *Chem. Biodivers*, 2007, 4, 1614–1648. [PubMed: 17712811]

365. Sharpless NE, White Oak, MD, 2019.
366. Gaoni Y and Mechoulam R, *J. Am. Chem. Soc.*, 1971, 93, 217–224. [PubMed: 5538858]
367. Mechoulam R and Shvo Y, *Tetrahedron*, 1963, 19, 2073–2078. [PubMed: 5879214]
368. Niesink RJM and van Laar MW, *Front. Psychiatry*, 2013, 4, 130. [PubMed: 24137134]
369. De Petrocellis L, Ligresti A, Moriello AS, Allarà M, Bisogno T, Petrosino S, Stott CG and Di Marzo V, *Br. J. Pharmacol.*, 2011, 163, 1479–1494. [PubMed: 21175579]
370. Laprairie RB, Bagher AM, Kelly MEM and Denovan-Wright EM, *Br. J. Pharmacol.*, 2015, 172, 4790–4805. [PubMed: 26218440]
371. Thomas A, Baillie GL, Phillips AM, Razdan RK, Ross RA and Pertwee RG, *Br. J. Pharmacol.*, 2007, 150, 613–623. [PubMed: 17245363]
372. Rock EM, Bolognini D, Limebeer CL, Cascio MG, Anavi-Goffer S, Fletcher PJ, Mechoulam R, Pertwee RG and Parker LA, *Br. J. Pharmacol.*, 2012, 165, 2620–2634. [PubMed: 21827451]
373. Russo EB, Burnett A, Hall B and Parker KK, *Neurochem. Res.*, 2005, 30, 1037–1043. [PubMed: 16258853]
374. Yamaori S, Kushihara M, Yamamoto I and Watanabe K, *Biochem. Pharmacol.*, 2010, 79, 1691–1698. [PubMed: 20117100]
375. De Petrocellis L, Vellani V, Schiano-Moriello A, Marini P, Magherini PC, Orlando P and Di Marzo V, *J. Pharmacol. Exp. Ther.*, 2008, 325, 1007 LP–1015. [PubMed: 18354058]
376. DeLong GT, Wolf CE, Poklis A and Lichtman AH, *Drug Alcohol Depend.*, 2010, 112, 126–133. [PubMed: 20619971]
377. Hanuš LO, Meyer SM, Muñoz E, Tagliatalata-Scafati O and Appendino G, *Nat. Prod. Rep.*, 2016, 33, 1357–1392. [PubMed: 27722705]
378. *Proc. Chem. Soc.*, 1964, 73.
379. Cascio MG, Gauson LA, Stevenson LA, Ross RA and Pertwee RG, *Br. J. Pharmacol.*, 2010, 159, 129–141. [PubMed: 20002104]
380. Fuhr L, Rousseau M, Plauth A, Schroeder FC and Sauer S, *J. Nat. Prod.*, 2015, 78, 1160–1164. [PubMed: 25938459]
381. Chicca A, Schafroth MA, Reynoso-Moreno I, Erni R, Petrucci V, Carreira EM and Gertsch J, *Sci. Adv.*, 2018, 4, eaat2166. [PubMed: 30397641]
382. Muhammad I, Li X-C, Jacob MR, Tekwani BL, Dunbar DC and Ferreira D, *J. Nat. Prod.*, 2003, 66, 804–809. [PubMed: 12828466]
383. Quaghebeur K, Coosemans J, Toppet S and Compennolle F, *Phytochemistry*, 1994, 37, 159–161. [PubMed: 7765609]
384. Matsuda LA, Lolait SJ, Brownstein MJ, Young AC and Bonner TI, *Nature*, 1990, 346, 561–564. [PubMed: 2165569]
385. Munro S, Thomas KL and Abu-Shaar M, *Nature*, 1993, 365, 61–65. [PubMed: 7689702]
386. Mechoulam R, Lander N, Varkony TH, Kimmel I, Becker O, Ben-Zvi Z, Edery H and Porath G, *J. Med. Chem.*, 1980, 23, 1068–1072. [PubMed: 7420350]
387. Howlett AC, *Prostaglandins Other Lipid Mediat.*, 2002, 68–69, 619–631.
388. Pertwee RG, Howlett AC, Abood ME, Alexander SPH, Di Marzo V, Elphick MR, Greasley PJ, Hansen HS, Kunos G, Mackie K, Mechoulam R and Ross RA, *Pharmacol. Rev.*, 2010, 62, 588–631. [PubMed: 21079038]
389. Bow EW and Rimoldi JM, *Perspect. Medicin. Chem.*, 2016, 8, 17–39. [PubMed: 27398024]
390. Vollner L, Bieniek D and Korte F, *Tetrahedron Lett.*, 1969, 10, 145–147.
391. Merkus FWHM, *Nature*, 1971, 232, 579–580. [PubMed: 4937510]
392. Linciano P, Citti C, Luongo L, Belardo C, Maione S, Vandelli MA, Forni F, Gigli G, Laganà A, Montone CM and Cannazza G, *J. Nat. Prod.*, 2020, 83, 88–98. [PubMed: 31891265]
393. Cascio MG, Zamberletti E, Marini P, Parolaro D and Pertwee RG, *Br. J. Pharmacol.*, 2015, 172, 1305–1318. [PubMed: 25363799]
394. Rock EM, Sticht MA, Duncan M, Stott C and Parker LA, *Br. J. Pharmacol.*, 2013, 170, 671–678. [PubMed: 23902479]

395. Citti C, Linciano P, Russo F, Luongo L, Iannotta M, Maione S, Laganà A, Capriotti AL, Forni F, Vandelli MA, Gigli G and Cannazza G, *Sci. Rep.*, 2019, 9, 20335. [PubMed: 31889124]
396. Ben-Shabat S, Fride E, Sheskin T, Tamiri T, Rhee M-H, Vogel Z, Bisogno T, De Petrocellis L, Di Marzo V and Mechoulam R, *Eur. J. Pharmacol.*, 1998, 353, 23–31. [PubMed: 9721036]
397. Mechoulam R and Ben-Shabat S, *Nat. Prod. Rep.*, 1999, 16, 131–143. [PubMed: 10331283]
398. Russo EB, *Br. J. Pharmacol.*, 2011, 163, 1344–1364. [PubMed: 21749363]
399. Carlini EA, Karniol IG, Renault PF and Schuster CR, *Br. J. Pharmacol.*, 1974, 50, 299–309. [PubMed: 4609532]
400. Stout JM, Boubakir Z, Ambrose SJ, Purves RW and Page JE, *Plant J.*, 2012, 71, 353–365. [PubMed: 22353623]
401. Taura F, Tanaka S, Taguchi C, Fukamizu T, Tanaka H, Shoyama Y and Morimoto S, *FEBS Lett.*, 2009, 583, 2061–2066. [PubMed: 19454282]
402. Gagne SJ, Stout JM, Liu E, Boubakir Z, Clark SM and Page JE, *Proc. Natl. Acad. Sci. U. S. A.*, 2012, 109, 12811–12816. [PubMed: 22802619]
403. US9765308B2, 2009.
404. Fellermeier M and Zenk MH, *FEBS Lett.*, 1998, 427, 283–285. [PubMed: 9607329]
405. Sirikantaramas S, Morimoto S, Shoyama Y, Ishikawa Y, Wada Y, Shoyama Y and Taura F, *J. Biol. Chem.*, 2004, 279, 39767–39774. [PubMed: 15190053]
406. Taura F, Sirikantaramas S, Shoyama Y, Yoshikai K, Shoyama Y and Morimoto S, *FEBS Lett.*, 2007, 581, 2929–2934. [PubMed: 17544411]
407. Morimoto S, Komatsu K, Taura F and Shoyama Y, *Phytochemistry*, 1998, 49, 1525–1529. [PubMed: 9862135]
408. Shoyama Y, Tamada T, Kurihara K, Takeuchi A, Taura F, Arai S, Blaber M, Shoyama Y, Morimoto S and Kuroki R, *J. Mol. Biol.*, 2012, 423, 96–105. [PubMed: 22766313]
409. Zirpel B, Kayser O and Stehle F, *J. Biotechnol.*, 2018, 284, 17–26. [PubMed: 30053500]
410. Jamieson CS, Ohashi M, Liu F, Tang Y and Houk KN, *Nat. Prod. Rep.*, 2019, 36, 698–713. [PubMed: 30311924]
411. Gao L, Su C, Du X, Wang R, Chen S, Zhou Y, Liu C, Liu X, Tian R, Zhang L, Xie K, Chen S, Guo Q, Guo L, Hano Y, Shimazaki M, Minami A, Oikawa H, Huang N, Houk KN, Huang L, Dai J and Lei X, *Nat. Chem.*, 2020, 12, 620–628. [PubMed: 32451436]
412. Ohashi M, Jamieson CS, Cai Y, Tan D, Kanayama D, Tang M-C, Anthony SM, V Chari J, Barber JS, Picazo E, Kakule TB, Cao S, Garg NK, Zhou J, Houk KN and Tang Y, *Nature*, 2020, 586, 64–69. [PubMed: 32999480]
413. Kuzuyama T, Noel JP and Richard SB, *Nature*, 2005, 435, 983–987. [PubMed: 15959519]
414. Zirpel B, Degenhardt F, Martin C, Kayser O and Stehle F, *J. Biotechnol.*, 2017, 259, 204–212. [PubMed: 28694184]
415. Kumano T, Richard SB, Noel JP, Nishiyama M and Kuzuyama T, *Bioorg. Med. Chem.*, 2008, 16, 8117–8126. [PubMed: 18682327]
416. Kumano T, Tomita T, Nishiyama M and Kuzuyama T, *J. Biol. Chem.*, 2010, 285, 39663–39671. [PubMed: 20937800]
417. Chatzivasileiou AO, Ward V, Edgar SM and Stephanopoulos G, *Proc. Natl. Acad. Sci.*, 2019, 116, 506 LP–511. [PubMed: 30584096]
418. Lund S, Hall R and Williams GJ, *ACS Synth. Biol.*, 2019, 8, 232–238. [PubMed: 30648856]
419. Brownstein MJ, *Proc. Natl. Acad. Sci. U. S. A.*, 1993, 90, 5391–5393. [PubMed: 8390660]
420. Singh A, Menéndez-Perdomo IM and Facchini PJ, *Phytochem. Rev.*, 2019, 18, 1457–1482.
421. Sigerist HE and Paracelsus, *Paracelsus in the light of four hundred years*, Columbia University Press, 1941.
422. Jurna I, *Schmerz*, 2003, 17, 280–283. [PubMed: 12923678]
423. Krenn L, Glantschnig S and Sorgner U, *Chromatographia*, 1998, 47, 21–24.
424. Waldhoer M, Bartlett SE and Whistler JL, *Annu. Rev. Biochem.*, 2004, 73, 953–990. [PubMed: 15189164]

425. Quock RM, Burkey TH, Varga E, Hosohata Y, Hosohata K, Cowell SM, Slate CA, Ehlert FJ, Roeske WR and Yamamura HI, *Pharmacol. Rev.*, 1999, 51, 503 LP–532. [PubMed: 10471416]
426. Minami M and Satoh M, *Neurosci. Res.*, 1995, 23, 121–145. [PubMed: 8532211]
427. Pogozheva ID, Lomize AL and Mosberg HI, *Biophys. J.*, 1998, 75, 612–634. [PubMed: 9675164]
428. Schmitz R, *Pharm. Hist.*, 1985, 27, 61–74. [PubMed: 11611724]
429. Robiquet P-J, *Ann. der Chemie*, 1833, 5, 82–111.
430. Rida PCG, Livecche D, Ogden A, Zhou J and Aneja R, *Med. Res. Rev.*, 2015, 35, 1072–1096. [PubMed: 26179481]
431. Ye K, Ke Y, Keshava N, Shanks J, Kapp JA, Tekmal RR, Petros J and Joshi HC, *Proc. Natl. Acad. Sci.*, 1998, 95, 1601 LP–1606. [PubMed: 9465062]
432. Ke Y, Ye K, Grossniklaus HE, Archer DR, Joshi HC and Kapp JA, *Cancer Immunol. Immunother.*, 2000, 49, 217–225. [PubMed: 10941904]
433. Samanani N and Facchini PJ, *J. Biol. Chem.*, 2002, 277, 33878–33883. [PubMed: 12107162]
434. Liscombe DK, MacLeod BP, Loukanina N, Nandi OI and Facchini PJ, *Phytochemistry*, 2005, 66, 2501–2520. [PubMed: 16342378]
435. Lichman BR, Gershtater MC, Lamming ED, Pesnot T, Sula A, Keep NH, Hailes HC and Ward JM, *FEBS J.*, 2015, 282, 1137–1151. [PubMed: 25620686]
436. Lichman BR, Sula A, Pesnot T, Hailes HC, Ward JM and Keep NH, *Biochemistry*, 2017, 56, 5274–5277. [PubMed: 28915025]
437. Pauli HH and Kutchan TM, *Plant J.*, 1998, 13, 793–801. [PubMed: 9681018]
438. Facchini PJ and Park SU, *Phytochemistry*, 2003, 64, 177–186. [PubMed: 12946416]
439. Gurkok T, Ozhuner E, Parmaksiz I, Özcan S, Turktas M, pek A, Demirtas I, Okay S and Unver T, *Front. Plant Sci.*, 2016, 7, 98. [PubMed: 26909086]
440. Bennett MR, Thompson ML, Shepherd SA, Dunstan MS, Herbert AJ, Smith DRM, Cronin VA, Menon BRK, Levy C and Micklefield J, *Angew. Chemie - Int. Ed.*, 2018, 57, 10600–10604.
441. Farrow SC, Hagel JM, Beaudoin GAW, Burns DC and Facchini PJ, *Nat. Chem. Biol.*, 2015, 11, 728–732. [PubMed: 26147354]
442. Winzer T, Kern M, King AJ, Larson TR, Teodor RI, Donninger SL, Li Y, Dowle AA, Cartwright J, Bates R, Ashford D, Thomas J, Walker C, Bowser TA and Graham IA, *Science (80-.)*, 2015, 349, 309–312.
443. Wijekoon CP and Facchini PJ, *Plant J.*, 2012, 69, 1052–1063. [PubMed: 22098111]
444. Lenz R and Zenk MH, *J. Biol. Chem.*, 1995, 270, 31091–31096. [PubMed: 8537369]
445. Grothe T, Lenz R and Kutchan TM, *J. Biol. Chem.*, 2001, 276, 30717–30723. [PubMed: 11404355]
446. Ziegler J, Brandt W, Geißler R and Facchini PJ, *J. Biol. Chem.*, 2009, 284, 26758–26767. [PubMed: 19648114]
447. Chen X, Hagel JM, Chang L, Tucker JE, Shiigi SA, Yelapaala Y, Chen HY, Estrada R, Colbeck J, Enquist-Newman M, Ibáñez AB, Cottarel G, Vidanes GM and Facchini PJ, *Nat. Chem. Biol.*, 2018, 14, 738–743. [PubMed: 29807982]
448. Farrow SC and Facchini PJ, *J. Biol. Chem.*, 2013, 288, 28997–29012. [PubMed: 23928311]
449. Unterlinner B, Lenz R and Kutchan TM, *Plant J.*, 1999, 18, 465–475. [PubMed: 10417697]
450. Kluza A, Niedzialkowska E, Kurpiewska K, Wojdyla Z, Quesne M, Kot E, Porebski PJ and Borowski T, *J. Struct. Biol.*, 2018, 202, 229–235. [PubMed: 29408320]
451. Winzer T, Gazda V, He Z, Kaminski F, Kern M, Larson TR, Li Y, Meade F, Teodor R, Vaistij FE, Walker C, Bowser TA and Graham IA, *Science (80-.)*, 2012, 336, 1704–1708.
452. Kutchan TM and Dittrich H, *J. Biol. Chem.*, 1995, 270, 24475–24481. [PubMed: 7592663]
453. Facchini PJ, Penzes C, Johnson AG and Bull D, *Plant Physiol.*, 1996, 112, 1669–1677. [PubMed: 8972604]
454. Gaweska HM, Roberts KM and Fitzpatrick PF, *Biochemistry*, 2012, 51, 7342–7347. [PubMed: 22931234]
455. Dang TTT and Facchini PJ, *Plant Physiol.*, 2012, 159, 618–631. [PubMed: 22535422]
456. Dang TTT and Facchini PJ, *FEBS Lett.*, 2014, 588, 198–204. [PubMed: 24316226]

457. Liscombe DK and Facchini PJ, *J. Biol. Chem.*, 2007, 282, 14741–14751. [PubMed: 17389594]
458. Lang DE, Morris JS, Rowley M, Torres MA, Maksimovich VA, Facchini PJ and Ng KKS, *J. Biol. Chem.*, 2019, 294, 14482–14898. [PubMed: 31395658]
459. Dang TTT and Facchini PJ, *J. Biol. Chem.*, 2014, 289, 2013–2026. [PubMed: 24324259]
460. Dang TTT, Chen X and Facchini PJ, *Nat. Chem. Biol.*, 2015, 11, 104–106. [PubMed: 25485687]
461. Chen X and Facchini PJ, *Plant J.*, 2014, 77, 173–184. [PubMed: 24708518]
462. Nakagawa A, Minami H, Kim JS, Koyanagi T, Katayama T, Sato F and Kumagai H, *Nat. Commun.*, 2011, 2, 326. [PubMed: 21610729]
463. Nakagawa A, Minami H, Kim JS, Koyanagi T, Katayama T, Sato F and Kumagai H, *Bioeng. Bugs*, 2012, 3, 49–53. [PubMed: 22179145]
464. Kim JS, Nakagawa A, Yamazaki Y, Matsumura E, Koyanagi T, Minami H, Katayama T, Sato F and Kumagai H, *Biosci. Biotechnol. Biochem.*, 2013, 77, 2166–2168. [PubMed: 24096658]
465. Thodey K, Galanie S and Smolke CD, *Nat. Chem. Biol.*, 2014, 10, 837–844. [PubMed: 25151135]
466. Fossati E, Ekins A, Narcross L, Zhu Y, Falgoutyret JP, Beaudoin GAW, Facchini PJ and Martin VJJ, *Nat. Commun.*, 2014, 5, 3283. [PubMed: 24513861]
467. Pyne ME, Kevvai K, Grewal PS, Narcross L, Choi B, Bourgeois L, Dueber JE and Martin VJJ, *Nat. Commun.*, 2020, 11, 3337. [PubMed: 32620756]
468. Trenchard IJ and Smolke CD, *Metab. Eng.*, 2015, 30, 96–104. [PubMed: 25981946]
469. French CE and Bruce NC, *Biochem. J.*, 1994, 301 (Pt 1), 97–103. [PubMed: 8037698]
470. Li Y, Li S, Thodey K, Trenchard I, Cravens A and Smolke CD, *Proc. Natl. Acad. Sci. U. S. A.*, 2018, 115, E3922–E3931. [PubMed: 29610307]
471. Li J, Lee E-J, Chang L and Facchini PJ, *Sci. Rep.*, 2016, 6, 39256. [PubMed: 27991536]
472. Flores-Bocanegra L, Raja HA, Graf TN, Augustinovi M, Wallace ED, Hematian S, Kellogg JJ, Todd DA, Cech NB and Oberlies NH, *J. Nat. Prod.*, 2020, 83, 2165–2177. [PubMed: 32597657]
473. Todd DA, Kellogg JJ, Wallace ED, Khin M, Flores-Bocanegra L, Tanna RS, McIntosh S, Raja HA, Graf TN, Hemby SE, Paine MF, Oberlies NH and Cech NB, *Sci. Rep.*, 2020, 10, 19158. [PubMed: 33154449]
474. Takayama H, *Chem. Pharm. Bull.*, 2004, 52, 916–928.
475. Yamamoto LT, Horie S, Takayama H, Aimi N, Sakai SI, Yano S, Shan J, Pang PKT, Ponglux D and Watanabe K, *Gen. Pharmacol.*, 1999, 33, 73–81. [PubMed: 10428019]
476. Stavriniades A, Tatsis EC, Caputi L, Foureau E, Stevenson CEM, Lawson DM, Courdavault V and O'Connor SE, *Nat. Commun.*, 2016, 7, 12116. [PubMed: 27418042]
477. Stavriniades A, Tatsis EC, Foureau E, Caputi L, Kellner F, Courdavault V and O'Connor SE, *Chem. Biol.*, 2015, 22, 336–341. [PubMed: 25772467]
478. Stavriniades AK, Tatsis EC, Dang TT, Caputi L, Stevenson CEM, Lawson DM, Schneider B and O'Connor SE, *ChemBioChem*, 2018, 19, 940–948. [PubMed: 29424954]
479. Trenti F, Yamamoto K, Hong B, Paetz C, Nakamura Y and O'Connor SE, *Org. Lett.*, 2021, 23, 1793–1797. [PubMed: 33625237]
480. Kong F, Ma Q, Huang S, Yang S, Fu L, Zhou L, Dai H, Yu Z and Zhao Y, *Nat. Prod. Res.*, 2017, 31, 1403–1408. [PubMed: 27834097]
481. Kamble SH, León F, King TI, Berthold EC, Lopera-Londono C, Siva Rama Raju K, Hampson AJ, Sharma A, Avery BA, McMahon LR and McCurdy CR, *ACS Pharmacol. Transl. Sci.*, 2020, 3, 1063–1068. [PubMed: 33344889]
482. Tsunematsu Y, Ishikawa N, Wakana D, Goda Y, Noguchi H, Moriya H, Hotta K and Watanabe K, *Nat. Chem. Biol.*, 2013, 9, 818–825. [PubMed: 24121553]
483. Ye Y, Du L, Zhang X, Newmister SA, McCauley M, Alegre-Requena JV, Zhang W, Mu S, Minami A, Fraley AE, Adrover-Castellano ML, Carney NA, Shende VV, Qi F, Oikawa H, Kato H, Tsukamoto S, Paton RS, Williams RM, Sherman DH and Li S, *Nat. Catal.*, 2020, 3, 497–506. [PubMed: 32923978]
484. Bonn-Miller MO, ElSohly MA, Loflin MJE, Chandra S and Vandrey R, *Int. Rev. Psychiatry*, 2018, 30, 277–284. [PubMed: 30179534]
485. Cristino L, Bisogno T and Di Marzo V, *Nat. Rev. Neurol.*, 2020, 16, 9–29. [PubMed: 31831863]

**Fig. 1.**

Four categories of psychoactive natural products or derivatives described in this review.

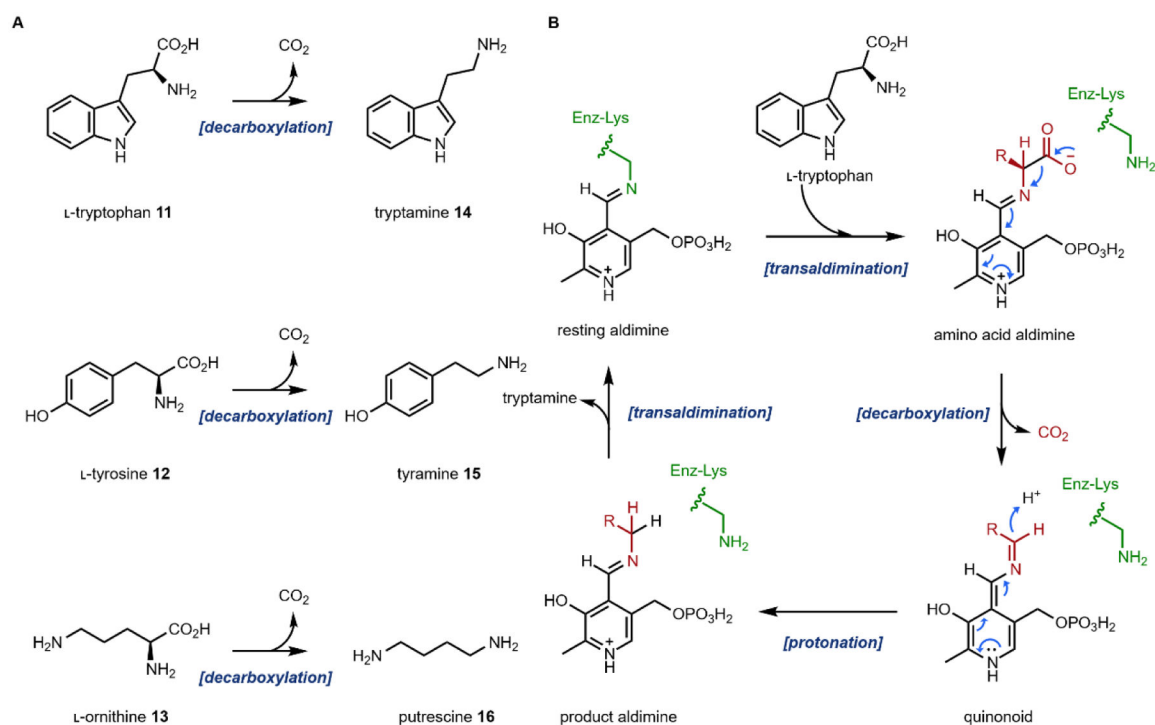


Fig. 2: PLP-Dependent amino acid decarboxylase.

(A) three amino acids are decarboxylated to give primary amines that are building blocks for alkaloids; (B) mechanism of the PLP-dependent tryptophan decarboxylase

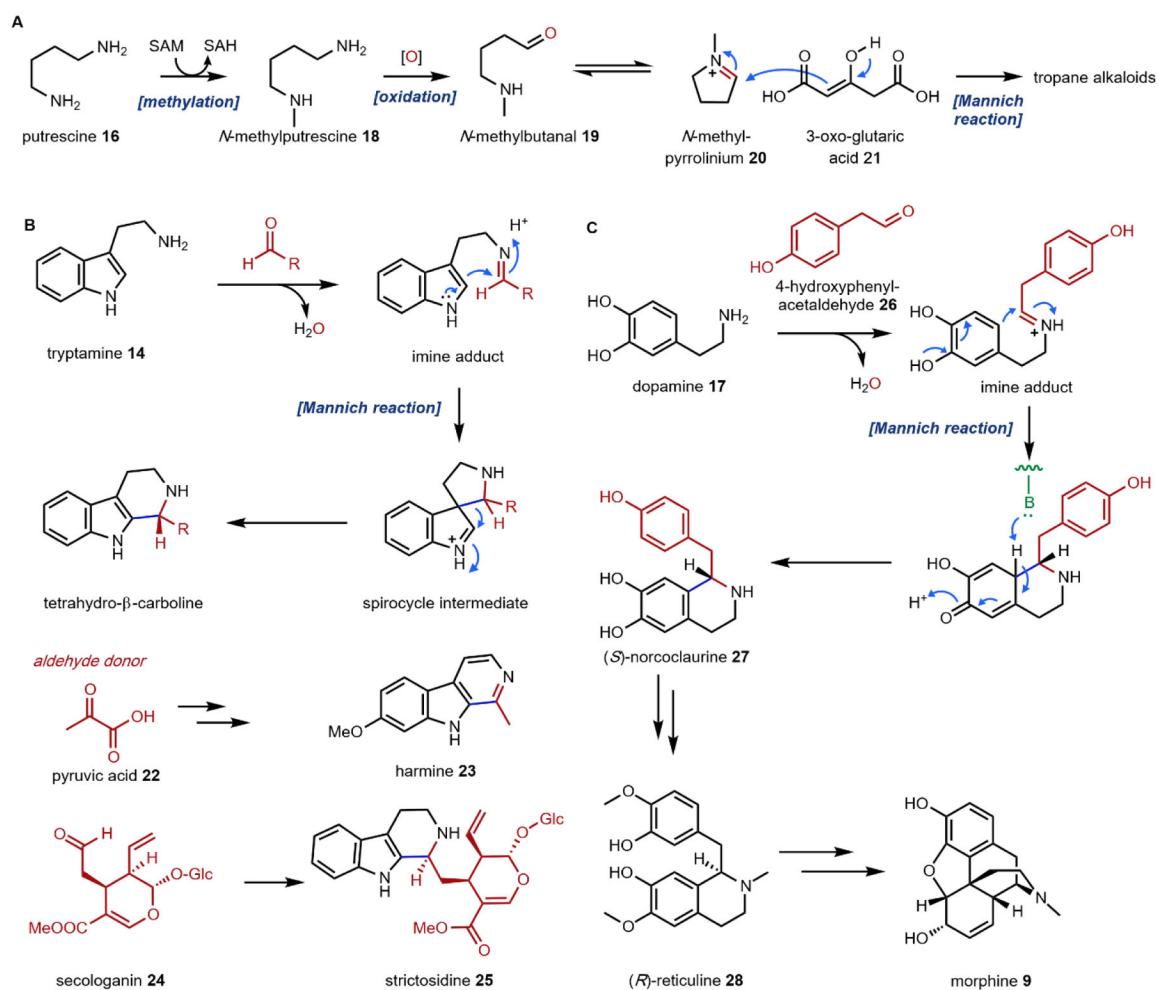


Fig. 3: Mannich reactions in alkaloid biosynthesis.

(A) formation of the pyrrolidine intermediate on pathway to tropane alkaloids; (B) the Pictet-Spengler reaction involving tryptamine to form tetrahydro- β -carboline intermediates; (C) the Pictet-Spengler reaction involving dopamine to form tetrahydroisoquinoline on pathway to morphine.

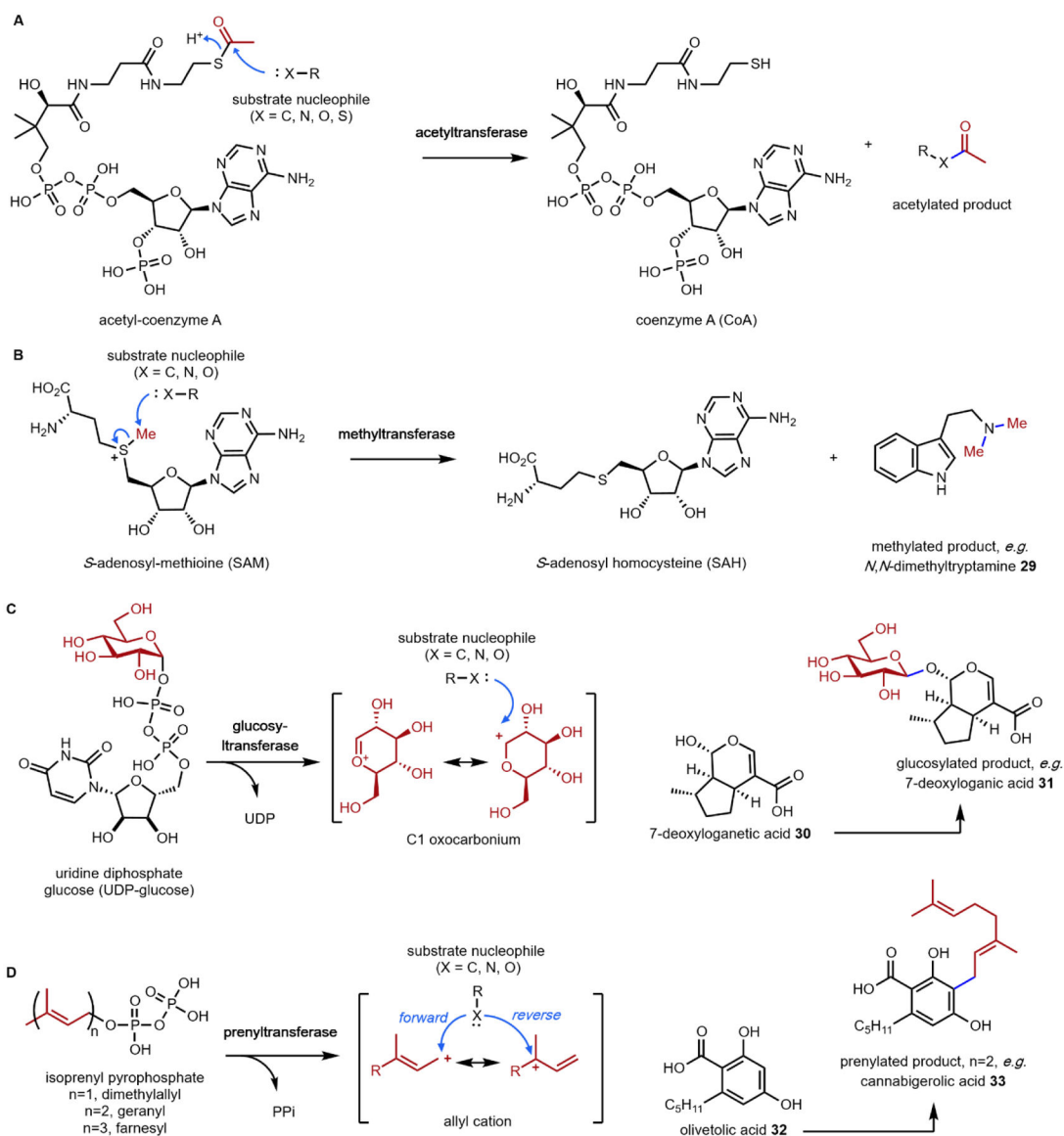


Fig. 4: Enzyme catalyzed group transfer reactions in biosynthesis.

(A) acetyltransferase-catalyzed acetyltransfer; (B) methyltransferase-catalyzed methyl transfer; (C) glucosyltransferase-catalyzed glucosyl transfer; and (D) prenyltransferase-catalyzed prenyl transfer.

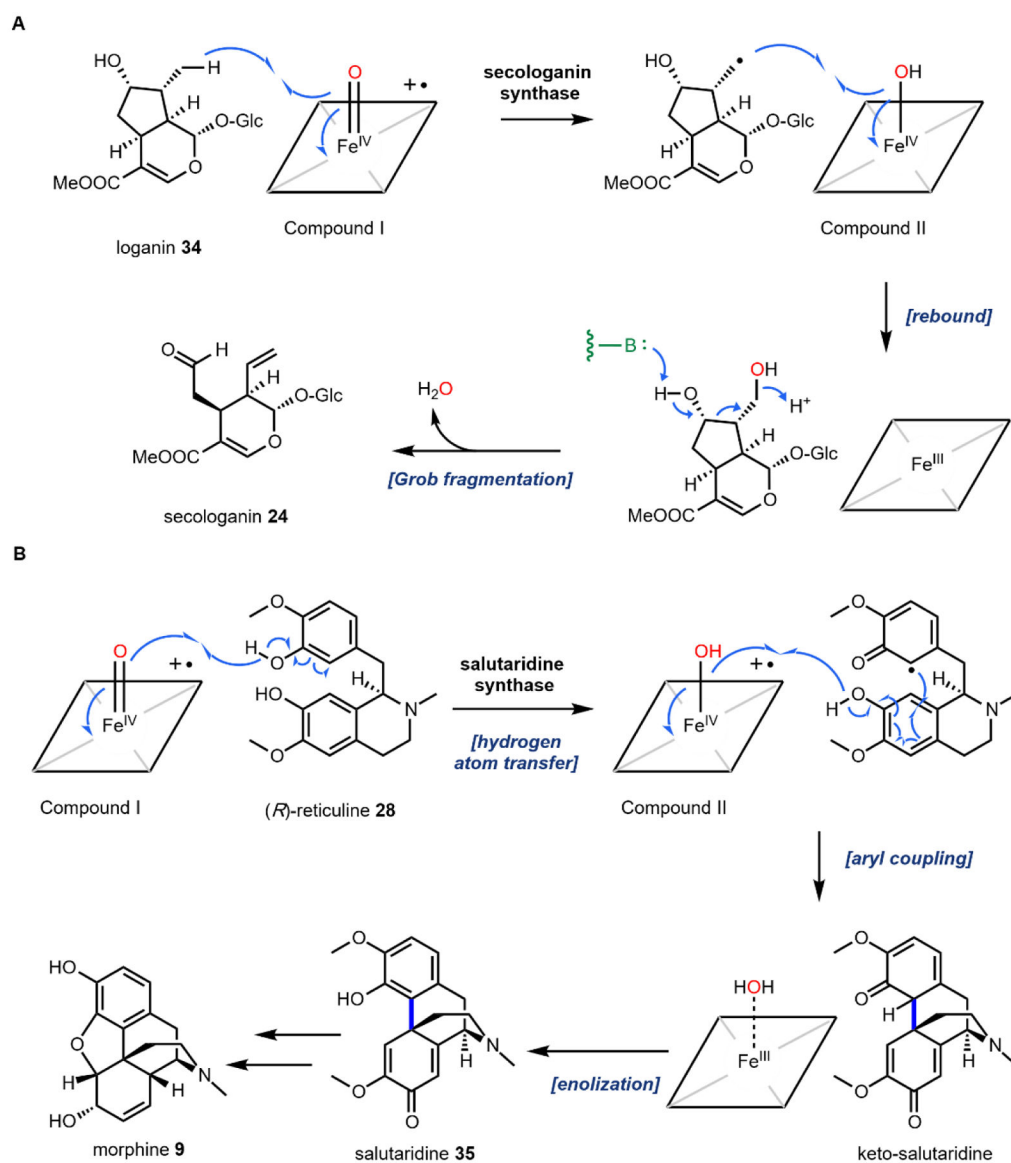


Fig. 5: Two examples of P450 catalyzed oxidative modifications in biosynthesis of plant natural products.

(A) secologanin synthase in biosynthesis of monoterpene indole alkaloids; (B) salutaridine synthase in biosynthesis of morphine family of opioids.

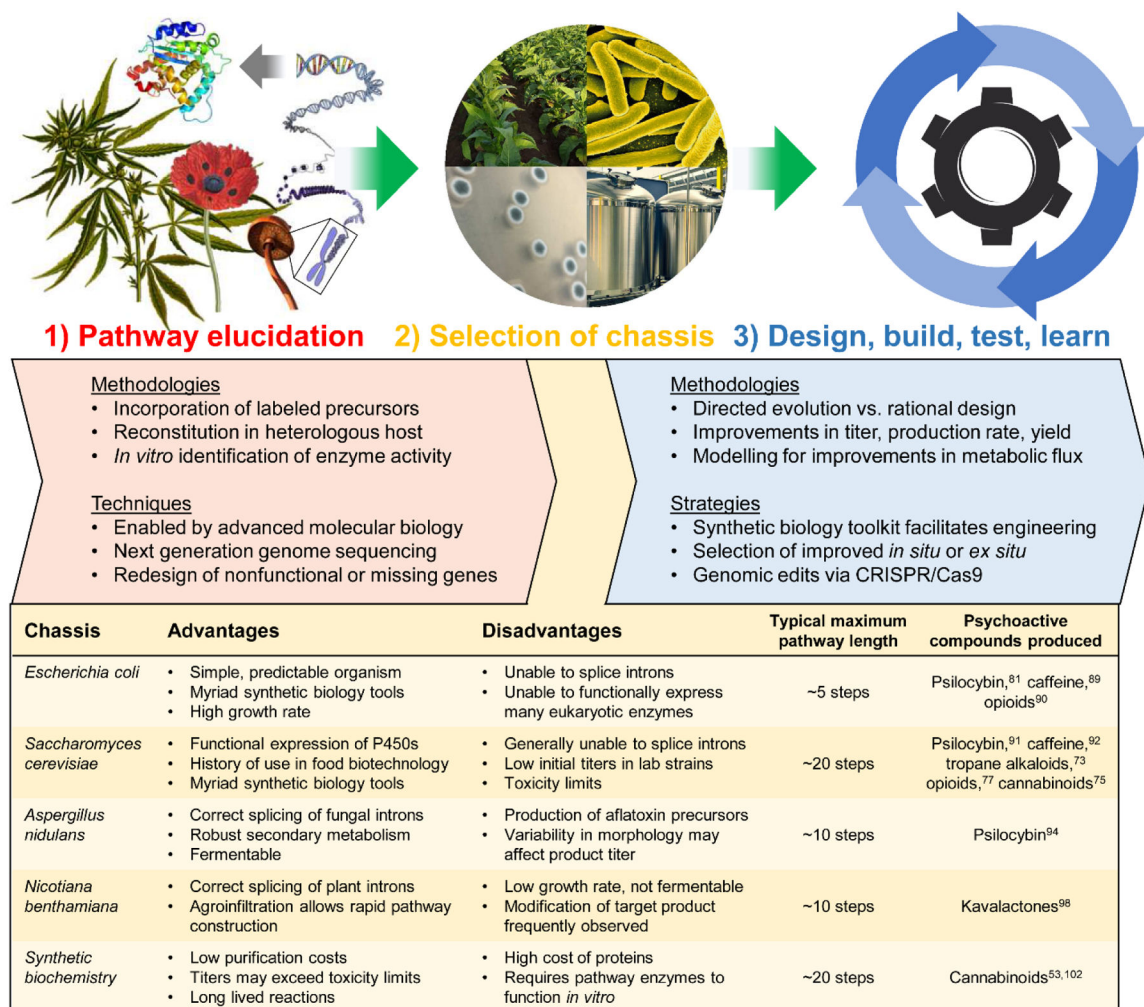


Fig. 6.
Strategies in synthetic biology.

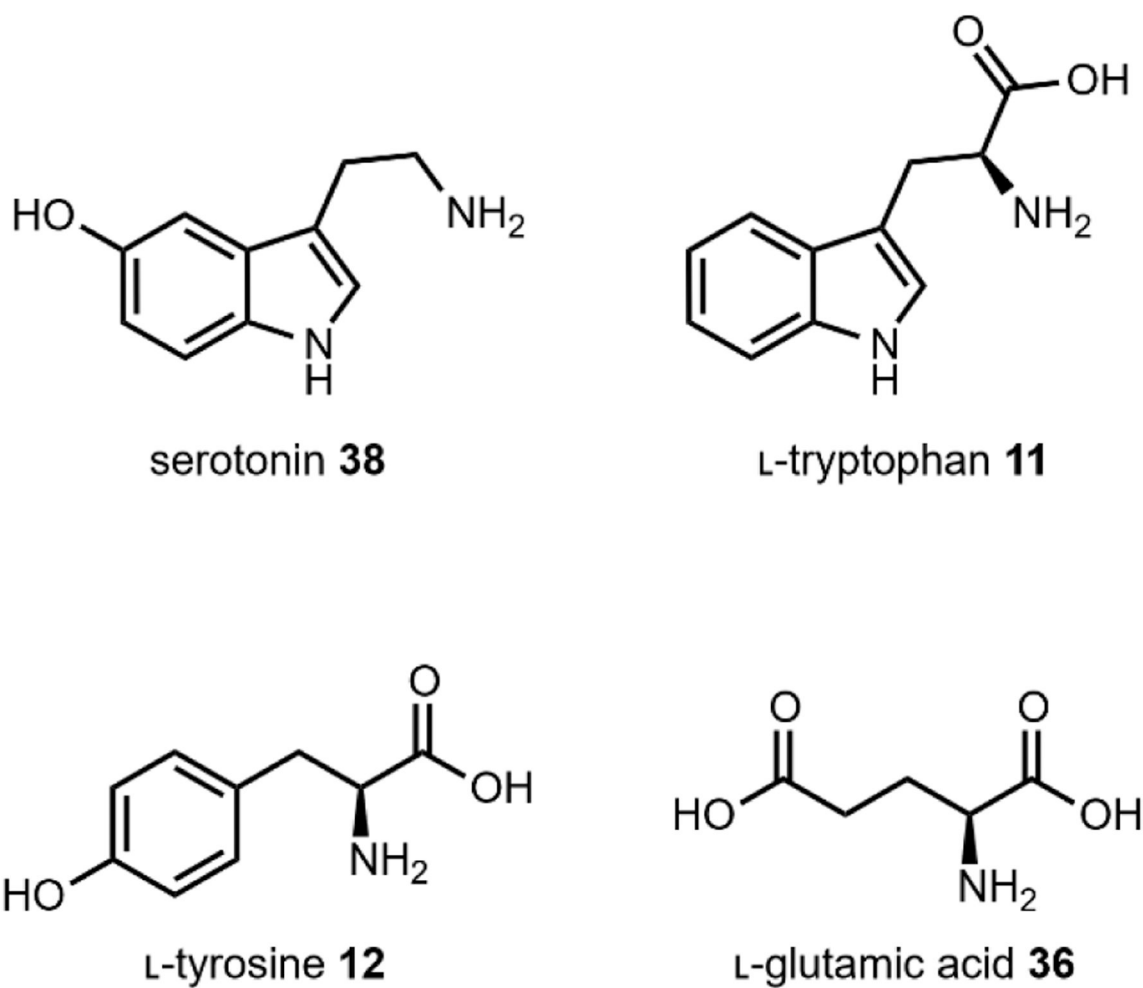


Fig. 7.
Amino acid building blocks for hallucinogens that target serotonin receptors.

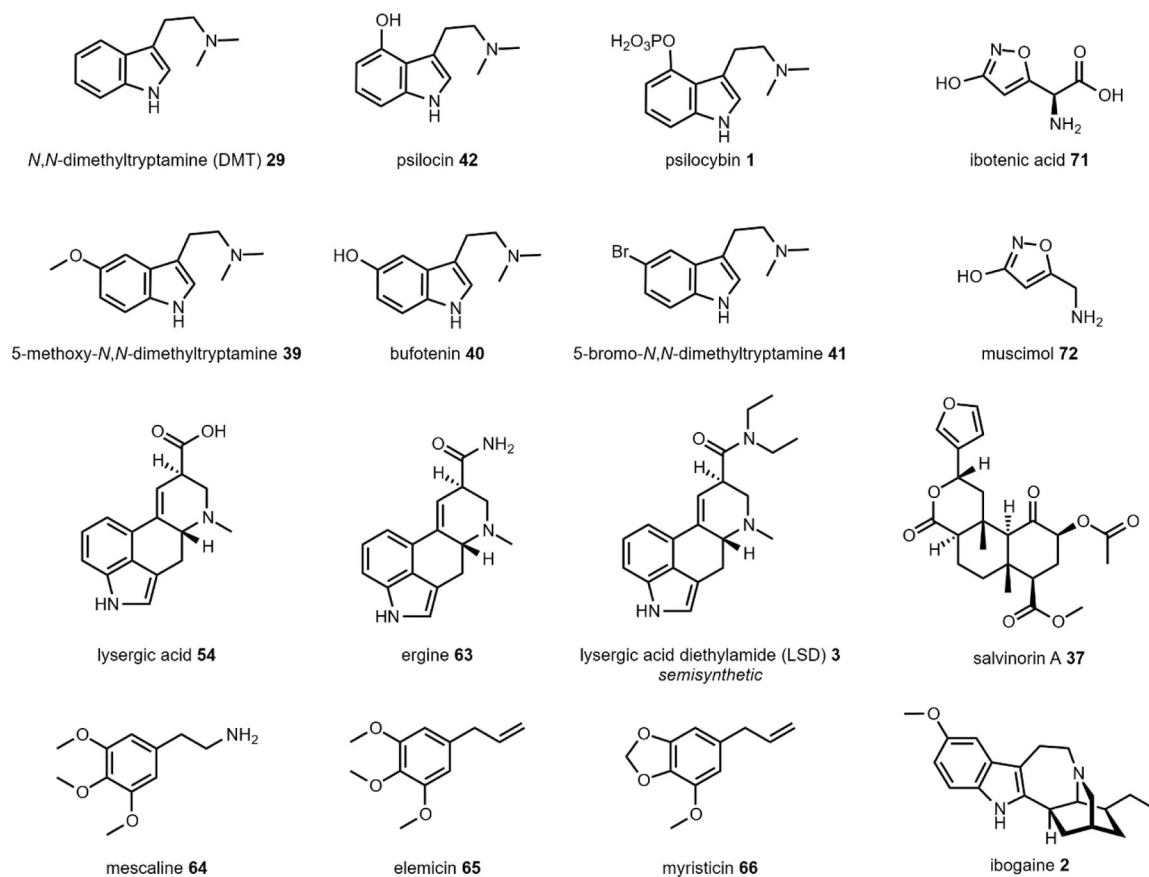
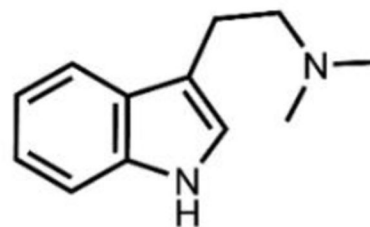


Fig. 8. Overview of hallucinogenic natural products.

*Note that LSD **3** is a semisynthetic compound derived from lysergic acid (Section 2.5).



Psychotria viridis



N,N-dimethyltryptamine (DMT) **29**

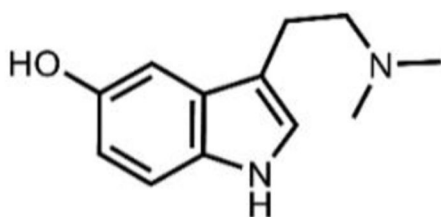
Fig. 9. *Psychotria viridis* is one of the common sources of DMT for ritual purposes.

Image on the left courtesy of Paulo Pedro P. R. Costa via. CC-4.0.

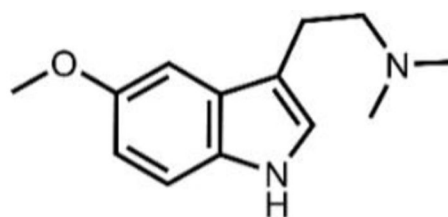
<https://upload.wikimedia.org/wikipedia/commons/0/01/PsychotriaviridisFrutoDSC75.jpg>



Incilius alvarius formerly known as *Bufo alvarius*



bufotenin **40**



5-methoxy-*N,N*-dimethyltryptamine **39**

Fig. 10. *Incilius alvarius*'s skin and exudates contain 5-methoxy-*N,N*-ditryptamine and bufotenin. Image on top courtesy of Wildfeuer via. CC-3.0. https://upload.wikimedia.org/wikipedia/commons/4/4f/2009-03-13Bufo_alvarius067.jpg

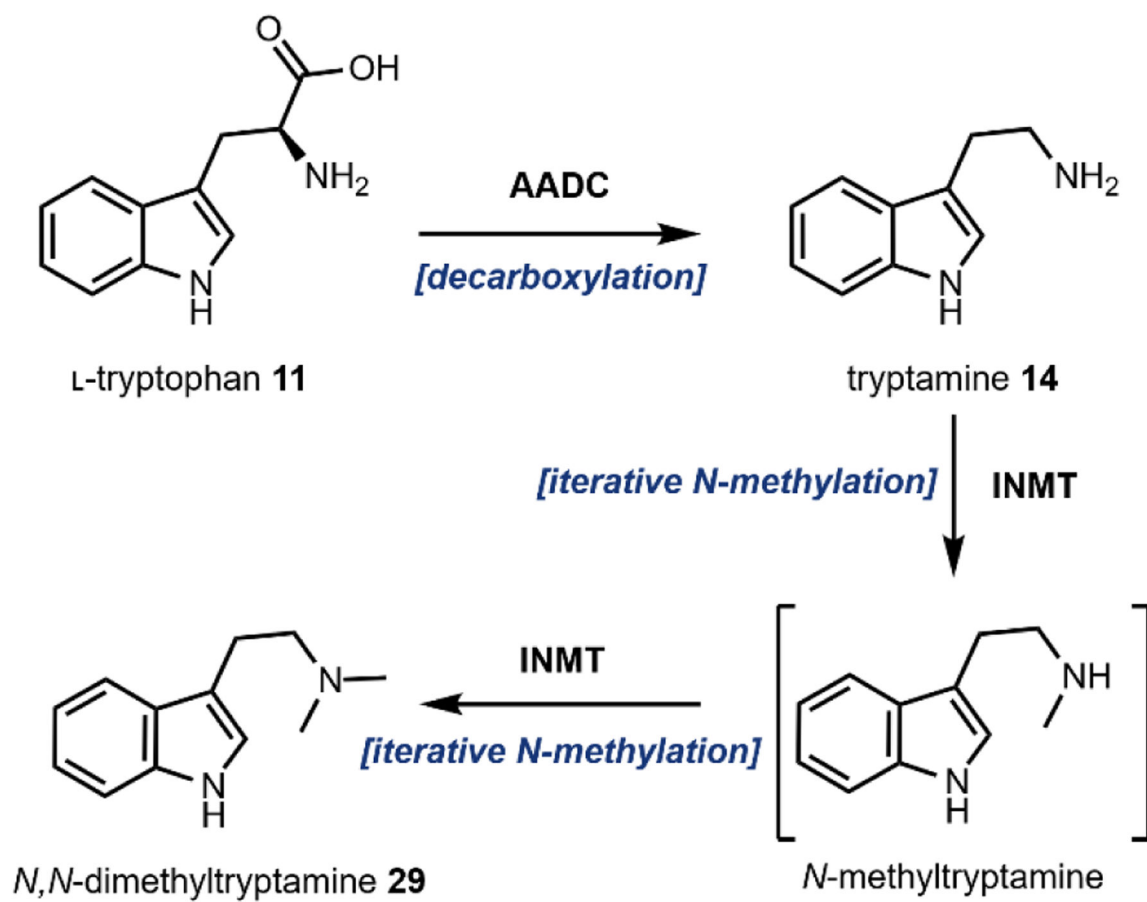
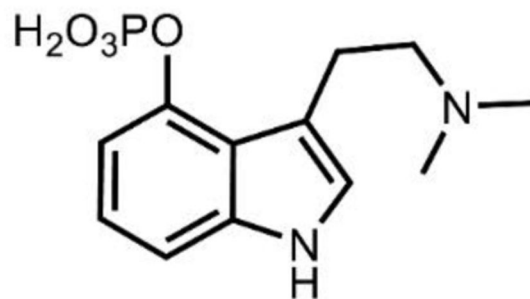


Fig. 11.
Biosynthesis of DMT.



Psilocybe mexicana



psilocybin **1**

Fig. 12. *Psilocybe mexicana* contains ~1% psilocybin.

Image on left courtesy of Alan Rockefeller via CC-3.0.

https://upload.wikimedia.org/wikipedia/commons/4/46/Psilocybe_mexicana_53960.jpg

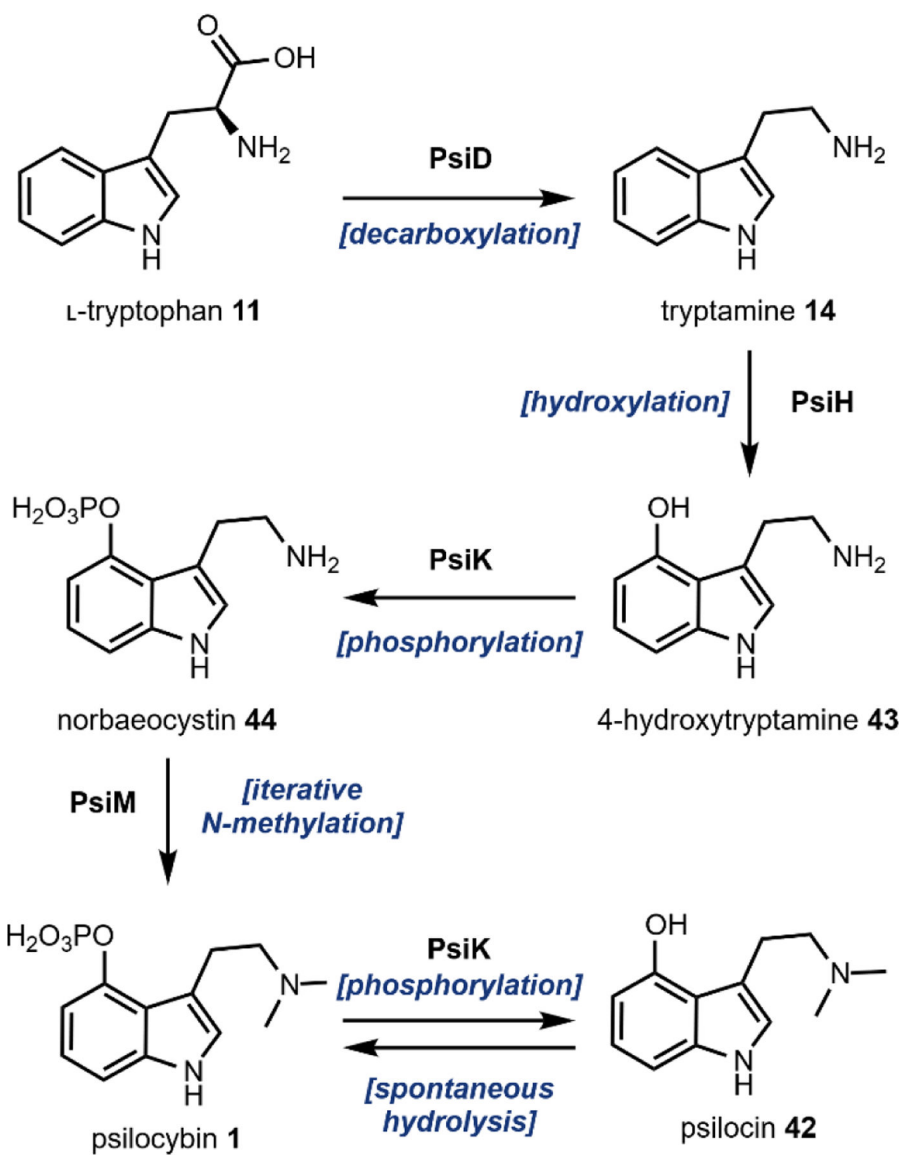


Fig. 13. Biosynthetic pathway of psilocybin and psilocin from L-tryptophan.

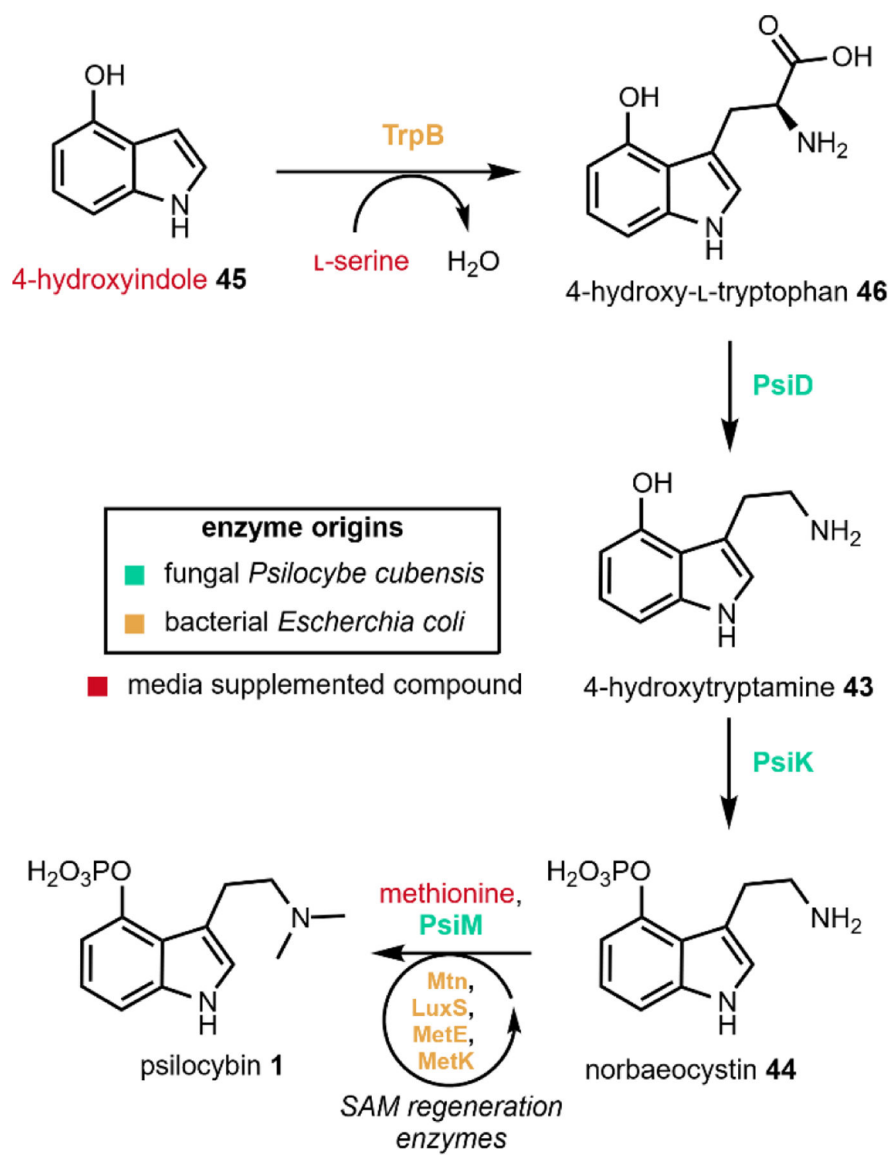


Fig. 14. Engineered production of psilocybin in *E. coli*.⁸¹

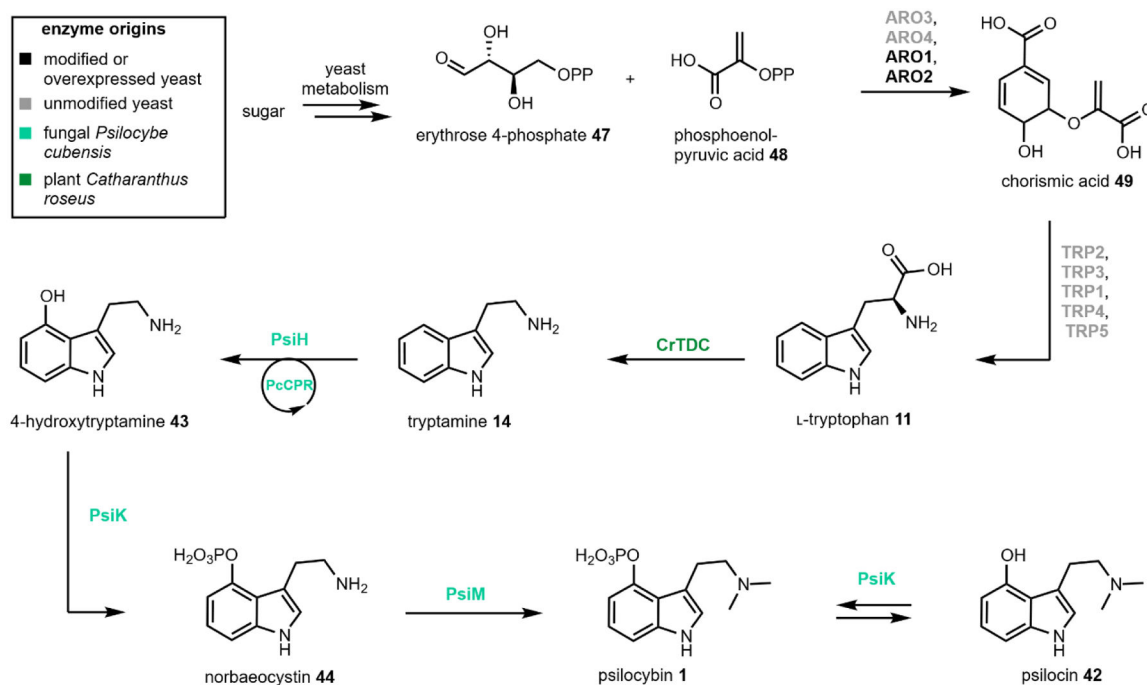
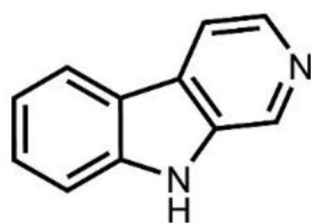


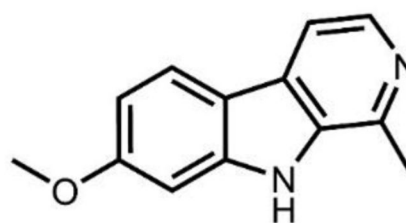
Fig. 15. Engineered production of psilocybin and psilocin in yeast.⁹¹



Banisteriopsis caapi



β -carboline scaffold



harmaline **23**

Fig. 16. *Banisteriopsis caapi* contains many compounds with the β -carboline scaffold, including harmine.

Image on left courtesy Forest and Kim Starr via CC-2.0. https://upload.wikimedia.org/wikipedia/commons/1/17/Starr-140222-0335-Banisteriopsis_caapi-leaves-Haiku-Maui_%2825240510635%29.jpg

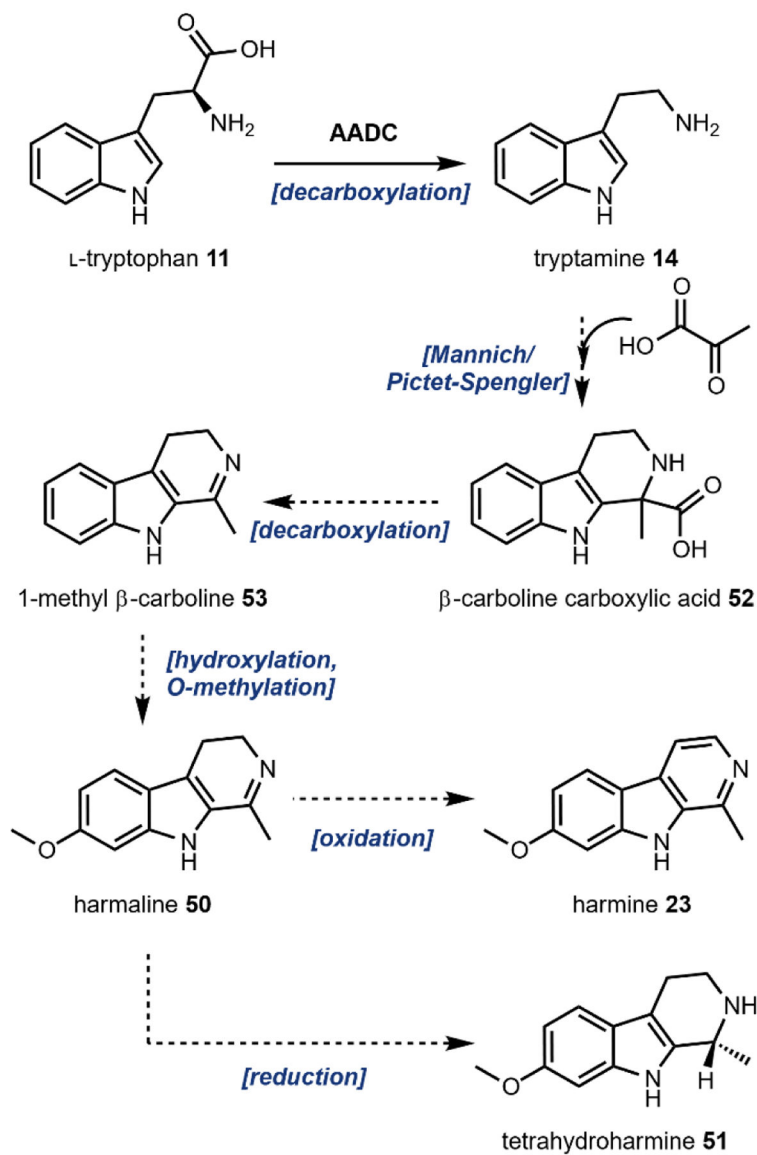
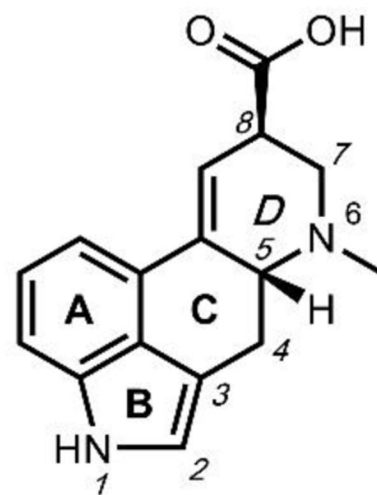


Fig. 17. Proposed biosynthesis of harmala alkaloids.¹⁶⁷



Claviceps purpurea



lysergic acid 54

Fig. 18. *Claviceps purpurea* (ergot fungus) infecting *Dactylis glomerata* (cat grass).
Image on the left courtesy of Bildoj via CC-3.0.

https://upload.wikimedia.org/wikipedia/commons/c/c4/Dactylis_026.JPG

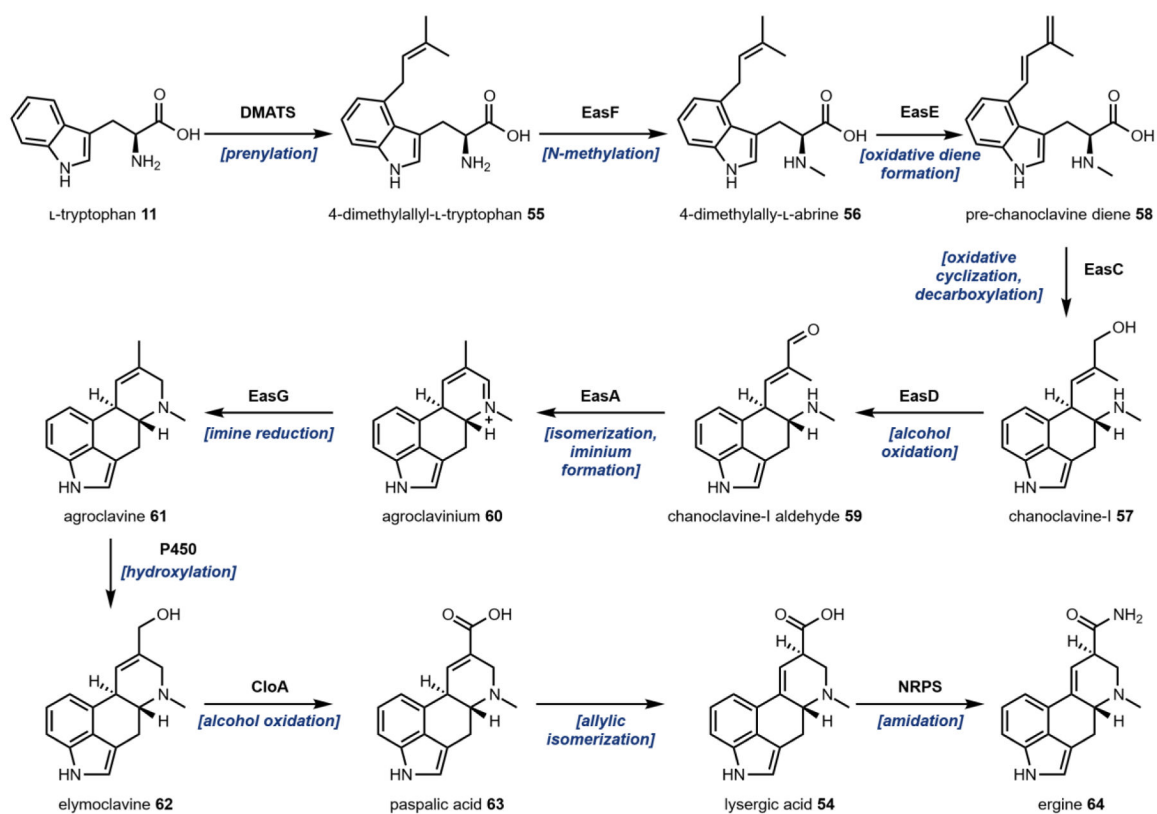
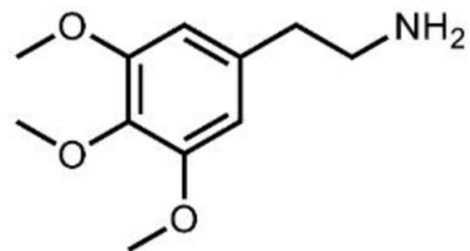


Fig. 19.
Biosynthesis of lysergic acid from L-tryptophan.



Lophophora williamsii



mescaline **65**

Fig. 20. *Lophophora williamsii*, one of the many cacti species that contain mescaline.

Image on the left courtesy of Peter A. Mansfeld via CC-3.0.

https://upload.wikimedia.org/wikipedia/commons/6/69/Lophophora_williamsii_pm.jpg

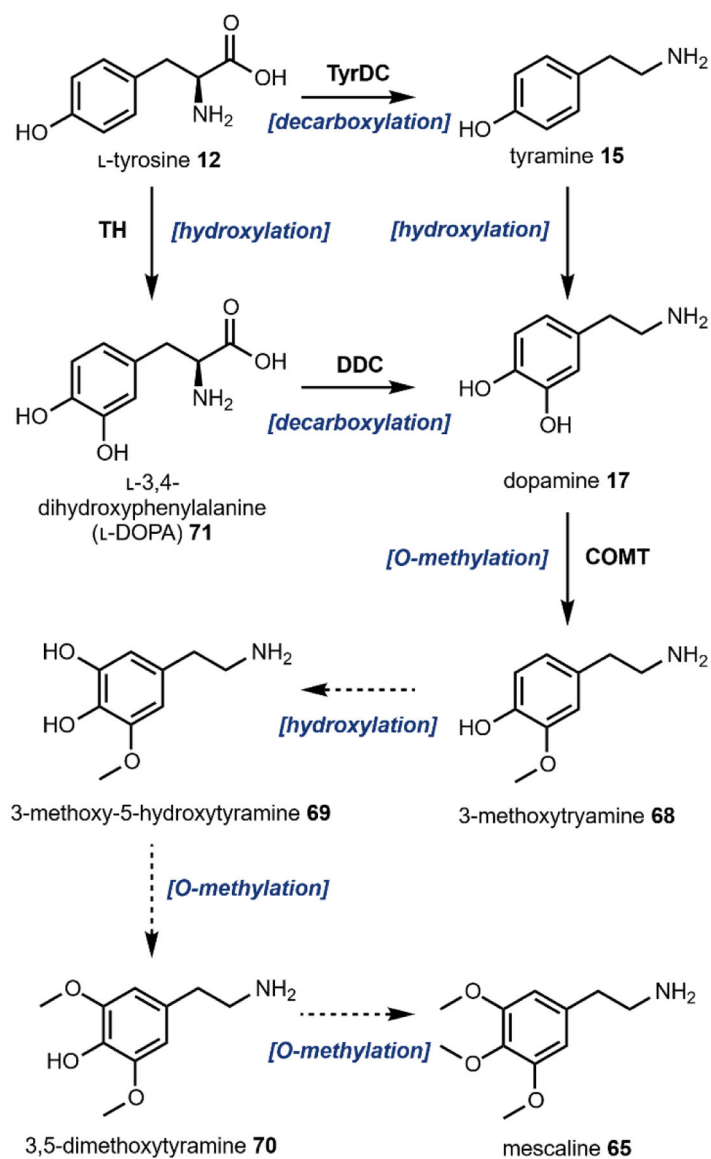
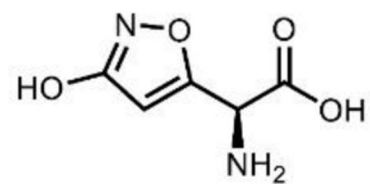


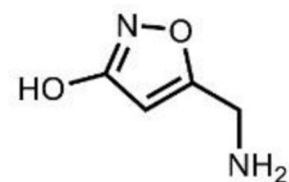
Fig. 21. Proposed biosynthesis of mescaline.²²¹



Amanita muscaria



ibotenic acid **72**



muscimol **73**

Fig. 22.

Amanita muscaria contains about ~100–1000 ppm of ibotenic acid and muscimol.

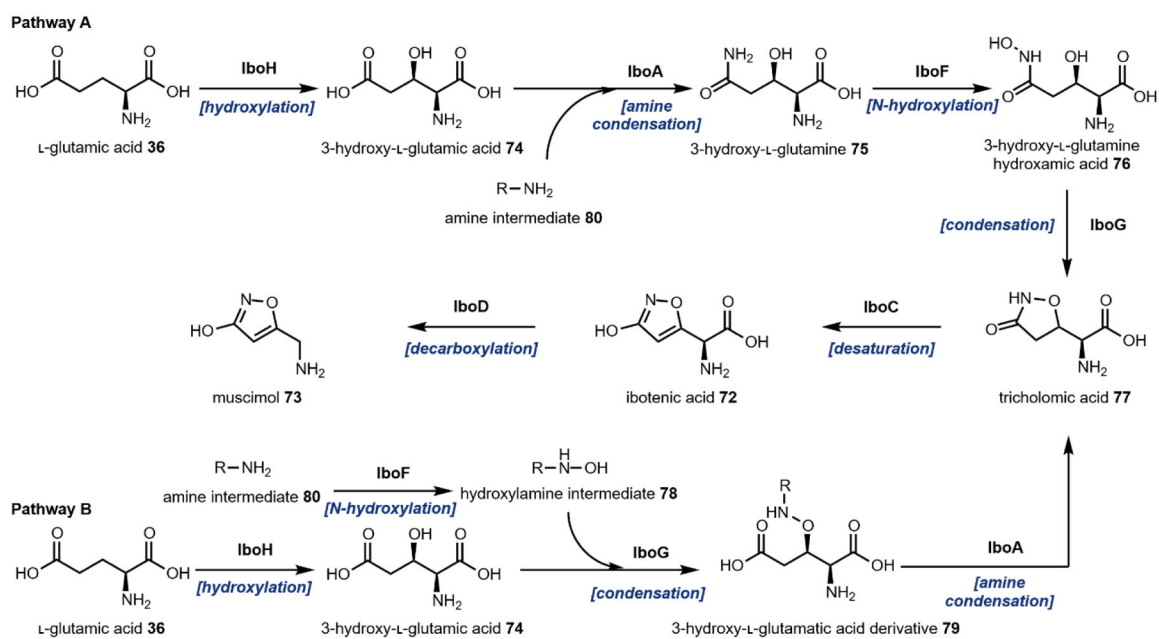
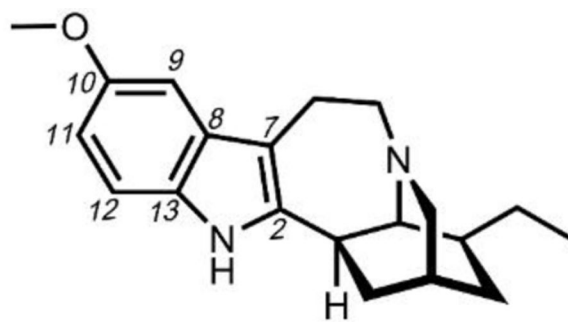


Fig. 23.
Biosynthesis of ibotenic acid and muscimol from L-glutamic acid.²²⁸



Tabernanthe iboga



ibogaine 2

Fig. 24. *Tabernanthe iboga* in fruit.

Image courtesy of Christian Kunath via CC-3.0.

<https://twitter.com/sesamothamnus/status/1031998713760231424>

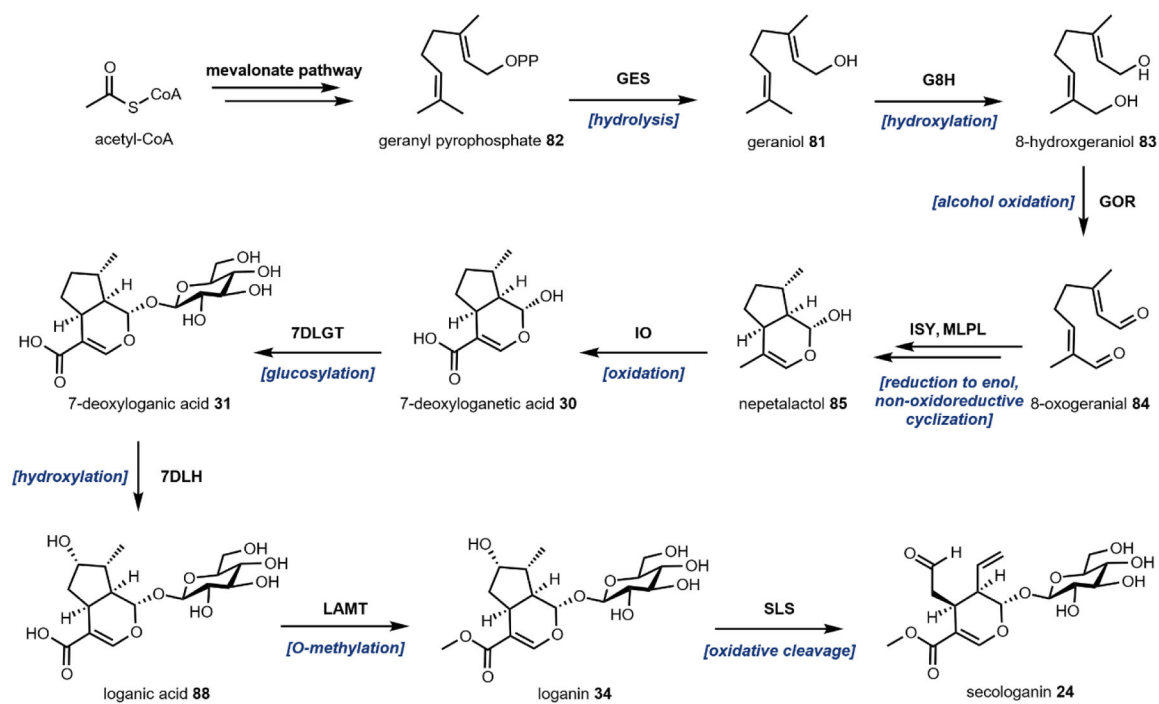


Fig. 25.
Biosynthesis of secologanin from geranyl pyrophosphate (GPP).

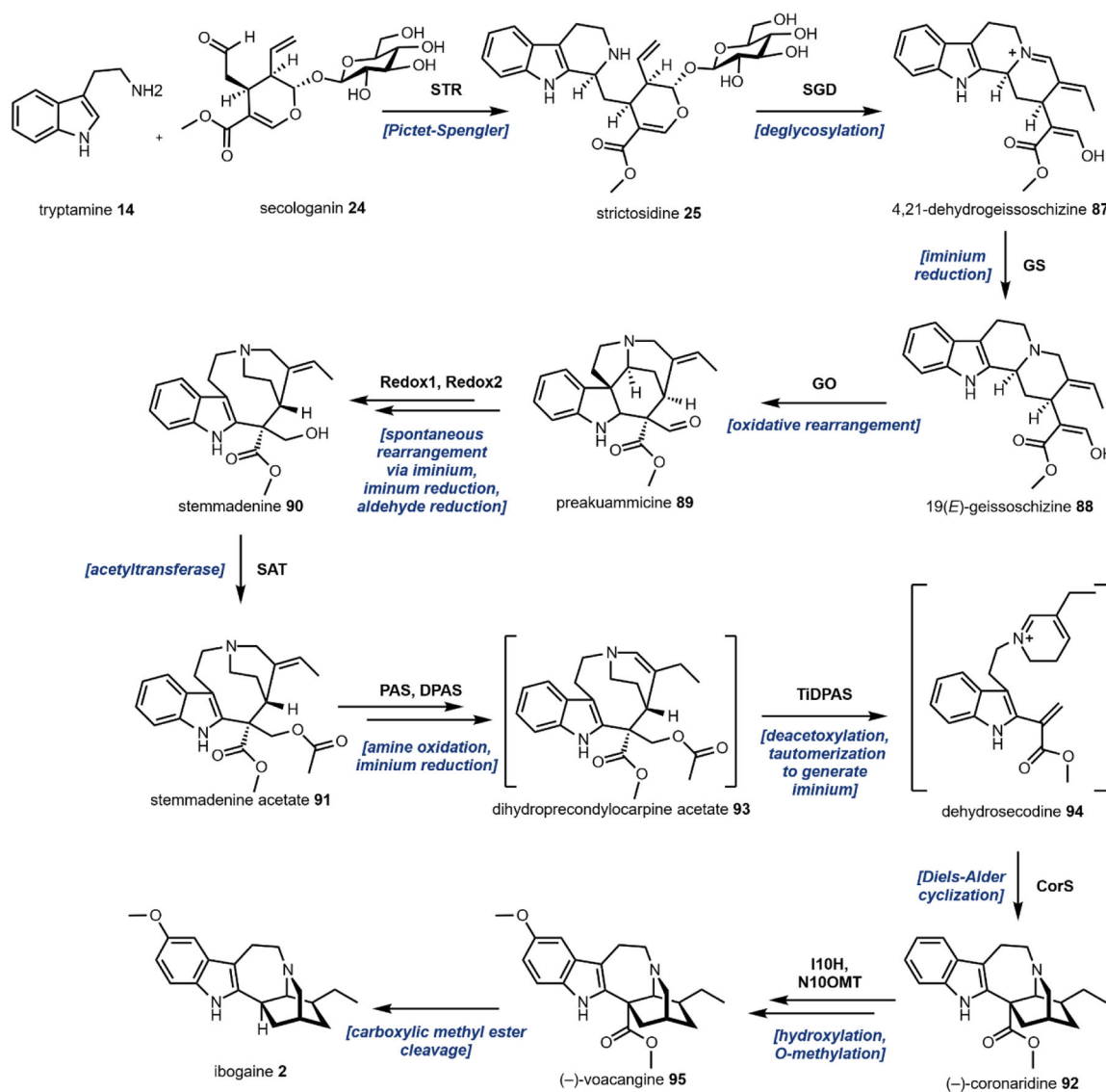


Fig. 26.
Biosynthesis of ibogaine from tryptamine and secologanin.

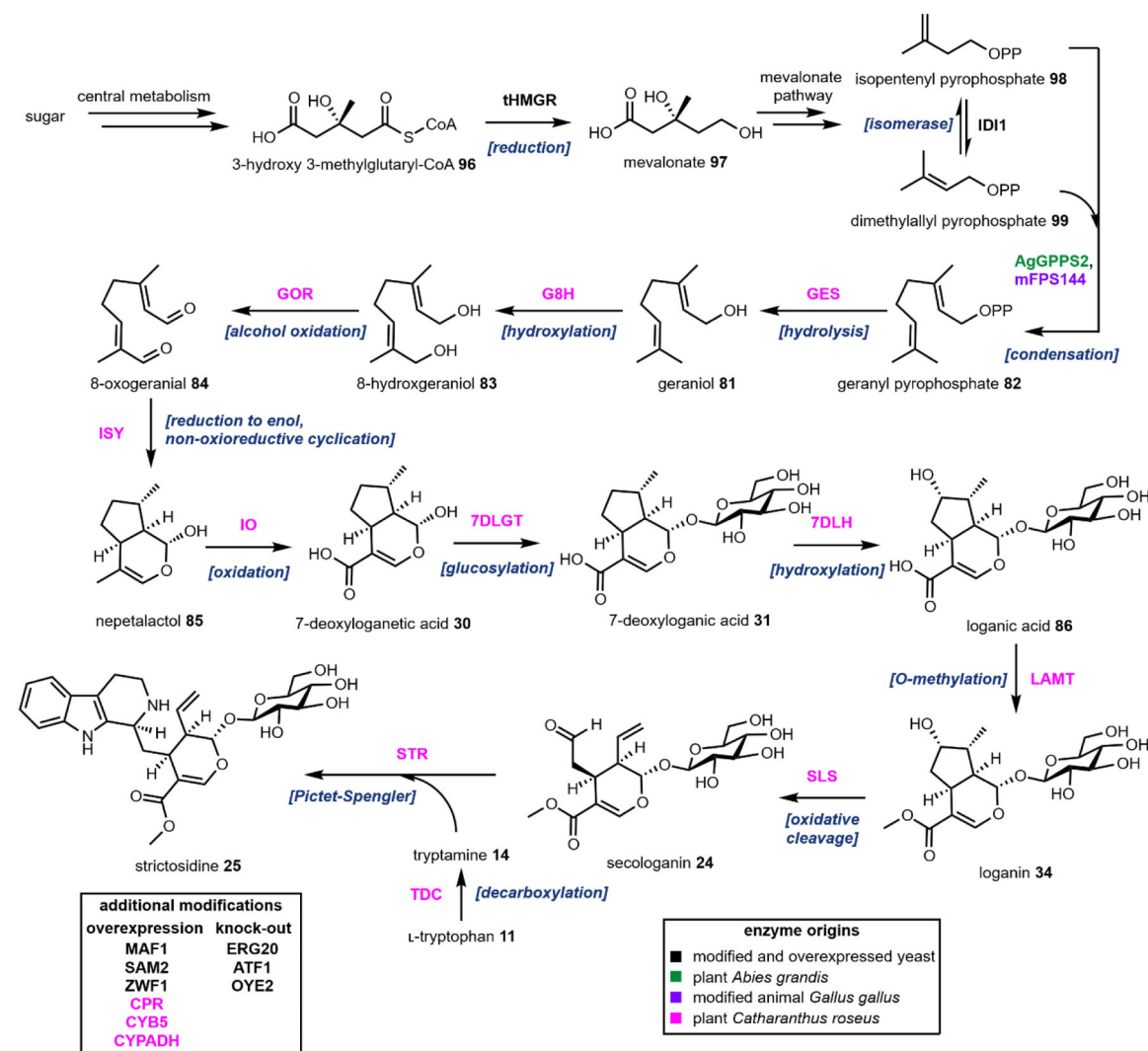
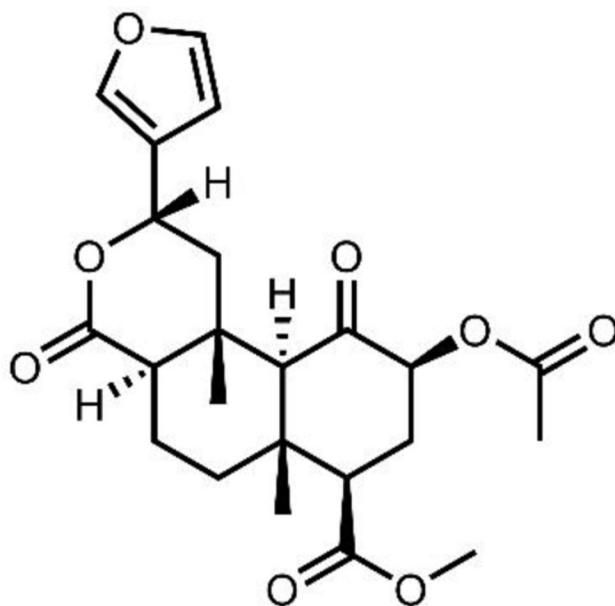


Fig. 27. Heterologous production of strictosidine in *S. cerevisiae*.⁷⁶



Salvia divinorum

salvinorin A **37**

Fig. 28.

Salvia divinorum contains salvinorin A, a structurally unique terpene hallucinogen. Image on the left courtesy of Eric Hunt via CC-2.5.

https://upload.wikimedia.org/wikipedia/commons/3/35/Salvia_divinorum_-1.jpg

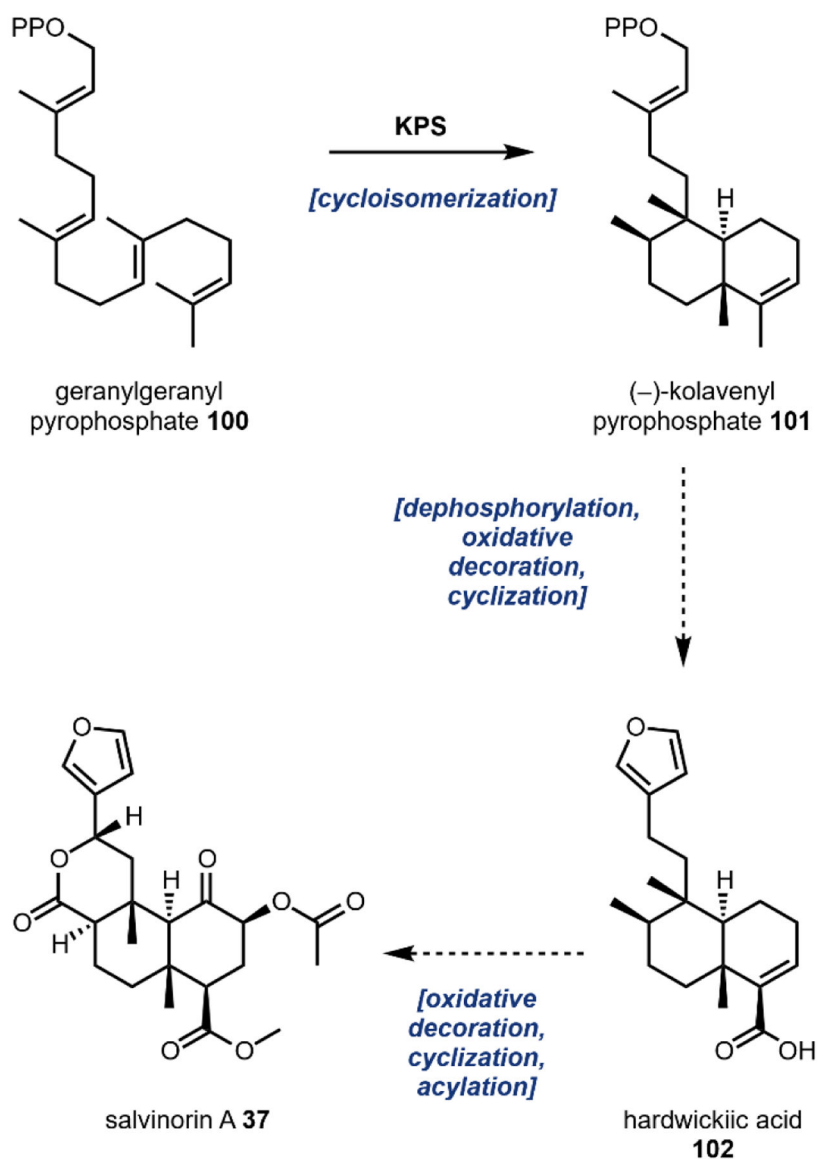
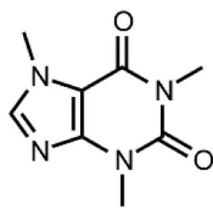
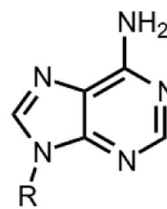
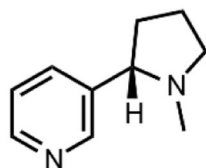
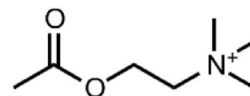
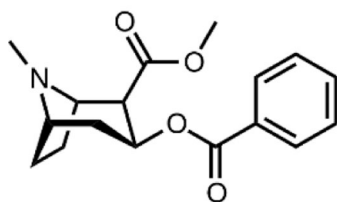
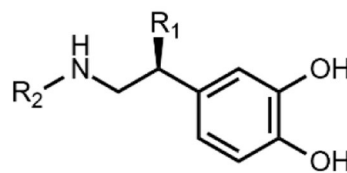
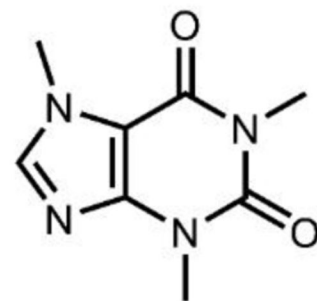


Fig. 29.
Proposed biosynthetic pathway for salvinorin A.²⁷⁹

caffeine **4**R = ribose; adenosine **105**
R = H; adenine **113**nicotine **5**acetylcholine **106**cocaine **6**R₁ = H, R₂ = H; dopamine **17**
R₁ = OH, R₂ = CH₃; epinephrine **103**
R₁ = OH, R₂ = H; norepinephrine **104****Fig. 30.**
Alkaloidal stimulants as structural mimics of neurotransmitters.



Coffea arabica beans



caffeine **4**

Fig. 31.

Coffea arabica (the dominant coffee cultivar) contains ~1.2 percent dry weight caffeine.

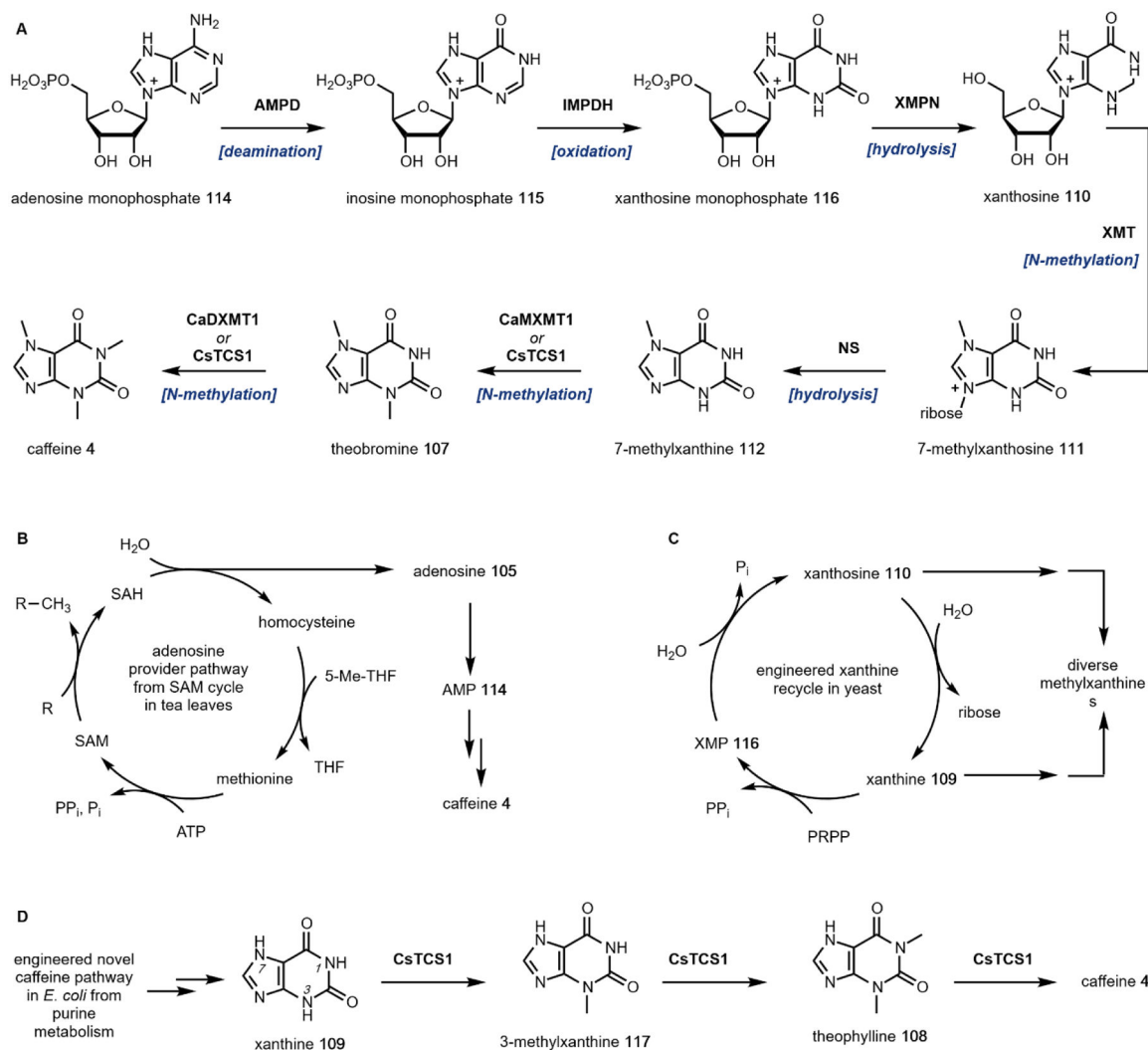
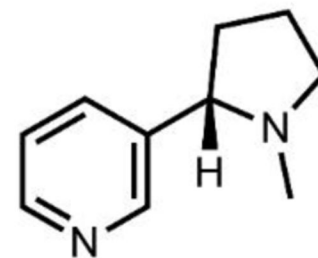


Fig. 32. Caffeine biosynthesis and microbial engineering strategies.

(A) Major caffeine biosynthetic route identified in *Camellia sinensis* and *Coffea arabica*. (B) SAH-derived adenosine may be funneled into purine metabolism in tea leaves following methyl transfer. (C) Xanthine recycle pathway utilized during heterologous production in yeast. (D) Novel xanthine-to-caffeine conversion pathway leveraged for caffeine production in *E. coli*.



Nicotiana tabacum



nicotine **5**

Fig. 33.

Nicotiana tabacum leaves contain 2 to 8 percent dry weight nicotine.

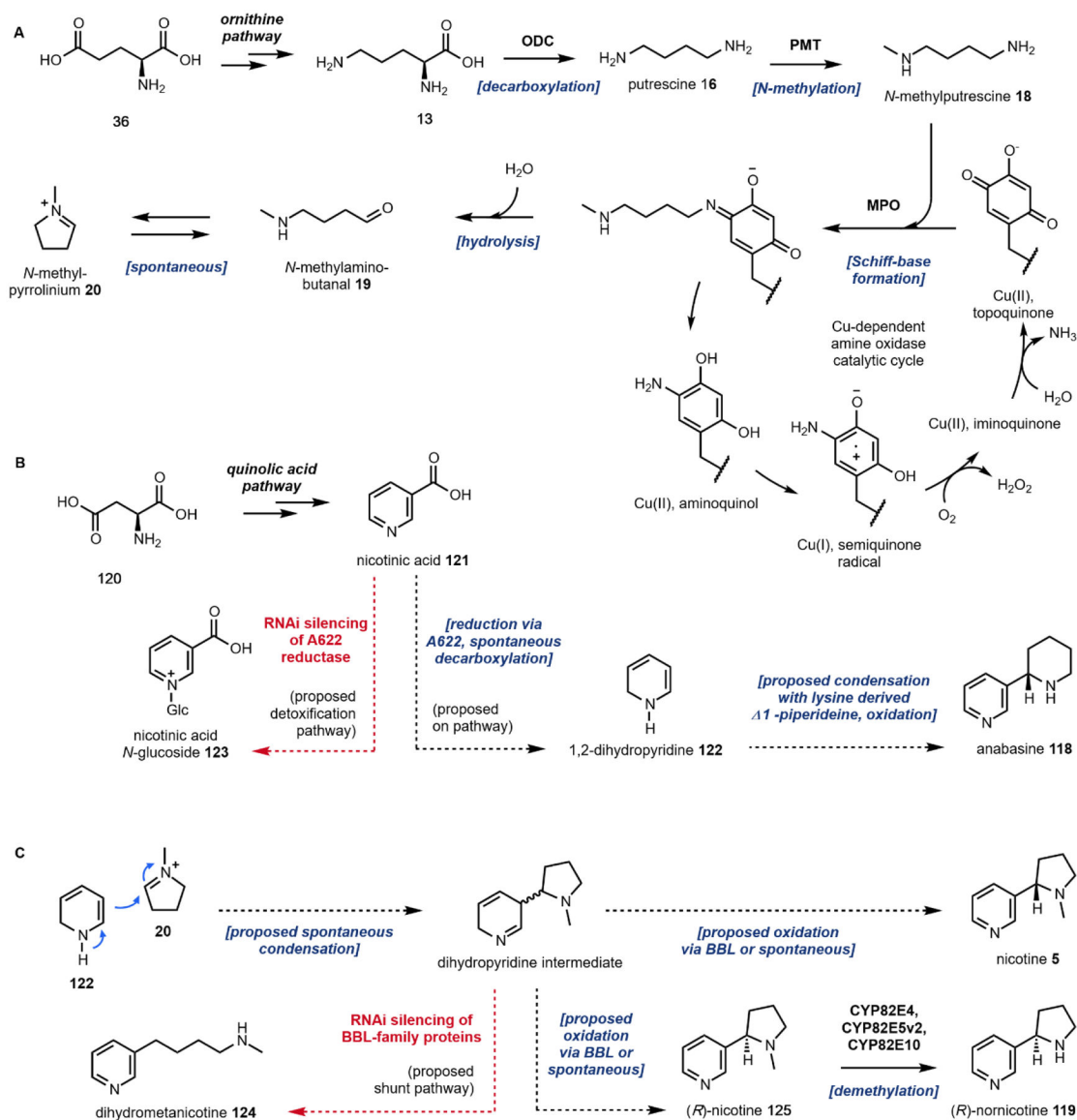
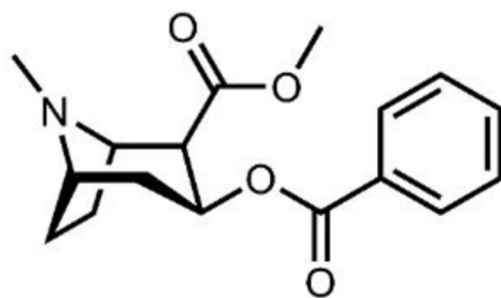


Fig. 34. Summary of the nicotine biosynthetic pathway, including known and proposed enzymatic steps.

(A) *N*-methylpyrrolinium formation via the polyamine pathway. (B) Proposed reduction of nicotinic acid via A622. (C) Proposed oxidation of condensation products via BBL towards nicotine, nornicotine.



Erythroxylum coca



cocaine **6**

Fig. 35. *Erythroxylum coca* leaves contain ~0.7 percent dry weight cocaine. Image on left courtesy of Danna Lizeth Guevara Prieto via CC-4.0. <https://www.inaturalist.org/photos/22483426>

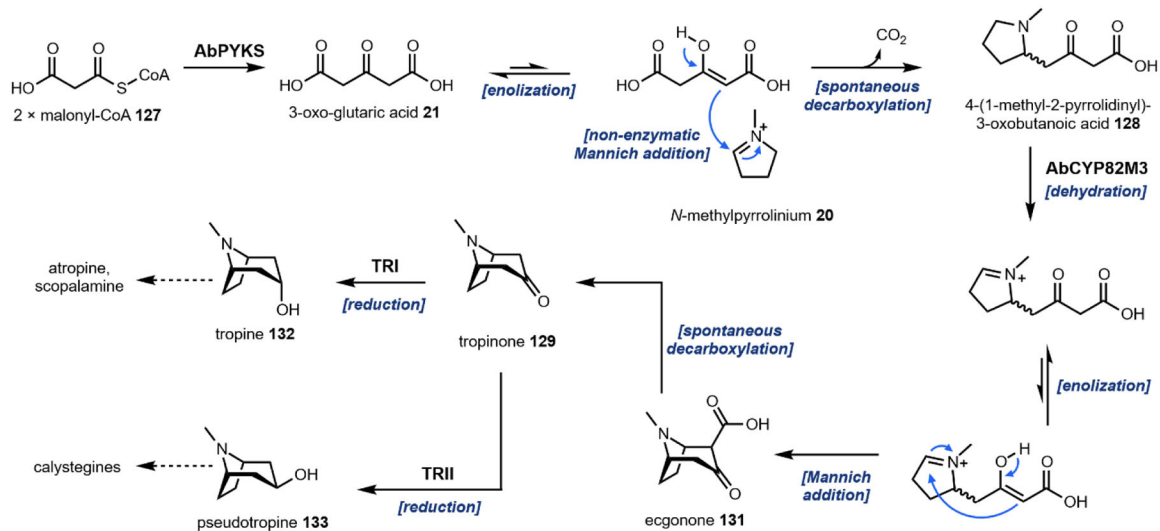


Fig. 36.
Formation of tropine, pseudotropine.

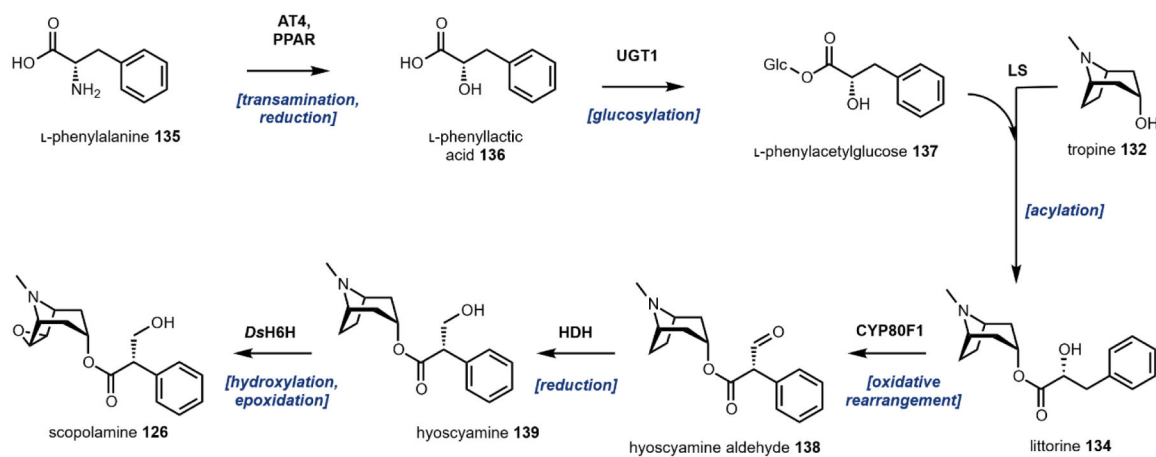


Fig. 37.
Scopolamine biosynthesis from phenylalanine and tropine.

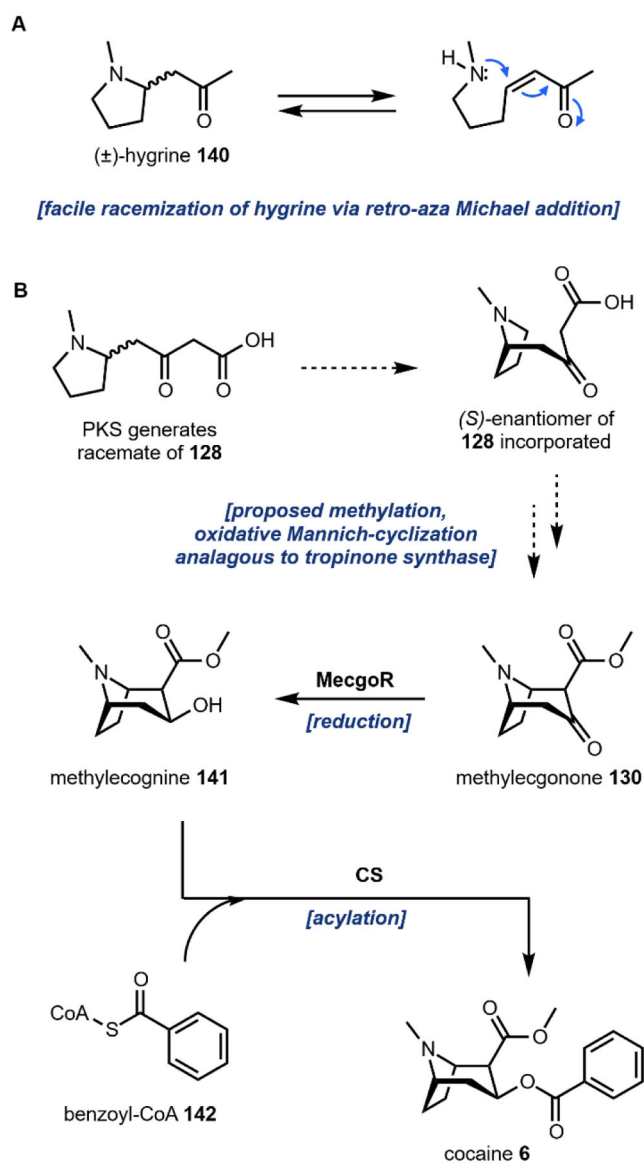


Fig. 38. Cocaine biosynthesis.

(A) Racemization of the cocaine pathway intermediate decarboxylation product hygrine. (B) Proposed biosynthesis of methylecgonone and subsequent formation of cocaine.

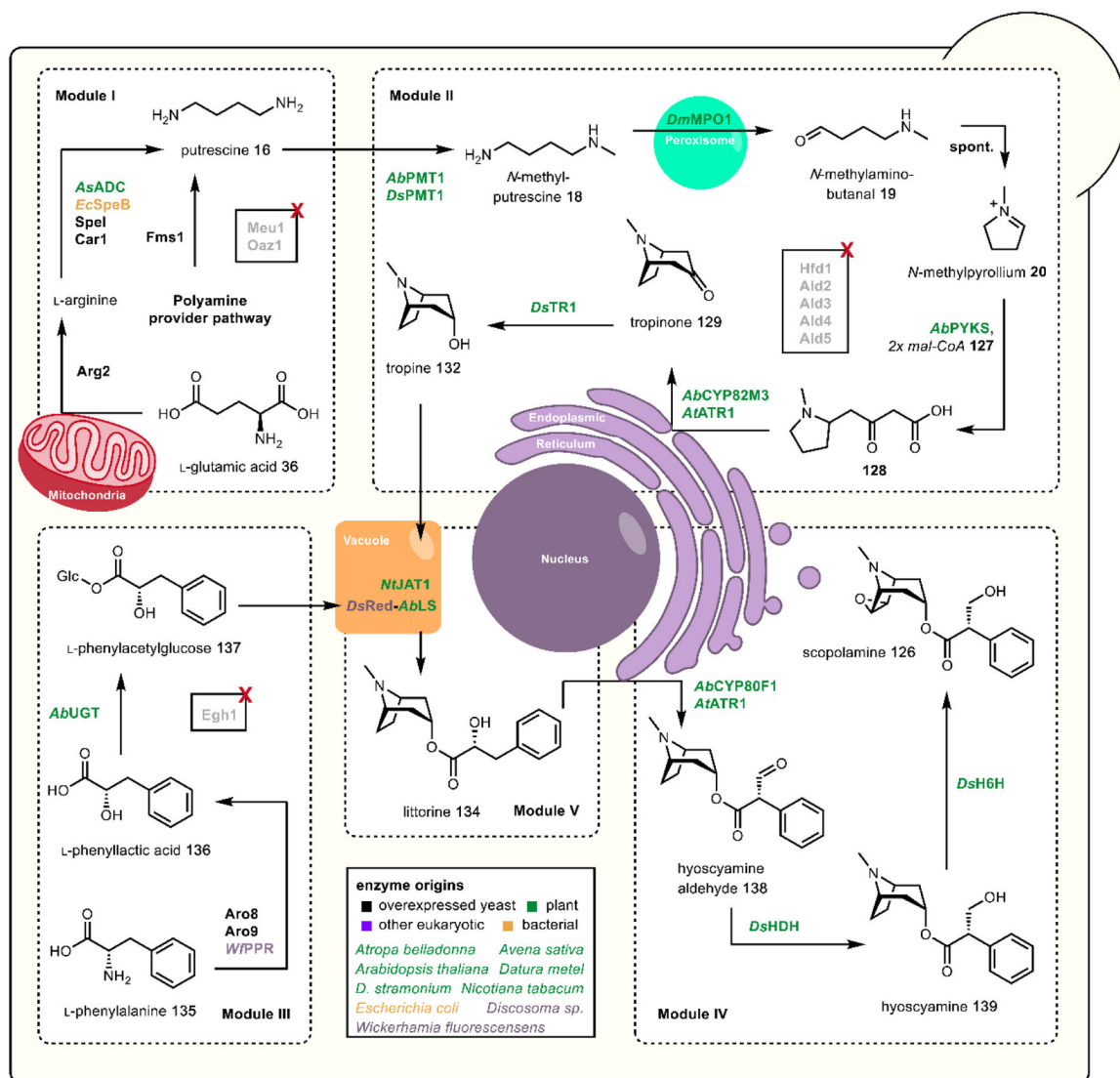
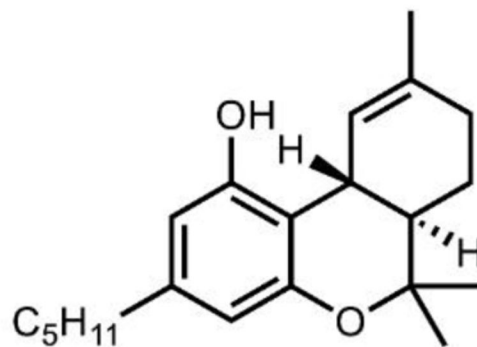


Fig. 39.
Production of tropane alkaloids in yeast.⁷³



Cannabis sativa



tetrahydrocannabinol 7

Fig. 40.

The *Cannabis sativa* plant typically contains 5–16% tetrahydrocannabinol (7).³⁶⁴

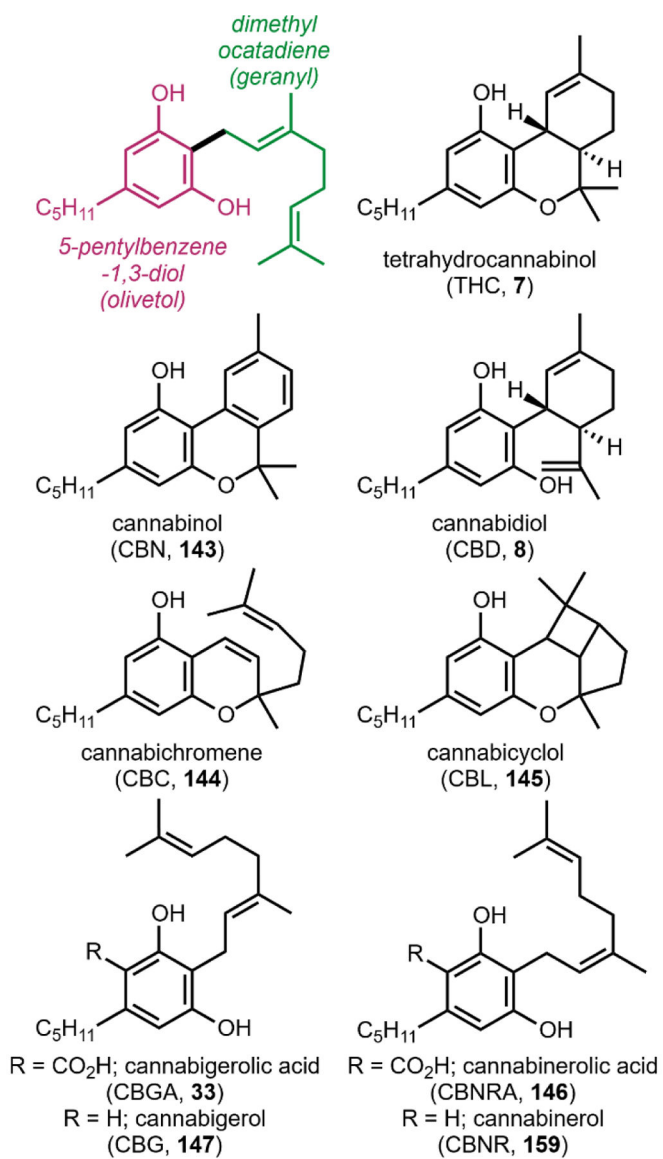
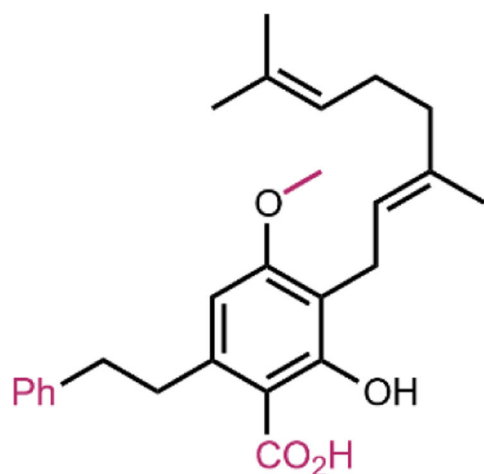
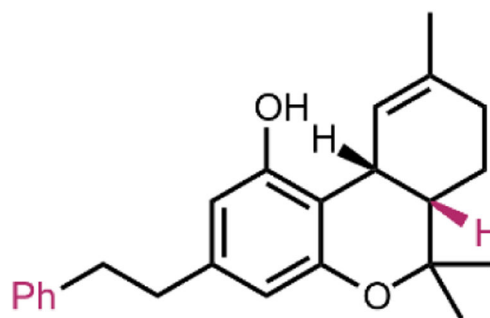


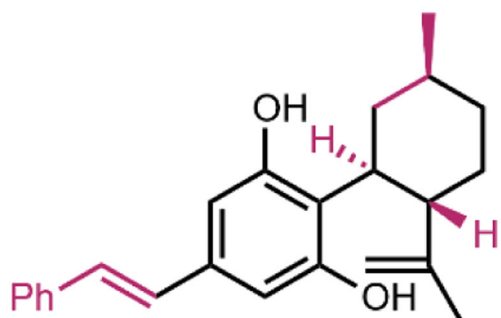
Fig. 41. Structural motifs and examples of isolated natural products from the *Cannabis* plant.



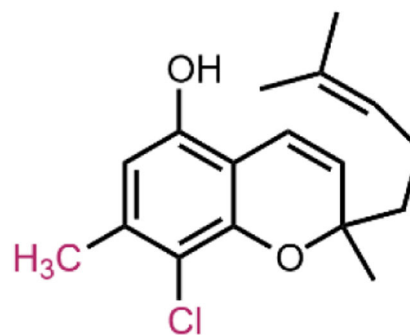
amorfrutin 2 (B) **148**
Amorpha fruticosa L.



(-)-*cis*-perrottetinene **149**
Radula perrottetii



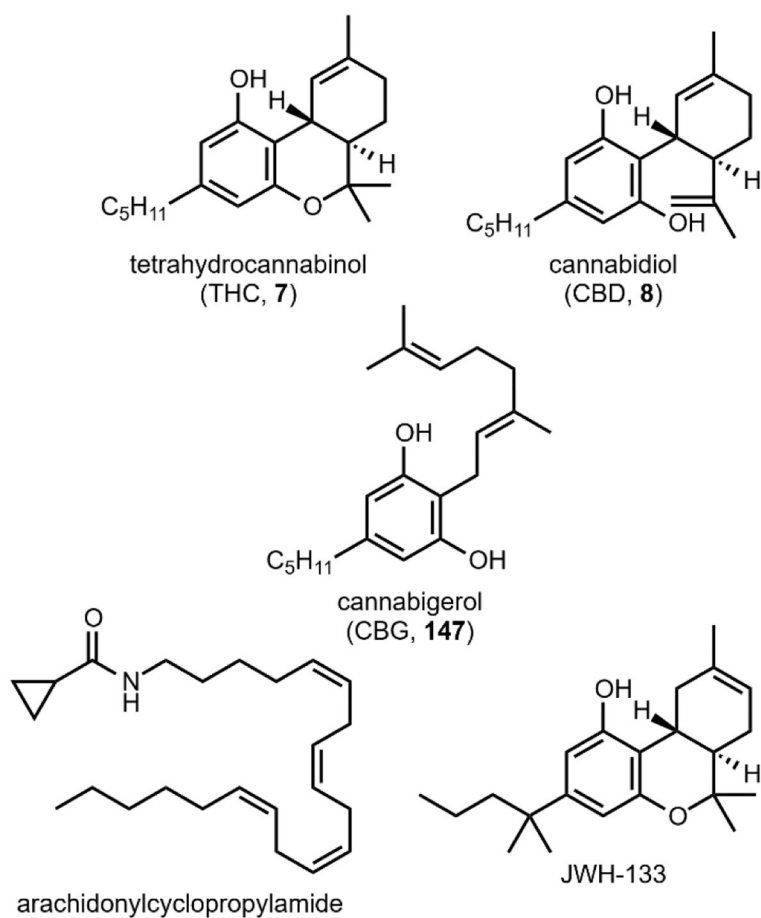
machaeridiol A **150**
Machaerium multiforum



6-chloro-cannabiorchichromene **151**
Cylindrocarpon olidum

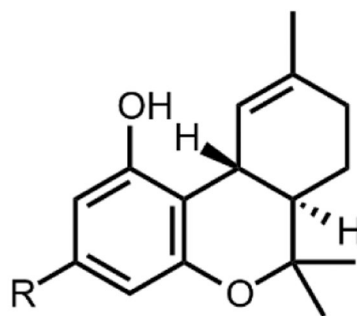
Fig. 42. Exemplary structurally related cannabinoid-like natural products isolated from other plant and fungal sources (*italics*).

Structural deviations highlighted in red. Amorfrutin 2 (B) (**148**) is a **148** derivative,³⁸⁰ (-)-*cis*-perrottetinene (**149**) is a **7** derivative,³⁸¹ machaeridiol (**150**) is a **8** derivative,³⁸² and 6-chloro-cannabiorchichromene (**151**) is a **144** derivative.³⁸³

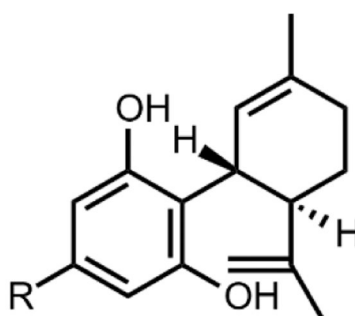


Structure	CB1 K _i (nM)	CB2 K _i (nM)
7	40.7	36.0
8	1,690	1,714
147	1,045	1,225
arachidonylcyclopropylamide	2.2	7.15
JWH-133	677	3.4

Fig. 43. CB1 and CB2 activity for 7, 8, 147, the natural endocannabinoid arachidonylcyclopropylamide, and synthetic analogue JWH-133.



Structure	CB1 K_i (nM)	CB2 K_i (nM)
R = C ₅ H ₁₁ ; 7 (THC)	40.7	36.0
R = C ₃ H ₇ ; 152 (THCV)	75.4	62.8
R = C ₇ H ₁₅ ; 154 (THCP)	1.2	6.2



Structure

- R = C₅H₁₁; **8** (CBD)
- R = C₃H₇; **153** (CBDV)
- R = C₇H₁₅; **155** (CBDP)

Fig. 44.

CB1 and CB2 activity of THC (**7**) with varying C3 alkyl chain lengths, propyl (varin, **152**) and heptyl (phorol, **154**). CBD alkyl chain length derivatives also shown for clarity.

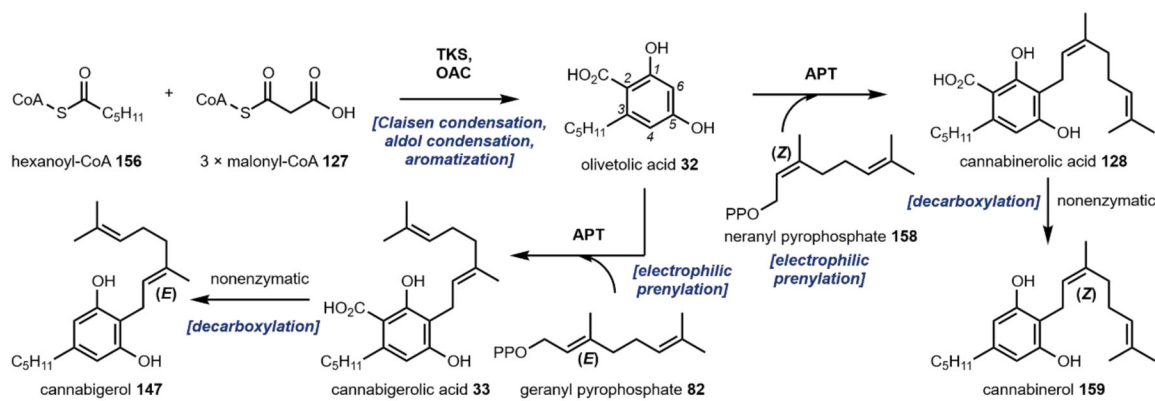


Fig. 45.
Biosynthesis of cannabigerol (147) and cannabinerol (159) from hexanoyl-CoA 156 and malonyl-CoA 127.

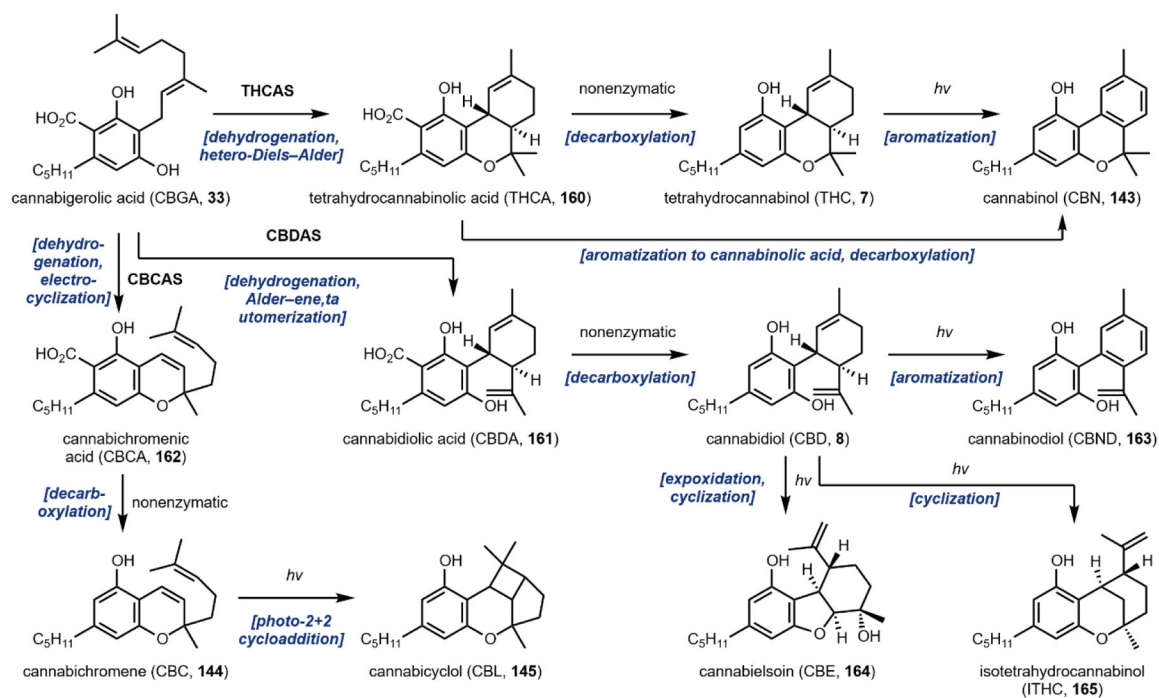


Fig. 46. Biosynthesis of tetrahydrocannabinol (7), cannabidiol (8), cannabichromene (144), and further nonenzymatic derivatized products.

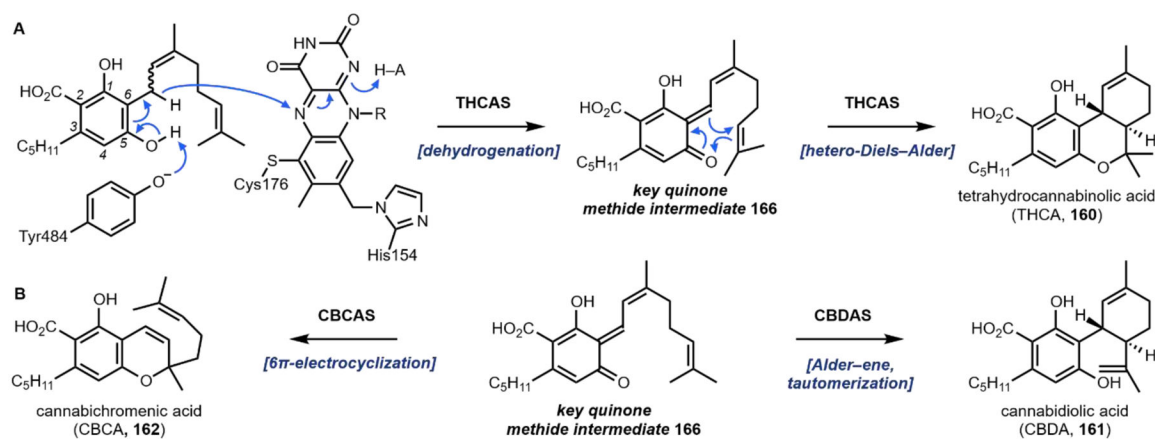


Fig. 47. Key proposed step in biosynthesis of cannabis natural products converting cannabigerolic or cannabimerolic acid to THCA (160).

(A) Enzymatic dehydrogenation reaction leads to a reactive quinone methide intermediate **166** that can undergo various pericyclic reactions to yield all cannabis scaffolds. Flavin adenine dinucleotide (FAD), R = C₁₆H₂₆N₅O₁₃P₂. (B) Related enzymatic transformations by CBCAS and CBDAS form CBCA (**162**) and CBDA (**161**)

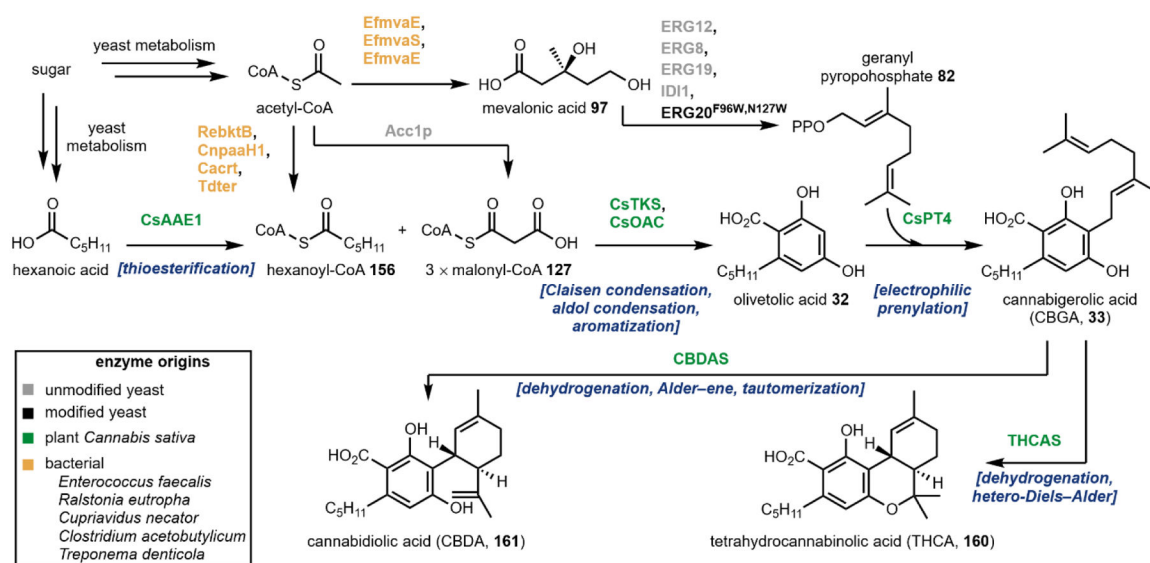


Fig. 48. Heterologous production of tetrahydrocannabinolic acid (160) and cannabidiolic acid (161).

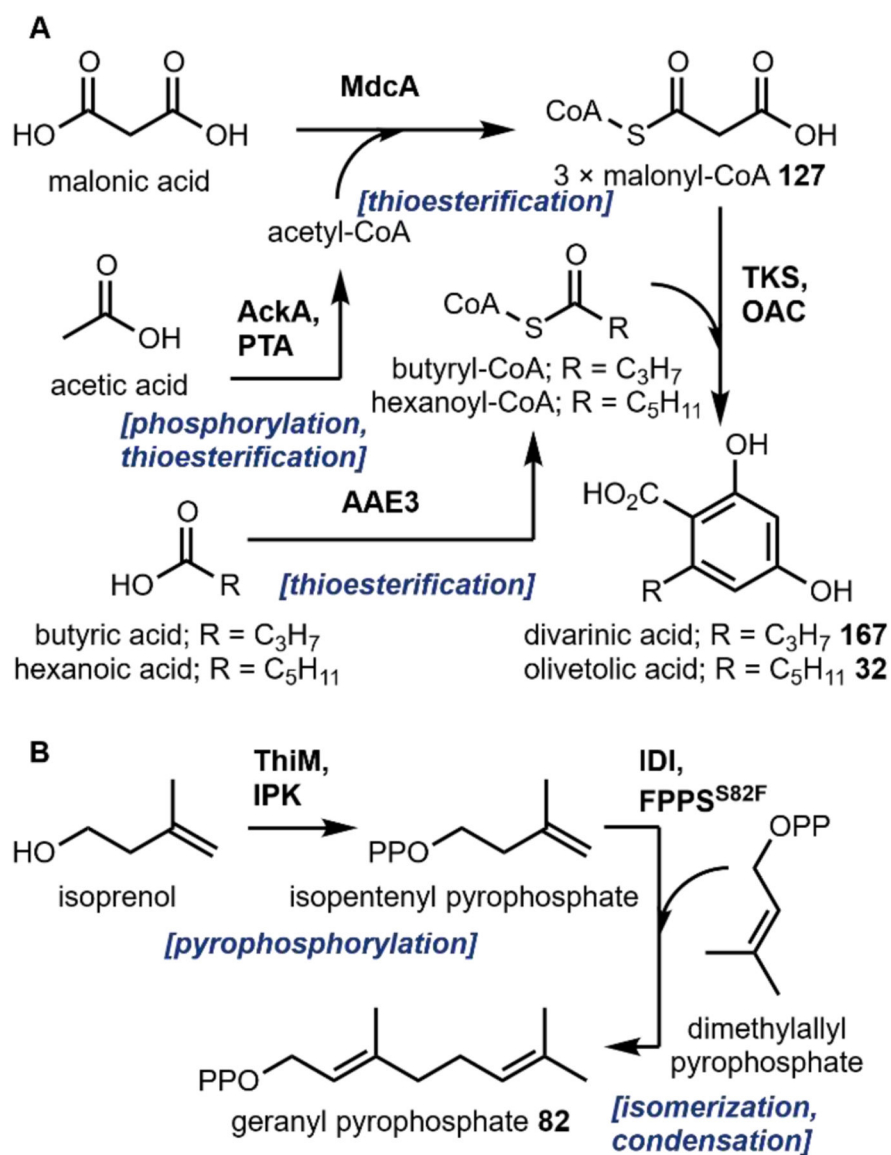
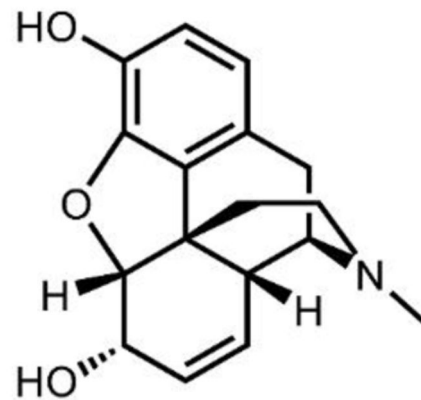


Fig 49. Cell-free system for improved olivetolic acid, divarinic acid, and geranyl pyrophosphate production.



Papaver somniferum



morphine **9**

Fig. 50. Image of bulbs and bloom of the poppy plant, *Papaver somniferum*.
On average, poppy bulbs contain 16% by weight morphine **9**.⁴²³

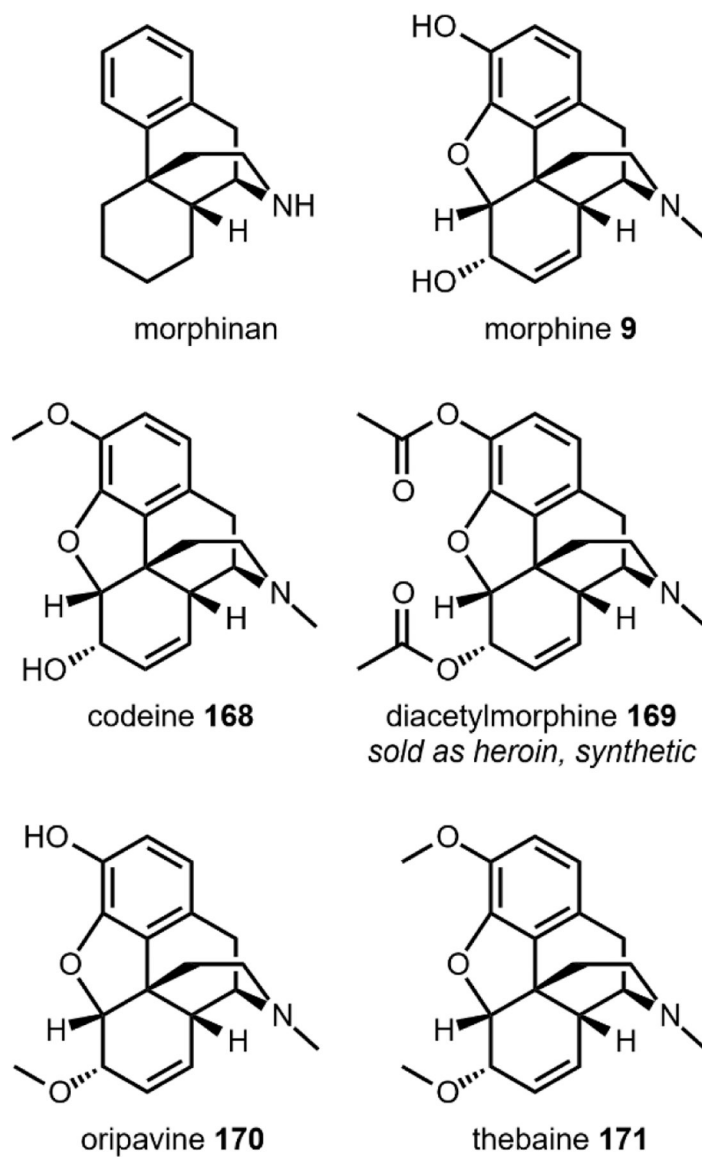


Fig. 51. Structures of natural morphinan opioids and synthetic compound diacetylmorphine (heroin, 169).

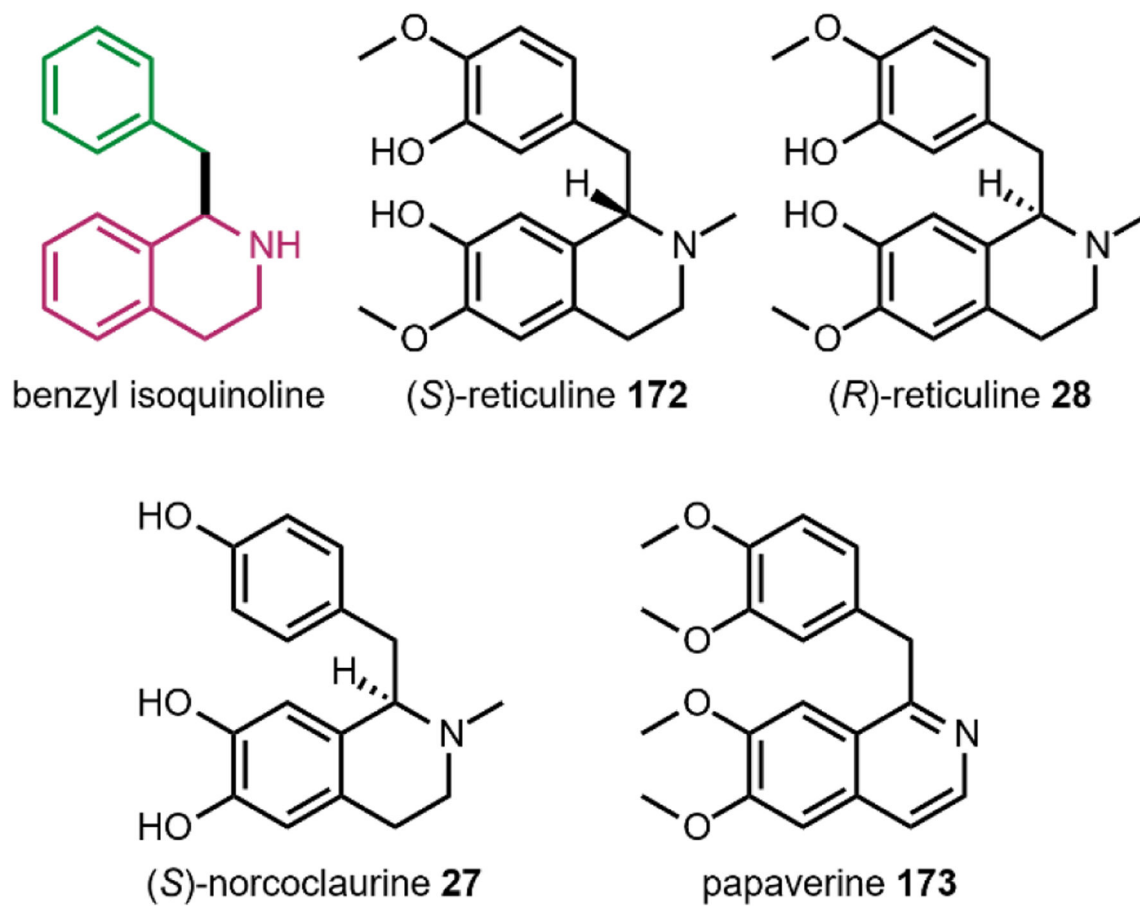


Fig. 52. Structures of simple benzyl isoquinolines that play key roles in opioid biosynthesis (172, 28, 27) and as antispasmodic drugs (173).

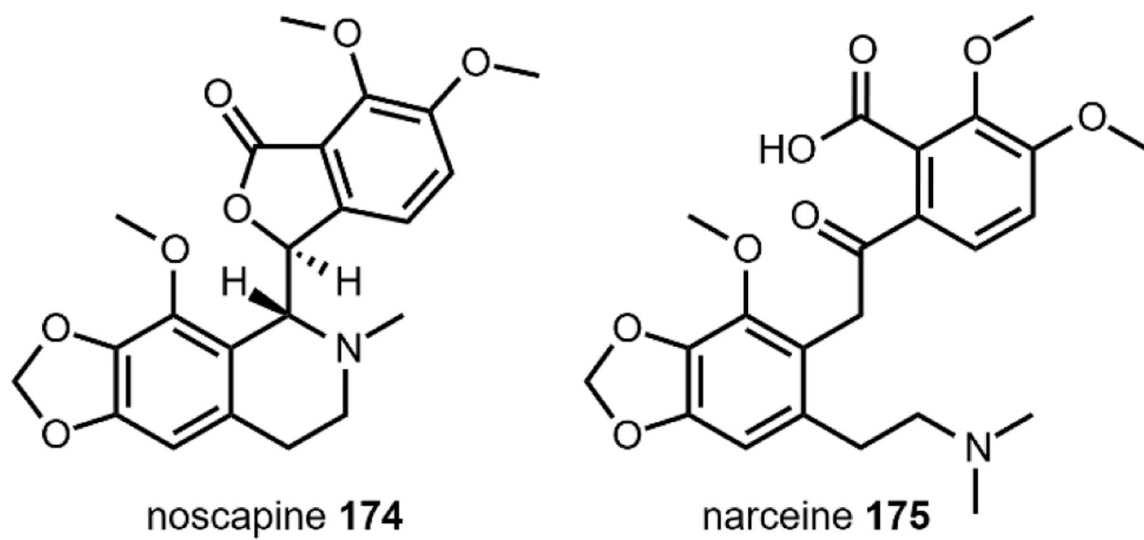
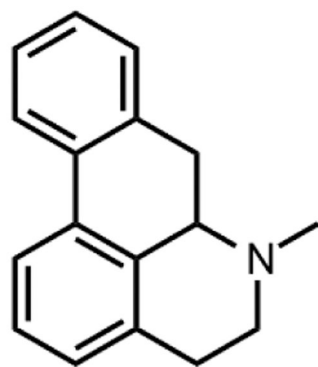


Fig. 53.
Phthalide isoquinoline opioid natural products, noscapine (174) and narceine (175).



aporphine

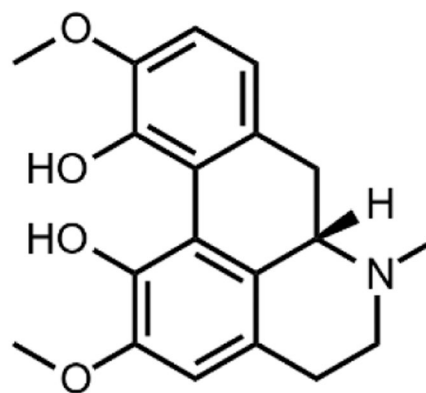
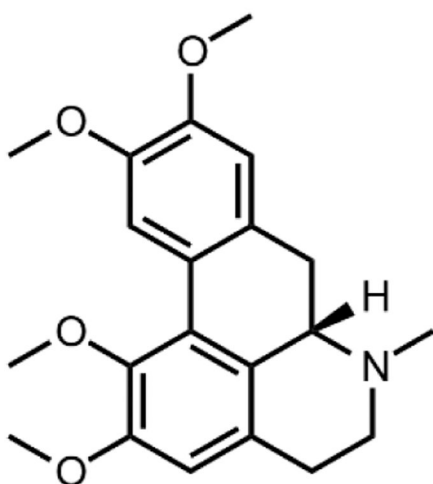
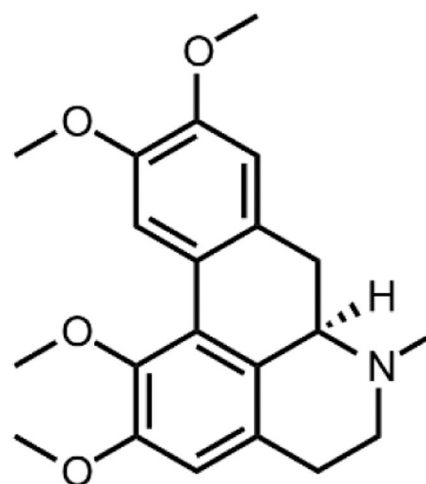
corytuberine **176***(S)*-glaucine **177***(R)*-glaucine **178**

Fig. 54. Aporphine opioids corytuberine (176), natural (*S*)-glaucine (177) and unnatural (*R*)-glaucine (178).

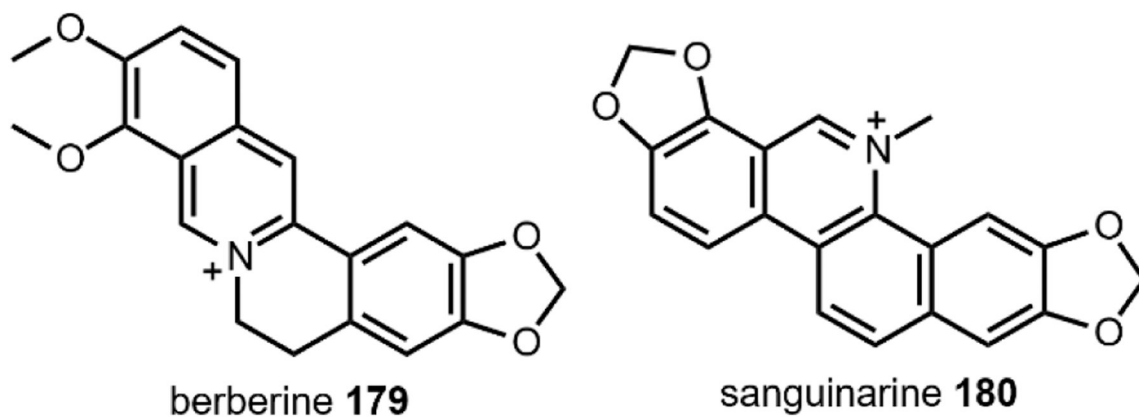


Fig. 55.
Examples of berberine opioids, berberine (179) and sanguinarine (180).

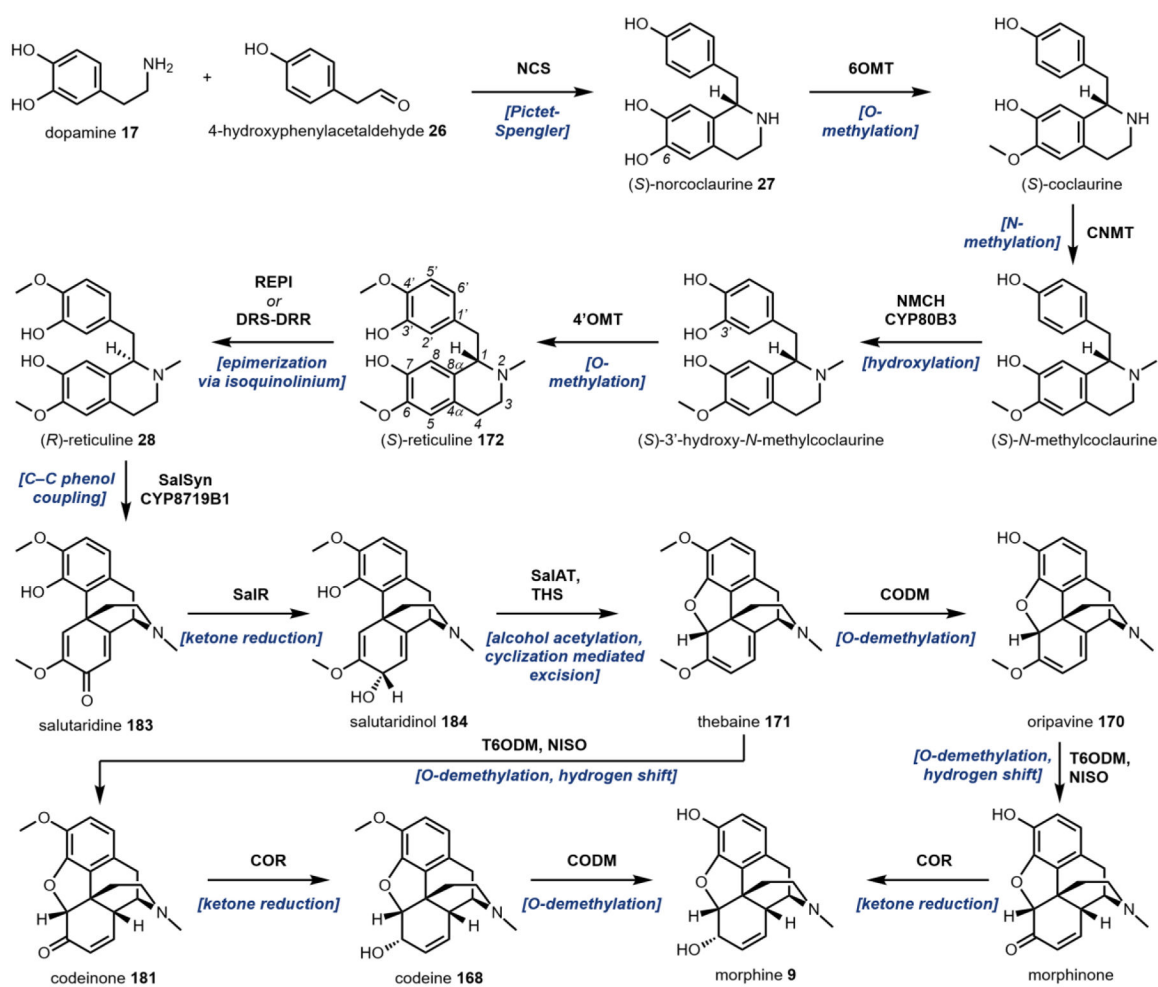


Fig. 56.
Biosynthesis of the morphine opioids from dopamine 17 and 4-hydroxyphenylacetaldehyde 26.

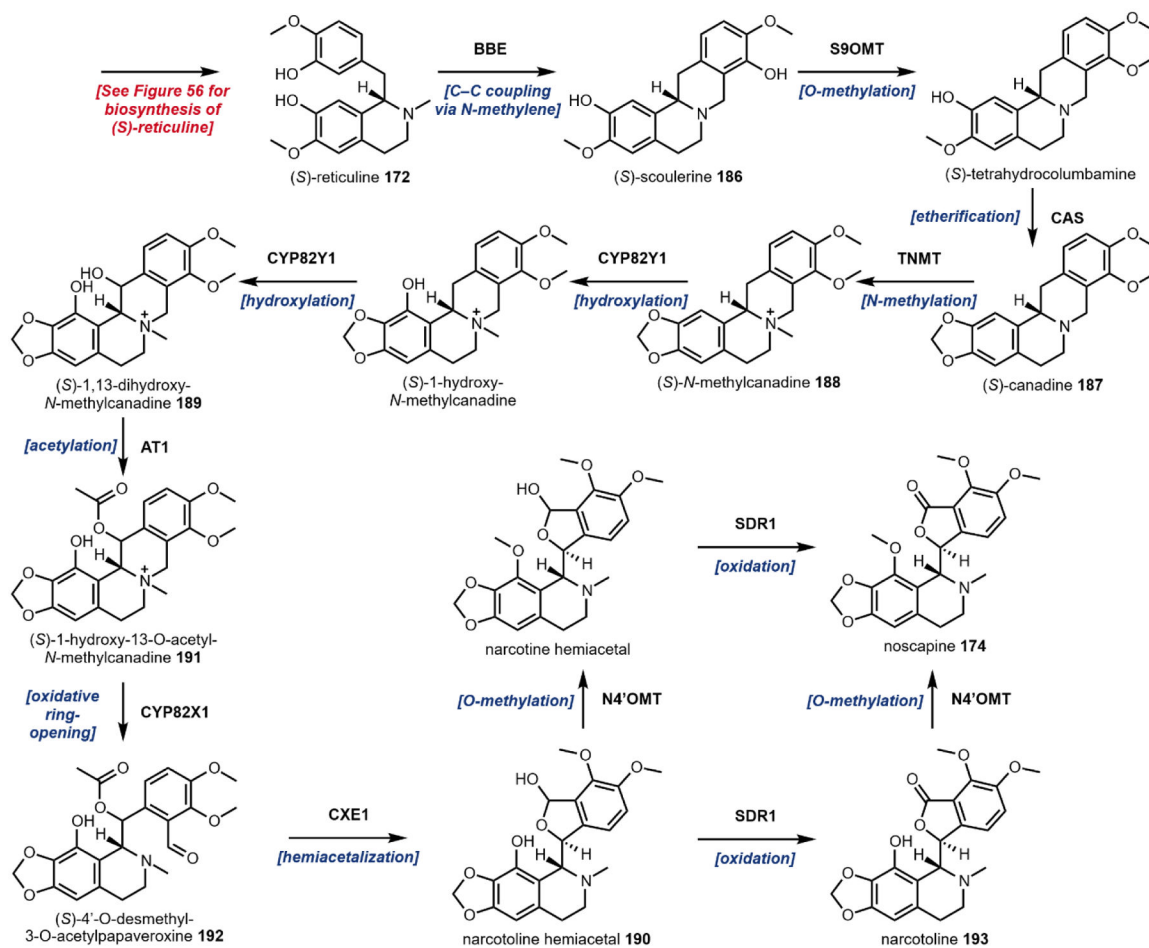


Fig. 57.
 Noscapine biosynthesis from (*S*)-reticuline.

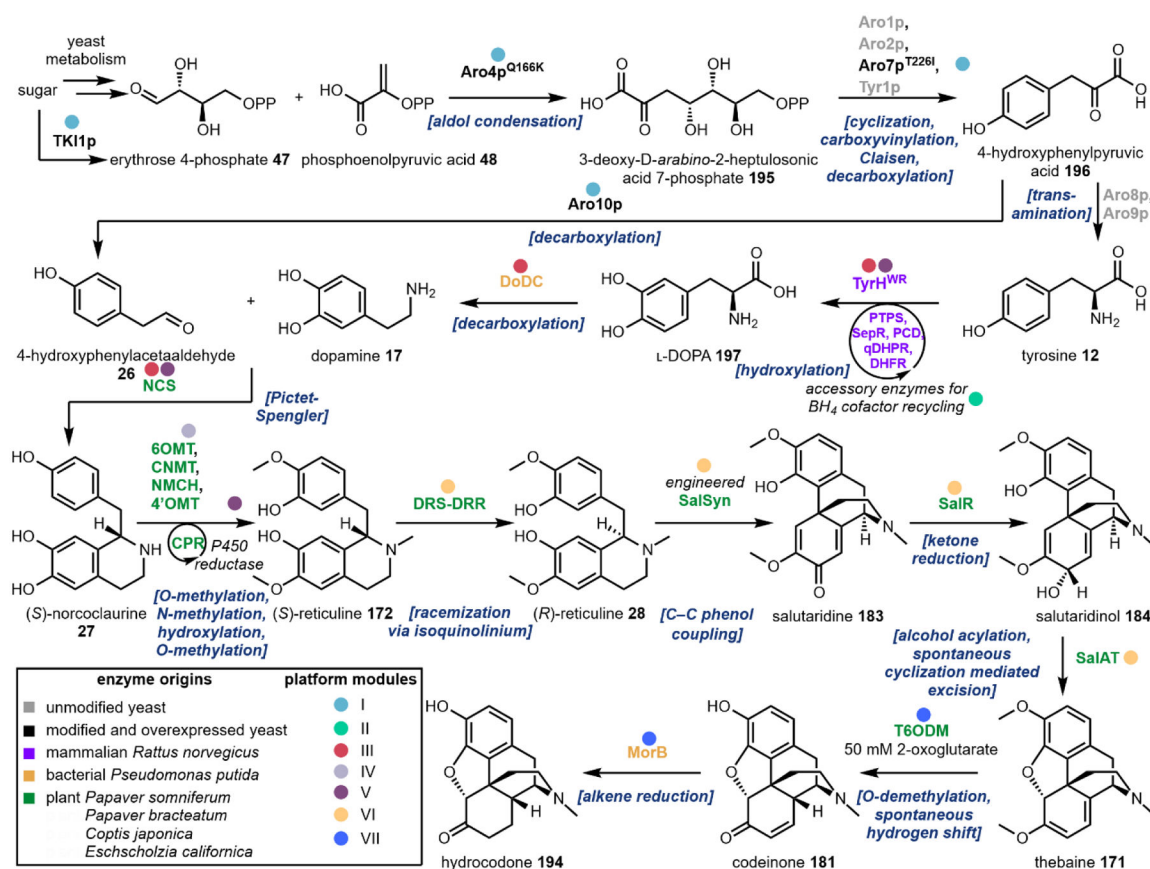
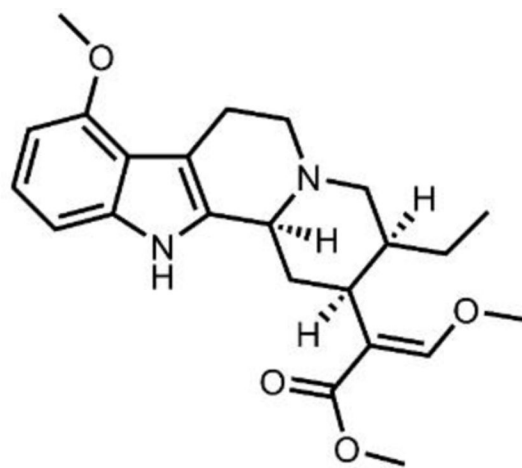


Fig. 58.

Heterologous production of thebaine and hydrocodone from sugar in yeast.



Mitragyna speciosa



mitragynine 10

Fig. 59. *Mitragyna speciosa* cultivars may contain up to one percent dry weight mitragynine. Image on left courtesy of Thor Porre via CC-3.0.

https://commons.wikimedia.org/wiki/File:Kratom_tree.jpg

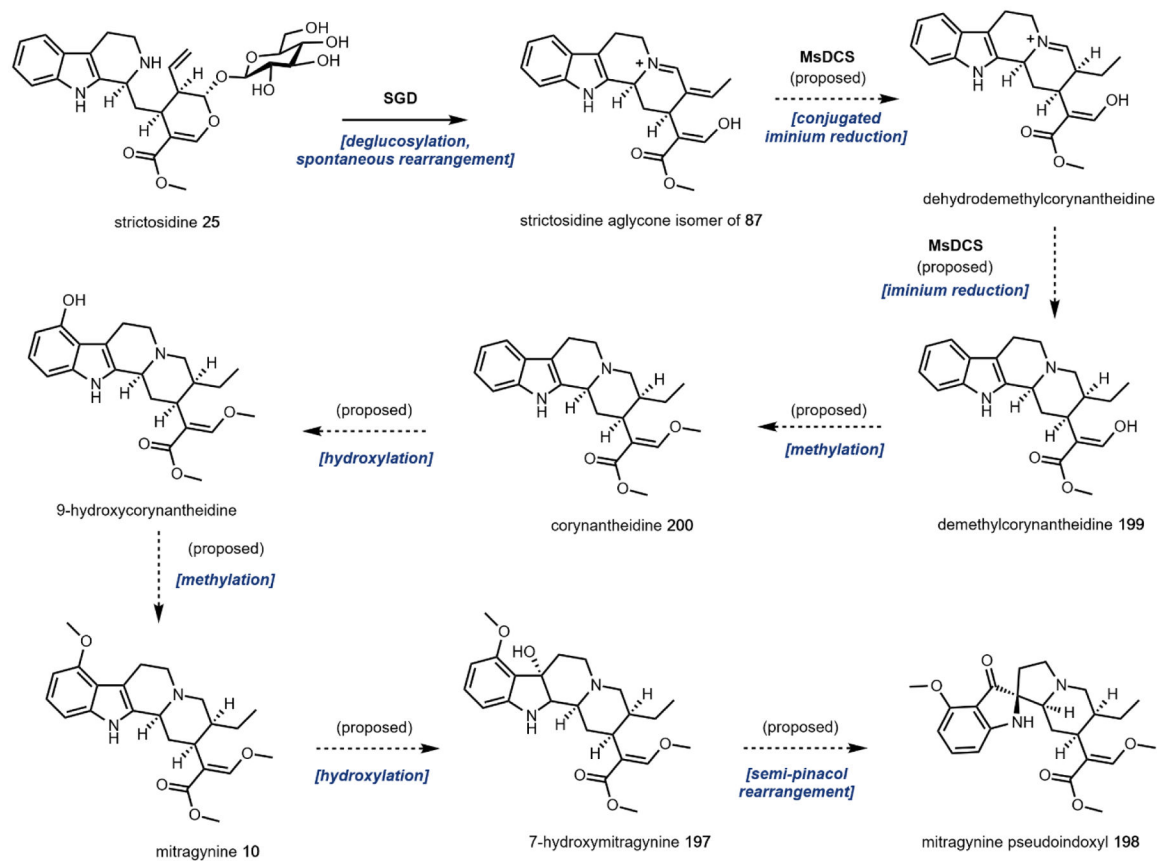


Fig. 60.
Proposed biosynthetic route to kratom alkaloids.